



# **The 10<sup>th</sup> Southeast Asia Collaborative Symposium on Energy Materials (SACSEM 10<sup>th</sup>)**

**October 2 – 4, 2024**

**University Hall at University of Tsukuba**



# **The 10th Southeast Asia Collaborative Symposium in Energy Materials (SACSEM 10th) 2-4, October. 2024**

**Invited Speaker: Presentation (20 min.) + Discussion (4 min.) + Change (1 min.)**

**Student Speaker: Presentation (10 min.) + Discussion (4 min.) + Change (1 min.)**

## **Participating Institutions**

Institut Teknologi Bandung (ITB, Indonesia)

Universiti Kebangsaan Malaysia (UKM, Malaysia)

Universiti Teknologi PETRONAS (UTP, Malaysia)

King Mongkut's University of Technology Thonburi (KMUTT, Thailand)

Universität Duisburg-Essen (UDE, Germany)

East China Normal University (ECNU, China)

University of Newcastle (Univ. Newcastle, Australia)

Politeknik STTT Bandung (STTT Bandung, Indonesia)

University of Trento (Univ. Trento, Italy)

Vietnam Academy of Science and Technology (VAST, Vietnam)

Kyushu University (Kyushu Univ.)

University of Tsukuba (UT, NIMS, AIST, KEK, Japan)



University of Tsukuba

To join, use the ZOOM link or QR code below:

<https://us02web.zoom.us/j/81018691900?pwd=4PsFGM0j1X57lq>

[J9ErbUbKa1oZxGph.1](https://us02web.zoom.us/j/81018691900?pwd=4PsFGM0j1X57lq)

Meeting ID: 810 1869 1900

Passcode: 925880



# Agenda

# SACSEM 10th Symposium Time Table

## DAY1 : October 2nd, Wednesday

Time	No	Affiliation	Presenter	Title
13:00-13:15	OP	U. Tsukuba	Mitsuyasu Kato(Vice President)	Opening Remarks
		U. Tsukuba	Yohei Yamamoto	
13:15-13:40	I01	ITB	Brian Yulianto	Metal Organic Framework Based Biosensors for Point of Care Detection of Infectious Disease
13:40-14:05	I02	UKM	Azizan Ahmad	Natural Rubber-Based Polymer Electrolytes for Electrochemical Devices: Modification, Challenges, Advances and Perspectives
14:05-14:30	I03	KMUTT	Surawut Chuangchote	Flexible and Stickable Perovskite Solar Cells
14:30-14:55	I04	NIMS	Yu Denis	Suppressing Formation of Zn-Mn-O Phases by In-situ Ti Decoration of MnO <sub>2</sub> for Long Lifespan MnO <sub>2</sub> -Zn Battery
<b>Break</b>				
15:20-15:45	I05	Univ. Newcastle	Ajayan Vinu	Nanoporous carbon based materials for clean hydrogen production
15:45-16:10	I06	ECNU	Shaoqiang Chen	Ultrafast lasing properties of perovskite microcavities
16:10-16:35	I07	AIST	Hiroshi Aoki	Biomedical and Environmental Analysis Based on DNA Sensor Arrays for Nucleotide Biomarkers
16:35-17:00	I08	UTP	Khairulazhar Jumbri	In-Situ Coated MOF UiO-66-NH <sub>2</sub> on Graphite for Improved Anode Performance in Lithium-Ion Batteries
17:00-17:25	I09	Univ. Trento	Narges Ataollahi	Transforming Waste PET Bottles into Proton Exchange Membranes for Electrochemical Applications
17:25-17:50	I10	U. Tsukuba	Masaki Hada	Local atomic motions in van der Waals heterostructures observed by complementary ultrafast probes
17:50-18:00		NIMS	Masanobu Naito	Introduction of STAM

Group Photo

19:00~ Welcome Dinner Hokkaido (close to Tsukuba Station)

## SACSEM 10th Symposium Time Table

### DAY2 : October 3rd, Thursday

Time	No	Affiliation	Presenter	Title
9:30-9:45	S01	U. Tsukuba	Ziwei Hu	Synthesis of Terminal-Modified Semiconducting Polymers and Elucidation of the Effect of Terminal Groups
9:45-10:00	S02	ITB	Xorell Ivanov Monov	Ambient-air processed perovskite CsPbBr <sub>3</sub> thin films for solar cell applications
10:00-10:15	S03	UKM	Chai Kai Ling	Synthesis and Characteristics of Non-Edible Jatropha Oil Based Polyurethane Acrylate (PUA) Gel Polymer Electrolyte For Dye
10:15-10:30	S04	UDE	Mohammed-Ali Sheik	Doped NaSICON-Type Solid Electrolytes for Sodium-Ion Batteries from Scalable Spray-Flame Synthesis
<b>Break</b>				
10:50-11:05	S05	U. Tsukuba	Wei-Sheng, Wang	Development of automatic synthesis system for materials research
11:05-11:20	S06	STTT-Bandung	Syahla Andini Putri	Study On A Potential Of PVA/AgNO <sub>3</sub> Nano Fiber As Anti Bacterial Materials Prepared By Electrospinning For Medical Application
11:20-11:35	S07	U. Tsukuba	Natsumi Noguchi	Assessment of Hydrogen Desorption and Absorption Properties of MgH <sub>2</sub> -Ni/HB composites
11:35-11:50	S08	UDE	Mena-Alexander Kräenbring	Coherent Workflows for Sustainable Electrocatalytic Hydrogenation Reactions with Pentlandite Catalysts
11:50-12:00		Daihatsu	Hidetomo Horikawa	Introduction of Daihatsu company
<b>Lunch</b>				
13:00-14:00	Poster Session			
<b>Break</b>				
14:15-14:40	I11	U. Tsukuba	Hiroko Tokoro	Direct observation of Magnetic Domain and Magnetization Reversal on Prussian Blue-based magnetic film
14:40-15:05	I12	KMUTT	Patiya Kemacheevakul	Wastewater Treatment by Photocatalytic Process Using Photocatalyst-coated Materials
15:05-15:30	I13	UKM	Lee Tian Khoon	Assessing the Efficacy of Natural rubber based functional methyl methacrylate binder for Lithium-ion batteries
15:30-15:55	I14	NIMS	Tang Daimin	Chirality Engineering for Ultimate Carbon Nanotube Electronics
<b>Break</b>				
16:15-16:40	I15	KEK	Tetsuya Yokoo	Neutron Scattering as a Common Technique for Energy Material Researches
16:40-17:05	I16	STTT-Bandung	Resty Maysepheny Hernawati	Natural Rubber Foam as Potential Blunt Trauma Pad for Soft Body Armor Application
17:05-17:30	I17	Kyushu Univ.	Junji Nakamura	Heterogeneous Catalysis Contributing to a Carbon-Neutral Society
17:30-17:55	I18	VAST	Nguyen Huy Dan	Research on manufacturing high coercivity hard magnetic materials

18:30~

Banquet

Soup Factory

## SACSEM 10th Symposium Time Table

### DAY3 : October 4th, Friday

Time	No	Affiliation	Presenter	Title
9:30-9:45	S09	U. Tsukuba	Kenji Hayashida	Activation mechanism of carbon catalyst for oxygen reduction reaction
9:45-10:00	S10	ITB	Miftahul Khoiri	Synthesis and Characterization of Nickel Cobalt Phosphate Electrode to Improve the Performance of Hybrid Supercapacitor
10:00-10:15	S11	Univ. Newcastle	Ayush Kumar	p-Nitrophenol reduction using transition metal supported zeolites
10:15-10:30	S12	UKM	Nurul Akmaliah	Graphene-Enhanced Lithium-Ion and Alternative Batteries: Pioneering Malaysia's National Green Economy
<b>Break</b>				
10:50-11:05	S13	U. Tsukuba	Muhammad Rezki	Enhancing Enzyme Electrode Performance Using Metal-Organic Frameworks for Advanced Biosensing Applications
11:05-11:20	S14	ECNU	Deyang Qin	High efficiency Sb <sub>2</sub> (S, Se) <sub>3</sub> thin-film solar cells by substrate-temperature-controlled vapor transport deposition method
11:20-11:35	S15	UDE	Adil Amin	Amorphous Silicon/Carbon Composite-Based Hierarchically Structured Supraparticles for Lithium-Ion Battery Anodes
11:35-11:50	S16	U. Tsukuba	Sota Nakayama	Near-unity angular anisotropy of circularly polarized luminescence from microspheres of monodispersed chiral conjugated polymer
11:50-12:05	S17	KMUTT	Kamonthip Singbumrung	Influence of Size and Shape of ZnO Photocatalysts in Natural Rubber Latex Foam on Antibacterial Applications
<b>Lunch</b>				
13:00-14:00	Poster Session			
<b>Break</b>				
14:15-14:40	I20	ITB	Arie Wibowo	Visible light-driven photocatalyst for synthetic dyes remediation
14:40-15:05	I21	UTP	Hayyiratul Fatimah Mohd Zaid	Molecular Interactions of Zinc-based Metal-Organic Framework Cluster and 1-Butyl-3-Methylimidazolium Chloride: Structural and
15:05-15:30	I22	NIMS	Yukari Katsura	Starrydata: A Data-Curation Project from Material Property Plots on Published Papers
15:30-15:55	I23	STTT-Bandung	Hendra	Micrometer-Scale Optical Web Made of Spider Dragline Fibers with Optical Gate Operations
15:55-16:20	I24	U. Tsukuba	Muneaki Hase	Diamond Nonlinear Photonics — Realizing Spatiotemporal Extreme Sensing Using Diamonds
16:20-16:30	Prize Announcement			
16:30-16:40	CL	U. Tsukuba	Muneaki Hase	Closing Remarks

17:30-19:00      Farewell Reception (Tsukuba Demi)



## Poster Session

DAY2 : October 3rd, Thursday

	Presenter	supervisor	Affiliation	title
1	Sarita Manandhar	Lok Kumar Shrestha	Univ. Tsukuba	Nanoarchitectonics of Biomass Carbon for Energy Storage Technology
2	Chenxiao YE	Denis YU	Univ. Tsukuba	Enhancement of Reversibility and Capacity of Silicon Based Electrodes through Various Parameters
3	Sabina SHAHI	Lok Kumar Shrestha	Univ. Tsukuba	Energy Performance Advancement by Tuning Nano-space of Hollow Carbon Spheres
4	Sabrina Schleich		UDE	Synthesis and characterization of high entropy oxide nanoparticles
5	Novi Dwi Widya Rini	Lok Kumar Shrestha	Univ. Tsukuba	3D Printed Scaffold using Polycaprolactone/Fullerene (C60) Nanorod for Bone Tissue Engineering
6	Yui Iwasaki	Masaki Hada	Univ. Tsukuba	Observing electronic dynamics in the conduction band of 2H-MoTe2 by using double-excitation ultrafast electron diffraction
7	YANG LUOTING		ECNU	T Perovskite photonic crystal of CsPbBr3 on patterned substrates and its laser properties
8	Sundas Rani	Yohei Yamamoto	Univ. Tsukuba	Chiral Gels of Polymer for the Fabrication of Organic Electrochemical Transistors
9	Mads Nybo Sørensen	Takashi Nakamura	Univ. Tsukuba	Synthesis and Properties of Azobenzene Containing Salen Based Macrocycles and Molecular Cages
10	Nurfauzi Abdullah	Takashi Suemasu	Univ. Tsukuba	Carrier Properties and The Possible Cause for Low Donor Activation of As-doped BaSi2 Thin Films
11	PEI ZHENHAO	Cheng Xiaohong	ECNU	Manganese-doped perovskite microcavities are used in laser resonators
12	Leon Müller		UDE	Spray-Flame Synthesis of Mn and V Substituted Perovskite-Type LaCoO3
13	Rabindra Nath Acharyya	Lok K. Shrestha	Univ. Tsukuba	Carbon Composites from Novel Metal Organic Framework on Fullerene Assemblies (MOFOF) for Energy Conversion Application
14	Toni Subagja	Sepehri Amin Hossein	Univ. Tsukuba	Influences of Co on the coercivity of (Sm8Zr2)(Fe1-xCox)TiyVzCu0.5-based magnets
15	Shunya Aoyagi	Yohei Yamamoto	Univ. Tsukuba	Highly dopable Excited-State Intramolecular Proton Transfer molecule-based microsphere WGM laser
16	Riku Seiki	Hiroko Tokoro	Univ. Tsukuba	Relationship between Heat Storage Properties and Crystallite Size of Lambda-Type Titanium Pentoxide
17	Zhichao Wei	Yasuo Norikane	Univ. Tsukuba	Effect of Alkyl Chain Length on Photoinduced Crystal-Liquid Phase Transition in Para-Alkoxy Azobenzenes

DAY3 : October 4th, Friday

	Presenter	supervisor	Affiliation	title
18	Ammara Firdous	Takashi SUEMASU	Univ. Tsukuba	Computational Insights into Schottky barrier height of vertical Graphene and Borophene with XS2N4 (X= Mo, W) monolayers
19	MARYAM HASSAN		UKM	Flower-like Cu2ZnSnS4 (CZTS) Transition Metal Sulphides (TMS) as a Micro-structured Electrode in Lithium Rechargeable Battery
20	KARIANA KUSUMA DEWI	Yohei Yamamoto	Univ. Tsukuba	Monodispersed Organic Microcavities from Inkjet Printer as Biological Optical Probes
21	Anmol Sharma	Takao Mori	Univ. Tsukuba	Enhanced Thermoelectric Properties of PANI/ZnSb nano nanocomposite flexible films
22	Makoto Okumura	Yohei Yamamoto	Univ. Tsukuba	Controlling the Rotational Behavior of Chiral Polymer Spheres with Optical Tweezers
23	Aamir Muhammad Fasih	Takao Mori	Univ. Tsukuba	Contact material optimization for the Mg3(Sb,Bi)2 based thermoelectric compounds
24	SINGH RAVI	Takahiro Kondo	Univ. Tsukuba	Systematic study of structural effects for proton and oxygen transport on nitrogen-doped carbon catalysts
25	Syadza Aisyah Hermadanti	Isa Anshori	ITB	Development of Flower like-nanocomposite Based Mg(Ti0.99Sn0.01)O3 Decorated on Reduced Graphene Oxide (rGO) as Supercapacitor Electrodes
26	LI WEIQI	Junpei Kuwabara	Univ. Tsukuba	Development of an efficient and air-stable Pd(II) precatalyst
27	Masato Kato	Yohei Yamamoto	Univ. Tsukuba	Electrically Switchable Organic Droplet Lasers for Laser Display
28	Xiong Tianya	Junpei Kuwabara	Univ. Tsukuba	Investigation of Regioselectivity and Reactivity in the Cross-Dehydrogenative Coupling Reaction of Disubstituted Benzenes with Polyfluoroarenes
29	Li Jinyu	Takahiro Kondo	Univ. Tsukuba	Exploration and evaluation of new elements of non-metallic substances r-BS by high-pressure synthesis
30	Valentinus Alphano Dabur	Arie Wibowo	ITB	he synthesis of visible-light-driven photocatalyst material using rGO/ZnO/Fe2O3 derived from zinc dross for synthetic dye degradation
31	Kushal Mehrotra	Takao Mori	Univ. Tsukuba	Enhancing Thermoelectric and Mechanical Properties of YbMg2(Bi,Sb)2 Zintl Phase through Anion site substitution
32	Angayarkanni Ramamurthy Dilipan	Sepehri-Amin Hossein	Univ. Tsukuba	Combinatorial sputtering synthesis of TbCu7-type Sm-Fe based compounds: A study on phase, composition, and extrinsic magnetic properties
33	Ayush Kumar	Univ. Newcastle	Univ. Tsukuba	p-Nitrophenol reduction using transition metal supported zeolites

# **Invited Speaker**

## **Metal Organic Framework Based Biosensors for Point of Care Detection of Infectious Diseases**

**Brian Yulianto, Muhammad Iqbal, Ni Luh Wulan Septiani,**

*Advanced Functional Materials Laboratory, Engineering Physics  
Department, Faculty of Industrial Technology, Institut Teknologi  
Bandung, Bandung 40132 Indonesia*



Metal-organic frameworks, or MOFs, are a type of porous material that have advantages such as a high surface area, abundant porosity, and surfaces that can be easily modified. MOFs with transition metals become interesting to utilize in electrochemical biosensors, especially if the MOF surface is terminated with metals as active sites, resulting in a high surface area with abundant available active sites. Several studies have successfully utilized MOFs as biosensor materials, particularly for virus detection. HKUST-1-based MOFs with a one-dimensional structure have been successfully used to detect the dengue virus. Modification was performed using high concentrations of triethanolamine to obtain a 1D structure with abundant metal centers. This strategy resulted in a biosensor with a detection limit of 0.9 pg/mL. Surface modification can also be performed by adding other transition metals to provide a variety of active sites. Nickel and copper were used as modifiers for HKUST-1. The presence of these metals reduced the detection limit to 0.7 pg/mL and 0.5 pg/mL, respectively. Another virus successfully detected using MOFs is Hepatitis B. Other copper-based MOFs were also modified to detect the Hepatitis B virus. MOFs with a spherical structure had high sensitivity and a detection limit of 730 pg/mL. Additionally, HKUST-1 was also used to detect Hepatitis B with a detection limit reaching 0.89 pg/mL. These research results demonstrate the high potential of MOFs for use in healthcare, particularly in biosensors.

***Keywords :*** *Biosensors, electrochemical, metal organic frameworks, virus, limit of detection*

# Natural Rubber-Based Polymer Electrolytes for Electrochemical Devices: Modification, Challenges, Advances and Perspectives



Azizan Ahmad<sup>1</sup>, Tian Khoon Lee<sup>1</sup>, Rawdah Whba<sup>2,3</sup>,  
Mohd Sukor Su'ait<sup>4</sup>

<sup>1</sup>*Department of Chemical Sciences, Universiti Kebangsaan Malaysia, Bangi 43600, Selangor, Malaysia.*

<sup>2</sup>*Department of Chemistry, Faculty of Applied Sciences, Taiz University, 6803 Taiz, Yemen*

<sup>3</sup>*Department of Engineering Physics, Istanbul Medeniyet University, 34700 Istanbul, Türkiye*

<sup>4</sup>*Solar Energy Research Institute (SERI), Universiti Kebangsaan Malaysia, Bangi 43600, Selangor, Malaysia.*

*E-mail: azizan@ukm.edu.my*

The issue of efficient energy storage is now becoming critical and mobilizing researchers and industrial companies worldwide. As energy demands grow, strict strategies will ensure that energy sources are available and accessible at a low cost and with the least possible effect on the environment. Polymer electrolytes (PEs) based on natural rubber (NR) and their derivatives are regarded as eco-friendly and have attracted increasing interest <sup>[1]</sup>. However, continuous efforts are still being made to improve this type of PEs for energy storage applications <sup>[2]</sup>. This review addresses the synthesis routes of modified natural rubbers (MNRs), challenges, and typical amendment methods to design flexible structures for electrochemical devices <sup>[3,4]</sup>. Furthermore, this review also discusses in depth the evolution of MNR-based PEs from the points of view of adaptable design strategies, fundamental thermomechanical and electrochemical characteristics, and future uses for energy storage <sup>[4,5]</sup>. Overall, this review highlights eco-friendly materials like rubber to open doors for novel approaches towards sustainable and renewable energy and boost the economy's value of NR.

## References

- [1] Lee, T.K et.al. *Electrochimica Acta*, 2019, 316, 283-291.
- [2] Whba, R. et.al. *Reactive and Functional Polymers*, 2021, 164, 104938.
- [3] Whba, R., et.al., *Polymer International*, 2023, 72(12), 1070-1078.
- [4] Whba, R et. al. *Journal of Energy Storage* 2024, 83, 110593.
- [5] Whba, R. et.al. *Solid State Ionics*, 2024, 116634.

# Flexible and Stickable Perovskite Solar Cells

Wassana Lekkla,<sup>1,2</sup> Taweewat Krajangsang,<sup>3</sup>  
Surawut Chungchote<sup>1,2,\*</sup>



<sup>1</sup> Department of Tool and Materials Engineering, Faculty of Engineering, King Mongkut's University of Technology Thonburi (KMUTT), 126 Prachauthit Rd., Bangmod, Thungkru, Bangkok 10140, Thailand.

<sup>2</sup> Research Center of Advanced Materials for Energy and Environmental Technology (MEET), King Mongkut's University of Technology Thonburi (KMUTT), 126 Prachauthit Rd., Bangmod, Thungkru, Bangkok 10140, Thailand.

<sup>3</sup> Solar Photovoltaic Research Team, National Energy Technology Center (ENTEC), National Science and Technology Development Agency (NSTDA), 111 Thailand Science Park, Phaholyothin Road, Klong Nueng, Klong Luang, Pathum Thani, 12120, Thailand

E-mail: [surawut.chu@kmutt.ac.th](mailto:surawut.chu@kmutt.ac.th)

Perovskite solar cells have achieved power conversion efficiencies exceeding 25% in recent years. The specialty of flexible perovskite solar cells is that they can be fabricated onto flexible substrates, making them lightweight, flexible, and wearable. They can be attached to equipment that requires low electrical power, such as solar vests, solar recharge backpacks, flexible solar panels, drones, and boats. This work presents an approach to fabricating flexible perovskite solar cells on adhesive label (stickable-removable) substrates. Different counter electrodes have been compared. The concept of utilizing adhesive label substrates in fabricating flexible perovskite solar cells, as well as a pathway for creating dependable power sources for stickable-removable electronic devices, will be presented.

# Suppressing Formation of Zn-Mn-O Phases by In-situ Ti Decoration of MnO<sub>2</sub> for Long Lifespan MnO<sub>2</sub>-Zn Battery

Denis Y. W. Yu,<sup>1</sup> Qiaohui Duan<sup>2</sup>

<sup>1</sup> National Institute for Materials Science, Tsukuba, Ibaraki, Japan

<sup>2</sup> City University of Hong Kong, Hong Kong

E-mail: yu.denis@nims.go.jp



Aqueous rechargeable MnO<sub>2</sub>-Zn batteries, featuring the use of low-cost and non-toxic materials, safe electrolyte, and moderate energy density is a promising candidate to replace toxic lead-acid batteries.<sup>1</sup> However, so far, MnO<sub>2</sub>-Zn batteries suffer from poor cyclability.<sup>2</sup> Even when Mn<sup>2+</sup> additive is added to the electrolyte, as commonly adopted by most researchers, the capacity still decreases with cycling due to the emergence of Zn-inserted phases in the cathode after cycling, whose formation mechanism is still under debate, and few facile and practical solutions have been proposed.<sup>3</sup> Here, we analyzed the cause of the cycle degradation, and proposed TiOSO<sub>4</sub> as an electrolyte additive to suppress the irreversible phase formation with an innovative in-situ decoration strategy, which achieves long lifespan of the MnO<sub>2</sub>-Zn batteries.<sup>4</sup>

Through characterizations such as X-ray diffraction (XRD), inductively-coupled plasma spectroscopy (ICP), etc. together with electrodeposition experiments, we found that continuous EMD dissolution-deposition reaction greatly contributes to the reversible capacity. The concomitant co-deposition of Mn<sup>2+</sup> and Zn<sup>2+</sup> generates Zn-Mn-O phases during cycling, leading to capacity fading. Inspired by the electrodeposition synthesis of Ti-doped EMD, we introduced TiOSO<sub>4</sub> as a facile electrolyte additive to form Ti-doped EMD during the cycling process, which can suppress the formation of the Zn-Mn-O phases. As a result, under a current of 1200 mA g<sup>-1</sup>, the EMD electrode still gives a capacity of 230 mAh g<sup>-1</sup> for over 1500 cycles. The superior cyclability is due to the improved stability of the as-formed Ti-doped EMD with TiOSO<sub>4</sub> additive and improved reversibility of Mn dissolution/deposition with cycling, as confirmed by XRD and ICP results. More characterizations and results will be shown during the meeting.

## References

- [1] Lopes, P.P. and Stamenkovic, V. R. *Science* **2020**, 369, 6506.
- [2] Becknell, N. et al., *Adv. Funct. Mater.* **2021**, 31, 35.
- [3] Aguilar, I. et al., *Energy Stor. Mater.* **2022**, 53.
- [4] Duan, Q. et al. *Small* **2024**, 2404368.

# Nanoporous carbon based materials for clean hydrogen production



Ajayan Vinu

<sup>1</sup> *The University of Newcastle, College of Engineering, Science and Environment, Callaghan 2308, Australia*  
E-mail: [ajayan.vinu@newcastle.edu.au](mailto:ajayan.vinu@newcastle.edu.au)

Nanoporous Materials with ordered porous structures and functional elements offer excellent textural features and catalytic properties. Among the nanoporous materials, nanoporous carbon nitrides are quite unique as they possess highly stable semiconducting CN framework with tunable band gaps and basicity. These CN nanomaterials can deliver successful energy and environment solutions - such as converting waste or seawater into clean hydrogen with only sunlight and developing innovative devices for energy storage and conversion. In this talk, I will present the development, capabilities, and current and future applications of multifunctional amorphous and crystalline nanoporous carbon nitride materials with different structures, band gaps, and nitrogen contents.<sup>1-9</sup> Especially, I will focus on the preparation of novel nanoporous amorphous and crystalline CN with different stoichiometries and their structural elucidation using different spectroscopic techniques. I will also demonstrate how the chemical composition, structure, porosity and the functionalization of these unique materials can be tuned.<sup>3,10-11</sup> In the last part of the talk, I will present on the energy storage and photocatalytic performance of these unique nanoporous carbon nitrides and their hybrids on water splitting to produce clean hydrogen from seawater. I will also demonstrate the utilization of this technology on converting the seawater from different beaches along the coastal side of Australia.

## References

1. Vinu et al., *Chem. Soc. Rev.* **2023**, 52 (21), 7602-7664
2. Vinu et al., *Adv. Mater.* **2024**, 36, 2306895.
3. Vinu et al., *Prog. in Mater. Sci.* **2023**, 135, 101104
4. Vinu et al., *Prog. in Mater. Sci.* **2024**, 101242
5. Vinu et al., *Adv. Mater.*, **2020**, 32, 1904635.
6. Vinu et al., *Chem. Soc. Rev.*, **2020**, 49, 4360.
7. Vinu et al., *Nano Energy*, **2020**, 72, 104702.
8. Vinu et al., *Angewandte Chemie*, **2018**, 130 (52), 17381.
9. Vinu et al., *Chem. Soc. Rev.*, **2018**, 47, 2680.
10. Vinu et al., *Nano Energy*, **2021**, 82, 105733.
11. Vinu et al., *Angewandte Chemie*, **2021**, 60 (39), 21242.

# Ultrafast lasing properties of perovskite microcavities

Shaoqiang Chen,<sup>1</sup> Zhan Su,<sup>1</sup> Guoen Weng,<sup>1</sup> and Hidefumi Akiyama<sup>2</sup>

<sup>1</sup> State Key Laboratory of Precision Spectroscopy, East China Normal University, Shanghai, China

<sup>2</sup> Institute for Solid State Physics, The University of Tokyo, Kashiwa, Japan

E-mail: sqchen@ee.ecnu.edu.cn



Perovskite materials have shown excellent optoelectronic properties in the field of not only solar cells but also light emitting devices, including LED and laser diodes, such as perovskite-based single-mode distributed feedback lasers and vertical cavity surface emitting lasers (VCSEL), where understanding the lasing mechanism is very important. To study the detailed lasing mechanisms in perovskite based microcavities, we have fabricated various kinds of CsPbBr<sub>3</sub> perovskite micro-cavities, such as micro-hemispheres, microplates, and micro-rods on different substrates. All the microcavities have shown lasing behaviors under femtosecond optical excitations, with Fabry-Perot mode and/or whispering-gallery mode. The time-resolved lasing spectra of the microcavities have been investigated with a streak camera, the results indicated that lasing dynamics is merged with the transient BGR effect and the transient change of refractive index in perovskite microcavities [1]. We also fabricated CsPbBr<sub>3</sub> perovskite nanocrystals based VCSEL, and single-mode lasing has been observed. The results indicated that with an excitation power over 2 times of the threshold, short pulses with a pulse width around 23 ps have been obtained, the lasing dynamics has been demonstrated to be related to the gain-switching mechanisms, indicating a potential application in short pulse generation of perovskite VCSELs [2].

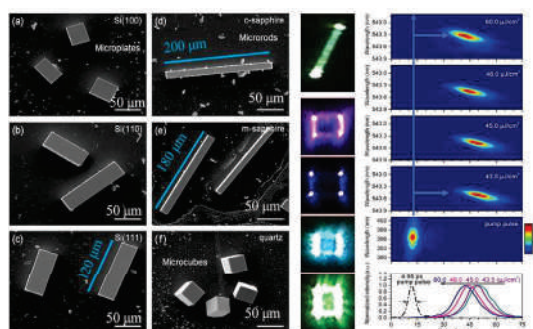


Fig.1 Various kinds of perovskite microcavities with the lasing images and time-resolved spectroscopies.

## References

- [1] Jiao Tian et al., *Communications Physics*. **2022**.5,160.
- [2] Yawen He et al., *Nanophotonics*. **2023**. 12(12): 2133–2143.



# Biomedical and Environmental Analysis Based on DNA Sensor Arrays for Nucleotide Biomarkers

Hiroshi Aoki<sup>1,2</sup>

<sup>1</sup> Environmental Management Research Institute, National Institute of Advanced Industrial Science and Technology (AIST), Tsukuba, Japan

<sup>2</sup> Materials Innovation Program Faculty, University of Tsukuba, Tsukuba, Japan

E-mail: aoki-h@aist.go.jp



Living things inhabiting the environment emit various information under the influence of the environment. Therefore, by focusing on information from living things, it is possible to evaluate the environment. Our research group is currently developing new environmental assessment methods by detecting and analyzing biomarkers as information emitted by living organisms. Here, we will introduce nucleotide sensor arrays that quickly and easily sensing DNAs or RNAs from the environments.

Based on the nucleotide detection principles using electrochemical signal switching upon sequence-specific hybridization with target nucleotide biomarkers, we developed sensor arrays enabling simultaneous analysis of multiple targets without labeling process. Synthesized probes composed of peptide nucleic acid (PNA) possessing target-responsive electroactive switches were immobilized on electrodes of a photo-lithographically fabricated 384-ch Au film electrode array chips to prepare the sensor array (Figure 1). The sensor array showed sequence-specific responses upon hybridization of the probes with target sequences complementary to the probes in contrast to mismatch versions. The target sequences from messenger RNAs (mRNAs) for chemical-responsive genes and microRNAs (miRNAs) for lung cancer biomarkers were successfully detected.<sup>[1]</sup> As more realistic cases, we also demonstrated the detection of DNAs from the environments to aim at an on-site DNA evaluation.<sup>[2]</sup> This talk will provide new insights of simple and rapid analysis based on the sensor arrays as one of the alternatives to DNA sequencers that are currently used in the biomedical and environmental fields, but need special skills and lab-installation.

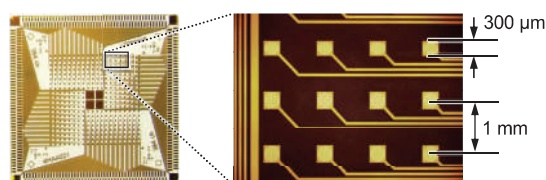


**Figure 1.** Photo-lithographically fabricated sensor array.

## References

- [1] Aoki, H.\*; Torimura, M.; Nakazato, T. *Biosens. Bioelectron.*, **2019**, *136*, 76–83.
- [2] Kawaguchi, M.; Aoki, H.\*; Kamo, H.; Miura, K.; Hiruta, Y.; Simizu, S.; Citterio, D.\* *Anal. Sci.* **2024**, *40*, 501–510.

# ***In-Situ* Coated MOF UiO-66-NH<sub>2</sub> on Graphite for Improved Anode Performance in Lithium-Ion Batteries**



Adam Azizi Abdul Azis,<sup>1</sup> Khairulazhar Jumbri,<sup>1</sup> Noor Fazriyana Hamidon<sup>1</sup>, Nurul Akmaliah Dzulkurnain<sup>2</sup>

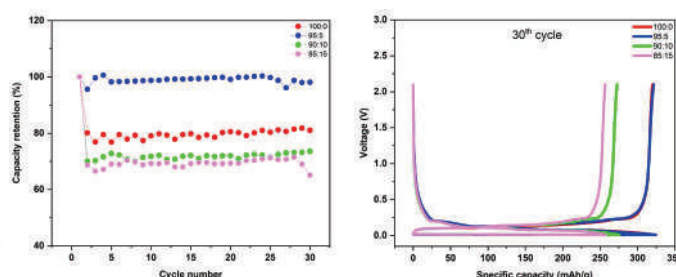
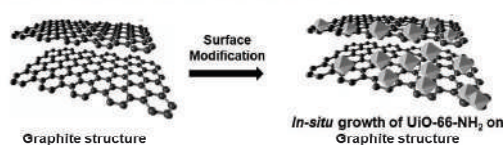
<sup>1</sup> Department of Fundamental and Applied Sciences, Universiti Teknologi PETRONAS, 32610 Seri Iskandar, Perak, Malaysia

<sup>2</sup> International Battery Center Sdn Bhd, Taman Teknologi, MRANTI, Bukit Jalil, 57000 Kuala Lumpur, Malaysia

E-mail: khairulazhar.jumbri@utp.edu.my

Lithium-ion batteries (LIBs) are essential for modern energy storage, but advancements in anode materials are needed to enhance their performance. This study explores graphite/UiO-66-NH<sub>2</sub> composites synthesized via *in-situ* solvothermal method. The objectives include developing the composites, optimizing the graphite to UiO-66-NH<sub>2</sub> ratio, and assessing their performance in coin cell batteries. Powder X-ray Diffraction (XRD) confirmed the successful integration of UiO-66-NH<sub>2</sub> into graphite without altering its crystal structure. BET surface area analysis showed that increasing UiO-66-NH<sub>2</sub> content enhanced the surface area of the composites, reaching 45 m<sup>2</sup>/g, 88 m<sup>2</sup>/g, and 155 m<sup>2</sup>/g for 5%, 10%, and 15% UiO-66-NH<sub>2</sub> loading, respectively. Field Emission Scanning Electron Microscopy (FESEM) revealed a uniform distribution of UiO-66-NH<sub>2</sub> on graphite surface. Electrochemical testing indicated that the 95:5 graphite/UiO-66-NH<sub>2</sub> composite achieved high charge and discharge capacities of 321.68 mAh/g and 324.23 mAh/g, respectively, with superior capacity retention compared to pristine graphite. The evaluation of the fabricated coin cells demonstrated promising life cycle performances, highlighting the potential of graphite/UiO-66-NH<sub>2</sub> composites as a viable anode material for future battery applications.

## RESEARCH ILLUSTRATION CONCEPT



*Incorporating UiO-66-NH<sub>2</sub> on graphite surface enhanced the overall performance of LIBs by improving the capacity, cycle and thermal stability*

# Transforming Waste PET Bottles into Proton Exchange Membranes for Electrochemical Applications



Narges Ataollahi,<sup>1</sup> Varun Donnakatte Neelalochana,<sup>1</sup> and Paolo Scardi <sup>1</sup>

<sup>1</sup> *Department of Civil, Environmental, and Mechanical Engineering, University of Trento, 38123 Trento, Italy*  
*E-mail: narges.ataollahi@unitn.it*

The extensive use of plastics in various industries has led to a significant increase in plastic waste over recent decades. Recycling PET bottles has emerged as a widely adopted solution to address this growing problem. This study focuses on the successful chemical modification <sup>[1]</sup> of waste PET bottles into proton exchange membranes (PEMs) and their potential application in electrochemical systems such as fuel cells, water electrolyzers, and vanadium redox flow batteries. The PET structure was modified through sulfonation reaction. The structural properties of the synthesized material were confirmed through NMR and FTIR analysis. To enhance the performance of the PEMs, the degree of sulfonation (SO<sub>3</sub>H) was carefully adjusted by varying the sulfonation concentration (50%, 60%, and 70%) under controlled time and temperature conditions. Among the different membranes, the one with 70% sulfonation demonstrated the best performance, exhibiting a maximum proton conductivity of 0.17 S/cm at 80°C, along with a water uptake of 37% at the same temperature. These results highlight the membrane's potential for effective proton conduction and hydration under operational conditions. This innovative PET-based membrane may contribute to sustainable energy solutions and promote the use of recycled materials in electrochemical applications which supports the principals of the circular economy by transforming waste into valuable resources.

## References

[1] Neelalochana, V. D.; Tomasino, E.; Di Maggio, R.; Cotini, O.; Scardi, P.; Mammi, S.; Ataollahi, N. *ACS Applied Polymer Materials* **2023**,5, 7548–7561.

# Local atomic motions in van der Waals heterostructures observed by complementary ultrafast probes



Masaki Hada<sup>1</sup>

<sup>1</sup>*Institute of Pure and Applied Sciences and Tsukuba Research Center for Energy Materials Science (TREMS), University of Tsukuba, 1-1-1 Tennodai, Tsukuba, Ibaraki 305-8573, Japan*

E-mail: hada.masaki.fm@u.tsukuba.ac.jp

## Content

In the last two decades, methods have been developed to directly observe the light-driven atomic motions of materials in real time. This progress is currently being made in elucidating the mechanisms of photoreactions and photoinduced phase transition phenomena in materials. [1,2]. These methodologies generally have a time resolution of  $10^{-14}$  to  $10^{-12}$  seconds (10 femtoseconds to 1 picosecond) and are called ultrafast measurements. Among the ultrafast measurement techniques, I will discuss ultrafast time-resolved electron diffraction measurements on solid-state materials in this presentation. Ultrafast time-resolved electron diffraction uses techniques like ultrafast time-resolved x-ray diffraction to measure the photoinduced changes of atomic or molecular coordinates.

The presentation shows the recent combined investigation of ultrafast time-resolved electron diffraction measurements, ultrafast transient absorption measurements, and first-principles calculations on a one-dimensional van der Waals heterostructure [3]. The heterostructure contains carbon nanotubes (CNTs) as an inner core and boron nitride nanotubes (BNNTs) as an outer core. We found peculiar charge transfer channels between CNTs and BNNTs through the heterostructures (Fig. 1).

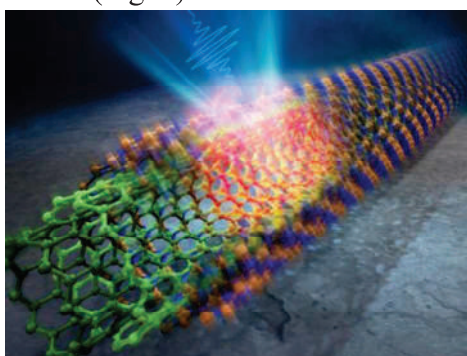


Fig. 1. Electron transfer channel observed in van der Waals heterostructures of a CNT and a BNNT.

## References

- [1] S. Koshihara, T. Ishikawa, Y. Okimoto, K. Onda, R. Fukaya, M. Hada, Y. Hayashi, S. Ishihata, T. Luty, *Physics Reports* 942, 1–61 (2022).
- [2] M. Hada, Y. Nishina, T. Kato, *Accounts of Chemical Research* 54, 731–743 (2021).
- [3] Y. Saida, T. Gauthier, H. Suzuki, S. Ohmura, R. Shikata, Y. Iwasaki, G. Noyama, M. Kishibuchi, Y. Tanaka, W. Yajima, N. Godin, G. Privault, T. Tokunaga, S. Ono, S. Koshihara, K. Tsuruta, Y. Hayashi, R. Bertoni, M. Hada, *Nature Communications* 15, 4600 (2024).

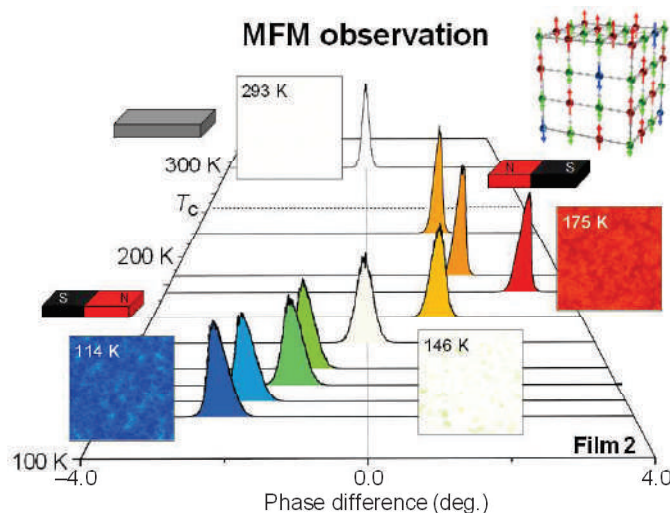
# Direct observation of Magnetic Domain and Magnetization Reversal on Prussian Blue-based magnetic film



Hiroko Tokoro

Department of Materials Science, Faculty of Pure and Applied Sciences,  
University of Tsukuba, Tsukuba, JAPAN  
E-mail: tokoro@ims.tsukuba.ac.jp

In molecule-based magnets, one can design magnetic properties, such as saturation magnetization, Curie temperature ( $T_C$ ), and coercive field, by selecting metal ions, radicals, and incorporated ligands. Herein, we study the magnetic domains of molecule-based magnets.<sup>1</sup> As target materials, two hexacyano-iron-chromate  $\text{Fe}_x\text{Cr}_{1-x}[\text{Cr}(\text{CN})_6]_{2/3} \cdot 5\text{H}_2\text{O}^2$  films ( $x = 0$ ; **Film 1** and  $x = 0.2$ ; **Film 2**) were prepared. The surface-magnetized states were measured using magnetic force microscopy. **Film 1** shows magnetic domain below  $T_C$  with a maze pattern. In **Film 2**, positive magnetic polarization appears below  $T_C$ , and magnetization becomes zero at a particular temperature ( $T_p = 146$  K), changing magnetic polarization to negative. Monte Carlo calculations implied that  $T_p$  is the compensation temperature. A direct observation of temperature-variable behaviour of compensation temperature has not been previously reported. This study can progress molecule-based magnets from magnetochemistry to magnetostatic engineering of bulk magnets, thereby opening a new field of molecule-based magnetostatic engineering.



## References

- [1] S. Nagashima, Y. Yahagi, M. Nishino, T. Yamaoka, K. Nakagawa, J. Wang, S. Ohkoshi, H. Tokoro *J. Am. Chem. Soc.*, **2023**, *145*, 22934.
- [2] S. Ohkoshi, A. Fujishima, K. Hashimoto, *J. Am. Chem. Soc.*, **1998**, *120*, 5349.

# Wastewater Treatment by Photocatalytic Process Using Photocatalyst-coated Materials

Krit Sirirerkratana,<sup>1</sup> Patiya Kemacheevakul,<sup>1,\*</sup> and  
Surawut Chuangchote<sup>2</sup>

<sup>1</sup> Department of Environmental Engineering, Faculty of Engineering, King  
Mongkut's University of Technology Thonburi, Bangkok, Thailand

<sup>2</sup> Department of Tool and Materials Engineering, Faculty of Engineering, King  
Mongkut's University of Technology Thonburi, Bangkok, Thailand

E-mail: [patiya.kem@kmutt.ac.th](mailto:patiya.kem@kmutt.ac.th)



In Thailand, there are many industrial factories. Each factory has different production processes which produce various types of wastewater. The color of wastewater comes from organic and inorganic pollutants. If the wastewater is not properly handled, it will affect humans and the environment.<sup>[2]</sup> The main purpose of this study is to reduce the color of wastewater by a photocatalytic process with TiO<sub>2</sub>-coated materials (*i.e.*, glass, ceramic tile, and stainless steel) using the sol-gel method under UV irradiations. The results showed that the optimum substrate and light source that yielded the highest color removal efficiency were TiO<sub>2</sub>-coated glass sheets under UV irradiation. The actual wastewater from the textile industry was tested in this study, and a high removal efficiency was obtained (92.2%). In addition, the reusability of the TiO<sub>2</sub>-coated glass sheet was also evaluated. It was found that the TiO<sub>2</sub>-coated glass sheet showed the same efficiencies for 5 times of reuse. This process can also decrease the time in the wastewater treatment process, which is not necessary to remove TiO<sub>2</sub> from the treated wastewater before releasing it into public water sources.

# Assessing the Efficacy of Natural rubber based functional methyl methacrylate binder for Lithium-ion batteries

Tian-Khoon Lee<sup>1,2,3\*</sup>, Nur Jafni Azaki<sup>1,2</sup>, Azizan Ahmad<sup>1,2,3</sup>, Nur Hasyareeda Hassan<sup>1,3</sup>



<sup>1</sup> Department of Chemical Sciences, Faculty of Science and Technology, Universiti Kebangsaan Malaysia, 43000 UKM Bangi, Selangor Malaysia.

<sup>2</sup>International Battery Center Sdn. Bhd, Incubator 3, Technology Park Malaysia, 57000 K.L., Malaysia

<sup>3</sup>Battery Technology Research Group (UKMBATT), Faculty of Science and Technology, Universiti Kebangsaan Malaysia, Bangi 43600, Selangor Darul Ehsan, Malaysia

Email: [tiankhoon@ukm.edu.my](mailto:tiankhoon@ukm.edu.my)

The binder plays a crucial role in batteries by providing adhesion for both active materials and substrates. Despite its importance, the binder has been less studied compared to cathodes, anodes, and electrolytes. In this study, a semicrystalline poly(methyl methacrylate) grafted natural rubber (MG49) was examined as a standalone rubber-based binder for graphite-based anodes in lithium-ion batteries. Three carbon additives—Super-P, C65, and KS6L—differing in particle size and shape were used as conducting agents in the graphite anodes. A thorough investigation of the physicochemical and electrochemical properties of these MG49-based electrodes was conducted. X-Ray diffraction analysis found that the MG49 based electrodes have shown good crystalline peaks which belong to the graphite comparing with PVDF and SBR+CMC based- electrodes. Similarly, the surface morphology and topography results of MG49-based electrodes and blank SBR+CMC have displayed a better distribution of graphite and Super P. This has led to enhance diffusion coefficient for the optimum electrode and a low of charge transfer resistance ( $R_{ct}$ ) of 153.4  $\Omega$  which is comparable to SBR/CMC (129.4  $\Omega$ ) and PVDF (570.5  $\Omega$ ). Equally, MG49 based electrode possessed a good reversibility redox reaction and low polarization. The super-P and C65-based electrodes showed good performance, whereas KS6L-based electrodes exhibited poor electrochemical results, attributed to their larger particle size and less optimal distribution. Battery performance evaluations indicated good cycling stability, with a capacity retention of 84.7% and a Coulombic efficiency maintained above 98.5%, highlighting the potential of MG49 rubber-based binders for lithium-ion battery applications.

## References

- [1] Nur, J.A.; Azizan, A.; Nur, H.H; Muhamma, A.A.M.A; Mohd, S.S.; Narges, A., Lee, T.K. *ACS Appl. Polym. Mater.* **2023**, *5*, 4953–4965
- [2] Khoon, L. T.; Fui, M.-L. W.; Hassan, N. H.; Su'ait, M. S.; Vedarajan, R.; Matsumi, N.; Bin Kassim, M.; Shyuan, L. K.; Ahmad, A. *J. Sol-Gel Sci. Technol.* **2019**, *90*, 665–675.
- [3] Li, S.; Liu, Y.-M.; Zhang, Y.-C.; Song, Y.; Wang, G.-K.; Liu, Y.X.; Wu, Z.-G.; Zhong, B.-H.; Zhong, Y.-J.; Guo, X.-D. *J. Power Sources* **2021**, 485,
- [4] Nowak, A. P.; Trzcinski, K.; Zarach, Z.; Li, J.; Roda, D.; Szkoda, M. *Applied Surface Science* **2022**, *606*, 154933.



# Chirality Engineering for Ultimate Carbon Nanotube Electronics



Daiming Tang<sup>1,2</sup>

<sup>1</sup> Research Center for Materials Nanoarchitectonics (MANA), National Institute for Materials Science (NIMS), Tsukuba, 305-0044, Japan.

<sup>2</sup> Institute of Pure and Applied Sciences, University of Tsukuba (Collaborative University), Tsukuba, 305-8571 Japan

E-mail: TANG.Daiming@nims.go.jp

Single-wall carbon nanotubes (SWCNTs) have a one-dimensional helical tubular molecular structure made up of hexagonally bonded  $sp^2$  carbon atoms. Conceptually, a SWCNT could be formed by rolling up a graphene sheet along a so-called chiral vector. The chirality of a SWCNT uniquely determines its atomic geometry and electronic structure, *i.e.* metallic or semiconducting. Currently, it is a great challenge to control the chirality of individual CNTs, hindering their applications in the promising energy-efficient nanotransistors.

We developed an in situ transmission electron microscopy (TEM) probing method to monitor the chirality transition and transport properties of individual CNTs. The chirality change is analyzed by nanobeam electron diffraction. The electronic transport properties are measured along with the structural changes, via fabricating transistors using the individual nanotubes as the suspended channels.<sup>[1]</sup> Controlled metal-to-semiconductor transition was realized to create nanotube transistors with a semiconducting nanotube channel covalently bonded between metallic nanotube source and drain. In addition, quantum transport at room temperature was demonstrated for the fabricated nanotube transistors with the channel length down to 2.8 nanometers.<sup>[2]</sup>

In this talk, I will discuss about the new understanding of the atomic mechanism and thermal properties of the CNT molecular junctions.<sup>[3]</sup> And an outlook of the ultimate CNT electronics enabled by the chirality engineering will be presented.<sup>[4]</sup>

## References

1. D.-M. Tang, D. G. Kvashnin *et al.*, *Ultramicroscopy* **2018**, 194, 108-116
2. D.-M. Tang, V. Erohin Sergey *et al.*, *Science* **2021**, 374, 1616-1620
3. O. Cretu, D.-M. Tang *et al.*, *Carbon* **2023**, 201, 1025-1029
4. D.-M. Tang, O. Cretu *et al.*, *Nature Reviews Electrical Engineering* **2024**, 1, 149-162

# Neutron Scattering as a Common Technique for Energy Material Researches



Tetsuya R. Yokoo<sup>1,2,3,4</sup>

<sup>1</sup>Graduated School of Pure and Applied Sciences, University of Tsukuba, 1-1-1 Tennodai, Tsukuba, Ibaraki 305-8573, Japan

<sup>2</sup>Institute of Materials Structure Science, High Energy Accelerator Research Organization, Oho 1-1 Tsukuba, Ibaraki 305-0801, Japan

<sup>3</sup>Materials and Life Science Division, J-PARC Center, Shirakata 2-4, Tokai, Ibaraki 319-1195, Japan

<sup>4</sup>Department of Advanced Studies, The Graduate University for Advanced Studies, SOKENDAI, Oho 1-1, Tsukuba, Ibaraki 305-0801, Japan

E-mail: tetsuya.yokoo@kek.jp

## Content

Neutron scattering is known to be one of powerful tools for investigating microscopic atomic/molecular positions and structures as well as their dynamical properties in material. In particular, an inelastic scattering enables us to see a dynamical motions of specific degrees of freedom in detail [1]. Even individual dynamics of a degree of freedom can be separately measured by utilizing so-called polarization analysis, which is quite new technique for pulsed neutron scattering [2]. POLANO is a recently constructed neutron spectrometer designed for the purpose of wide momentum ( $Q$ ) and energy ( $E$ ) range inelastic measurements with polarization analysis capability (see Fig. 1). Using all these neutron techniques, wide field in material science can be investigated as well as energy materials. In the talk, some typical applications, in particular the research field of quantum spin systems and energy materials will be presented.

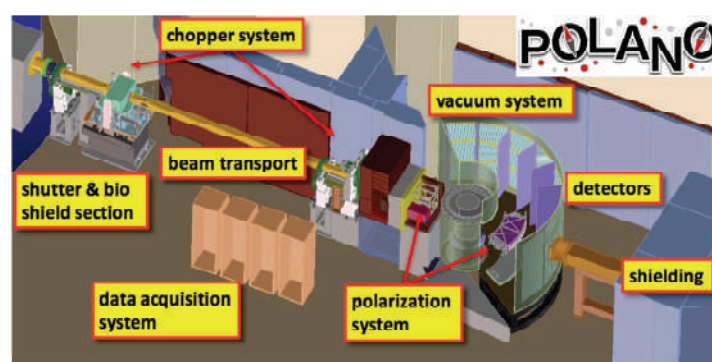


Fig. 1. Schematic 3D view of the POLANO.

## References

- [1] Materials and Life Science Experimental Facility (MLF) at the Japan Proton Accelerator Research Complex (J-PARC), MDPI Books, Quantum Beam Science (2019).
- [2] T. Yokoo, *et. al.*, EPJ Web of Conferences **83**, 03018 (2015).

# Natural Rubber Foam as Potential Blunt Trauma Pad for Soft Body Armor Application

Resty Maysepheny Hernawati,<sup>1</sup> Onny Aulia Rachman,<sup>2</sup> Steven,<sup>2</sup> and Mardiyati<sup>2</sup>

<sup>1</sup> Textile Engineering Department, Politeknik STTT Bandung, Indonesia

<sup>2</sup> Faculty of Mechanical and Aerospace Engineering, Institut Teknologi Bandung, Indonesia

E-mail: resty.maysepheny.h@gmail.com



Indonesia's lack of ability to independently produce blunt trauma pads (BTP) for soft body armor underlies this research. Various selected materials continue to be developed to manufacture BTP which is designed to mitigate and reduce blunt force trauma, including natural rubber. This research aims to manufacture alternative BTP made from natural rubber material. The natural rubber compound made by adding sodium bicarbonate using a double roll mill machine was molded using compression molding with or without pressing. The resulting rubber foam was then tested for morphology, foam density, and energy absorption using SEM and a rebound resilience tester. The result showed that natural rubber foam-based BTP has the morphology of open-cell foam and energy absorption of 30 - 35%. These findings suggest that BTP based on natural rubber and sodium bicarbonate can be potentially an alternative BTP in Body Armor systems.

## References

- [1] Critchley, B. R., et al. *Advanced Engineering Materials* **2013**, 1–6.
- [2] Cannon, L., *Journal of the Royal Army Medical Corps* **2001**, 147, 87–96.
- [3] Charoeythornkhajhornchai, P., et al. *Journal of Cellular Plastics* **2017**, 53(3), 287–303.
- [4] Harnnarongchai, W. et al. *Applied Mechanics and Materials* **2015**, 804(1), 25–29.
- [5] Obi, B. E. *Polymeric Foams Structure-Property-Performance*, Elsevier Inc. **2017**, 189–205.
- [6] Pinto, J.,;Solo, E., Rodriguez-perez, et al, *Journal of Cellular Plastics* **2013**, (7).
- [7] Roberts, J. C., et al. *The Journal of TRAUMA Injury, Infection, and Critical Care* **2001**, 62(5), 1127–1133.

# Heterogeneous Catalysis Contributing to a Carbon-Neutral Society

Junji Nakamura

*International Institute for Carbon-Neutral Energy Research (I2CNER), Kyushu University, 744 Motoooka Nishi-Ku, Fukuoka, 819-0395 Japan*

E-mail: nakamura.junji.700@m.kyushu-u.ac.jp



Scientific research has confirmed that climate change is driven by anthropogenic CO<sub>2</sub> emissions. To combat this, urgent measures are required to capture CO<sub>2</sub> at emission sources and implement renewable energy solutions efficiently on a global scale, necessitating collaboration among scientists, engineers, and policymakers. One key solution is the conversion of captured CO<sub>2</sub> into an energy carrier. Among various options, methanol stands out as the most suitable. This conclusion is the result of 30 years of my dedicated research on methanol synthesis catalysts from CO<sub>2</sub>. Catalytic chemistry plays a pivotal role in producing sustainable fuels, offering a viable alternative to cheap fossil fuels.

In this presentation, I will briefly explain why methanol is an effective energy carrier. True innovation lies in technology that can be applied in any country. Methanol synthesis from CO<sub>2</sub> is globally feasible, using inexpensive copper as a catalyst. The energy required for this process, conducted at 250°C and 50 atm, is relatively low. Furthermore, methanol presents advantages such as easy handling, compatibility as a fuel for internal combustion engines and fuel cells, and utility in chemical processes like the MTO (methanol to olefin) process. Most importantly, methanol is an ideal energy carrier that promotes CO<sub>2</sub> recycling.

Next, I will introduce useful catalytic mechanisms that contribute to carbon neutrality [1,2]. The first mechanism involves CO<sub>2</sub> activation. When the bending mode of the linear CO<sub>2</sub> molecule is excited, its acidity increases due to a reduction in the LUMO level. This allows CO<sub>2</sub> to react with hydrogen on the copper surface without the need for catalyst heating [1]. The second mechanism involves the role of pyridinic nitrogen in nitrogen-doped carbon catalysts [3,4]. Pyridinic nitrogen readily reacts with protons to form NH<sup>+</sup> species. Upon reduction, an electron enters the π\* orbital, forming a radical electron. Oxygen molecules then react with these radical electrons. This O<sub>2</sub> adsorption and NH<sup>+</sup> reduction occur in a coupled manner, reducing the potential corresponding to the O<sub>2</sub> adsorption energy. Lastly, I will introduce the mixed-potential-driven catalytic mechanism. When different metal components within a single catalyst particle come into contact with an electrolyte, they form nanoanode and nanocathode regions, creating a short-circuit state. The net free energy from anodic and cathodic reactions is converted into an overpotential that drives the reaction, similar to corrosion phenomena. I will present the theoretical framework of this mixed-potential-driven catalysis, including catalytic activity parameters [5].

## References

- [1] J. Quan, F. Muttaqien, T. Kondo, T. Kozarashi, T. Mogi, T. Imabayashi, Y. Hamamoto, K. Inagaki, I. Hamada, Y. Morikawa, J. Nakamura, *Nature Chem.* 11, 722-729 (2019).
- [2] Kotaro Takeyasu, Yasutaka Sawaki, Takumi Imabayashi, Septia Eka Marsha Putra, Harry Handoko Halim, Jiamei Quan, Yuji Hamamoto, Ikutaro Hamada, Yoshitada Morikawa, Takahiro Kondo, Tadahihiro Fujitani, and Junji Nakamura, *J.Am.Chem.Soc.*, 144, 12158-12166 (2022).
- [3] D. Guo, R. Shibuya, C. Akiba, S. Saji, T. Kondo, J. Nakamura, *Science* 351, 6271, 361-365 (2016).
- [4] K. Takeyasu, M. Furukawa, Y. Shimoyama, S. K. Singh, J. Nakamura, *Angew. Chem. Int. Ed.*, 60 (10), 5121-5124 (2020).
- [5] Mo Yan, Nuning Anugrah Putri Namari, Junji Nakamura, and Kotaro Takeyasu, *Communications Chemistry*, 7, 69 (2024).

# Research on manufacturing high coercivity hard magnetic materials



Pham Thi Thanh<sup>1,2</sup>, Nguyen Huy Ngoc<sup>1,2</sup>, Truong Viet Anh<sup>1</sup>, Nguyen Hai Yen<sup>1,2</sup>, Kieu Xuan Hau<sup>1,2</sup>, Nguyen Mau Lam<sup>3</sup>, Nguyen Van Duong<sup>3</sup>, Jung-Goo Lee<sup>4</sup>, Nguyen Huy Dan<sup>1,2,\*</sup>

<sup>1</sup>*Institute of Materials Science, Vietnam Academy of Science and Technology, 18 Hoang Quoc Viet, Ha Noi, Viet Nam*

<sup>2</sup>*Graduate University of Science and Technology, Vietnam Academy of Science and Technology, 18 Hoang Quoc Viet, Ha Noi, Viet Nam*

<sup>3</sup>*Hanoi Pedagogical University 2, 32 Nguyen Van Linh, Xuan Hoa, Phuc Yen, Vinh Phuc, Viet Nam*

<sup>4</sup>*Korea Institute of Materials Science, 797 Changwondaero, Seongsan-gu, Changwon, Gyeongnam, 51508, South Korea*

\*E-mail: dannh@ims.vast.ac.vn

Hard magnetic materials, so-called permanent magnets, are widely applied in practice such as motors, generators, control devices, computers, magnetic resonance imaging machines... Many applications require materials with high coercivity to improve energy conversion efficiency. This report presents our results of research on fabrication technology to enhance coercivity for some hard magnetic materials including rare earth and rare earth-free hard magnetic materials (Nd-Fe-B, Mn-Bi, Co-Zr...). The produced high coercivity hard magnetic materials were tested for application in motors and generators and the results showed that the performance of the devices were significantly improved.

# Visible light-driven photocatalyst for synthetic dyes remediation



Arie Wibowo<sup>1,2</sup>

<sup>1</sup>Materials Science and Engineering Research Group, Faculty of Mechanical and Aerospace Engineering, Institut Teknologi Bandung, Bandung 40132, Indonesia,

<sup>2</sup>Research Center for Nanoscience and Nanotechnology, Institut Teknologi Bandung, Bandung 40132, Indonesia.

E-mail: [ariewibowo@itb.ac.id](mailto:ariewibowo@itb.ac.id)

Photocatalytic degradation is one of attractive strategies to eliminate persistent organic pollutants (POPs) from water stream because it utilizes the abundant solar energy source to generate powerful hydroxyl radical to degrade POPs and produce H<sub>2</sub>O and CO<sub>2</sub> as the final degradation products. TiO<sub>2</sub> is one of the popular photocatalyst because it is photochemically stable, non-toxic, commercially available, and cheap. However, TiO<sub>2</sub> is not efficient enough to harvest energy from sunlight due to its high bandgap (3.22 eV) so that it can only absorb energy in UV light region, which is only 5% of sunlight irradiation. Here, we report fabrication of black TiO<sub>2</sub> through microwave heating to decrease the bandgap of TiO<sub>2</sub> [1], utilization of graphitic carbon nitride [2] and ZnO-Fe<sub>2</sub>O<sub>3</sub> heterojunction [3] as visible light-driven photocatalyst to improve its performance in visible-light region of solar energy. Furthermore, we also report several efforts to tackle weaknesses of TiO<sub>2</sub> such as fast recombination, high density and particle agglomeration.

## References

- [1] R. Rachmantyo, A. A. Afkauni, R. Reinaldo, L. Zhang, A. Arramel, M. D. Birowosuto, **A. Wibowo\*** and H. Judawisastra\*, "Fabrication of Black TiO<sub>2</sub> Through Microwave Heating for Visible Light-driven Photocatalytic Degradation of Rhodamine 6G", *Reaction Chemistry and Engineering*, **2024**, *accepted*.
- [2] I. J. Budiarso, S. Fujita, S. Saito, H. Judawisastra, K. Takeyasu, and **A. Wibowo\***, "Facile Fabrication of Graphitic Carbon Nitride/Polydopamine/Polyurethane Foam as Floating Photocatalyst for Synthetic Dye Remediation", *Reaction Chemistry and Engineering*, **2024**, *Advance Article* (DOI: 10.1039/D4RE00193A)
- [3] W. J. Budiman, A. Hardiansyah, V. A. Dabur, N. Yudasari, Isnaeni, L. J. Diguna, D. Kowal, M. D. Birowosuto, and **A. Wibowo\***, "Fabrication of reduced graphene oxide/zinc oxide/iron oxide from zinc dross for photocatalytic degradation of synthetic dye under visible light irradiation", *International Journal of Environmental Science and Technology*, under review.

# Molecular Interactions of Zinc-based Metal-Organic Framework Cluster and 1-Butyl-3-Methylimidazolium Chloride: Structural and Density Functional Theory Study



Hayyiratul Fatimah Mohd Zaid<sup>1</sup>, and Mohd Faridzuan Majid<sup>2</sup>

<sup>1</sup>Chemical Engineering Department, Universiti Teknologi PETRONAS, 32610, Bandar Seri Iskandar, Perak, Malaysia, <sup>2</sup>Fundamental and Applied Sciences Department, Universiti Teknologi PETRONAS, 32610, Bandar Seri Iskandar, Perak, Malaysia, <sup>1,2</sup>Center of Innovative Nanostructures and Nanodevices (COINN), Universiti Teknologi PETRONAS, 32610, Bandar Seri Iskandar, Perak, Malaysia

E-mail: [hayyiratul.mzaid@utp.edu.my](mailto:hayyiratul.mzaid@utp.edu.my)

A metal-organic framework (MOF) is a crystalline compound characterized by a three-dimensional structure composed of organic ligands and metal ions. The interconnection between these organic ligands and metal ions forms a network of coordination polymers, creating adjustable voids with a notably large total surface area. This distinctive feature of MOFs allows them to engage in host-guest interactions with small molecules, such as ionic liquids (ILs), which have the capacity to modify phase behavior and enhance performance in energy storage systems. However, comprehending the molecular interactions between MOFs and ILs has proven challenging due to the limited number of computational studies in this area. In this investigation, we employed a combined experimental and computational approach to analyze the structural parameters of a specific zeolitic imidazolate framework (ZIF-L) and 1-butyl-3-methylimidazolium chloride ([BMIM][Cl]). Upon loading IL, observable distortions in bond lengths and bond angles occurred within the ligand-metal region, attributed to an increase in electron density surrounding the framework. This perturbation disrupted the tetrahedral symmetry, signifying a flexible MOF system when impregnated with IL. Furthermore, an augmentation in molecular orbital energy, resulting from the confinement of IL, contributed to the stabilization of this hybrid structure. The findings from our molecular interactions study suggest that ZIF-L and [BMIM][Cl] hold promise as potential candidates for electrolyte materials in energy storage systems.

*Keywords - metal-organic framework, ionic liquid, zeolitic imidazolate framework, density functional theory, structural parameters, intermolecular forces.*

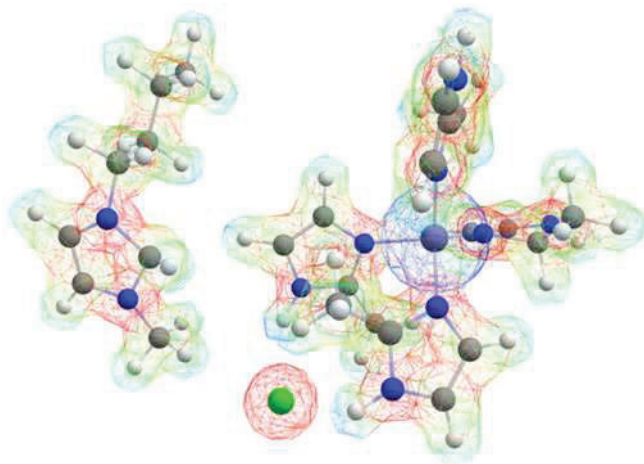


Figure 1. The molecular electrostatic potential isosurface of ZIF-L MOF cluster and [BMIM][Cl]. Red color represents the attraction of the atom by the concentrated electron density in the molecules, blue color represents the repulsion of the atom by the atomic nuclei in regions where low electron density can be found and the nuclear charge is incompletely shielded.

# Starrydata: A Data-Curation Project from Material Property Plots on Published Papers

Yukari Katsura,<sup>1,2,3</sup>

<sup>1</sup>*National Institute for Materials Science, Tsukuba, Japan*

<sup>2</sup>*University of Tsukuba, Tsukuba, Japan*

<sup>3</sup>*RIKEN, Tokyo, Japan*

E-mail: [KATSURA.Yukari@nims.go.jp](mailto:KATSURA.Yukari@nims.go.jp)



Experimental datasets for materials informatics are difficult to obtain. In the papers of material sciences, most of the experimental data are provided as plot images. A typical plot image contains both the good samples and the other samples for comparison. The original experimental data can be extracted by tracing the plots. Such scientific data can be shared freely, without violating the copyrights of the publishers. We have developed Starrydata web system [1], an open database of experimental materials data collected by tracing plot images in literature. This web system allows users, including our data curators to share experimental data, with figure captions, sample information and other short explanatory text. The data on Starrydata are open to the public, and it can be used freely both for commercial and non-commercial purposes.

As an example of data collection using Starrydata, we introduce our dataset collected temperature dependences of thermoelectric properties from plot images in published papers. This thermoelectric materials database is our largest data collection project on Starrydata, containing curves obtained from ~50,000 physical samples reported in ~10,000 papers, with chemical compositions and fabrication methods when available. Data collection by the human curators were accelerated by improving the data digitizer, and implementing an automatic retrieval system of sample information from given text, by using Large Language Models (LLM).

## Acknowledgments:

This project has received support from the Japan Science and Technology Agency (JST) CREST grant number JPMJCR19J1, KAKENHI JP19H05818, JP19H05818, JP19H05820, the Kazuchika Okura Memorial Foundation, as well as fundings from collaborating companies.

## References:

[1] Yukari Katsura et al., *Sci. Technol. Adv. Mater.*, 20:1, 511-520. URL: <https://www.starrydata2.org/>



# Micrometer-Scale Optical Web Made of Spider Dragline Fibers with Optical Gate Operations

Hendra<sup>1,2</sup>, Hiroshi Yamagishi<sup>2</sup>, Wey Yih Heah<sup>2</sup>, Ali D. Malay<sup>3</sup>, Keiji Numata<sup>3</sup>, and Yohei Yamamoto<sup>2</sup>



<sup>1</sup>Department of Textile Engineering Politeknik STTT Bandung  
Jakarta Street No. 31, Bandung 40272, Indonesia.

<sup>2</sup>Faculty of Pure and Applied Sciences and Tsukuba Research Center for Energy Materials Science (TREMS) University of Tsukuba 1-1-1 Tennodai, Tsukuba, Ibaraki 305–8573, Japan

<sup>3</sup>Biomacromolecules Research Team RIKEN Center for Sustainable Resource Science 2-1 Hirosawa, Wako-shi, Saitama 351-0198, Japan

<sup>4</sup>Department of Materials Chemistry Kyoto University Kyotodaigaku-Katsura, Nishikyo-ku, Kyoto 615–8510, Japan.

Dragline silk fibers produced by spiders are a masterpiece structural protein that is durable even in the wild conditions. Dragline silk fibers are known to have excellent mechanical toughness and flexibility and further possess optical transparency, which are highly promising as textiles, sensors, and optical devices. Here, the authors show that the dragline silk microfibers act as good optical waveguides with the optical loss coefficient as small as 0.03 decibel per micrometer. The light transportation in the dragline silk fiber is performed by fluorescence energy transfer between two microspheres located on a suspended dragline silk microfiber. By utilizing a micromanipulation equipment, micrometer-scale spider web-like structures are fabricated. The experimentally observed optical waveguiding properties of the weaves match well with simulation results using simple mathematical models. Furthermore, optical logic gate operations are demonstrated using photoswitchable micro sphere resonators attached on the dragline fibers.

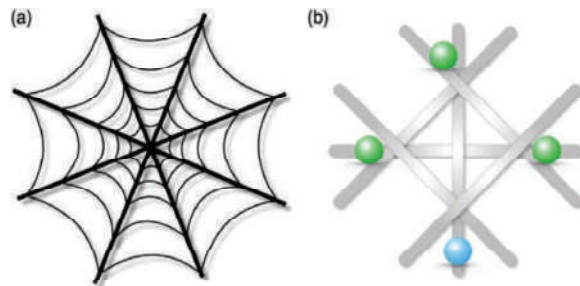


**Figure 1.** Schematic representations of: a) the spider orb-web and b) micrometer-scale spider web using dragline silk optical fibers. In (b), one blue-fluorescent microsphere and three green-fluorescent microspheres are drawn, which are represented as an emitter and detectors, respectively. *Adv. Optical Mater.* **2022**, 2202563

## References

- [1]. Hendra, A. Takeuchi, H. Yamagishi, O. Oki, M. Morimoto, M. Irie, Y. Yamamoto, *Adv. Funct. Mater.* **2021**, 31, 2103685.
- [2]. D. Okada, T. Nakamura, D. Braam, T. D. Dao, S. Ishii, T. Nagao, A. Lorke, T. Nabeshima, Y. Yamamoto, *ACS Nano* **2016**, 10, 7058.
- [3]. A. D. Malay, T. Suzuki, T. Katashima, N. Kono, K. Arakawa, K. Numata, *Sci. Adv.* **2020**, 6, eabb6030.
- [4]. S. Kushida, D. Braam, T. D. Dao, H. Saito, K. Shibasaki, S. Ishii, T. Nagao, A. Saeki, J. Kuwabara, T. Kanbara, M. Kijima, A. Lorke, Y. Yamamoto, *ACS Nano* **2016**, 10, 5543.

# Diamond Nonlinear Photonics — Realizing Spatiotemporal Extreme Sensing Using Diamonds

Muneaki Hase<sup>1</sup>, Daisuke Sato<sup>1</sup>, Junjie Guo<sup>1</sup>, Takuto Ichikawa<sup>1</sup>,  
Dwi Prananto<sup>2</sup>, Toshu An<sup>2</sup>, Paul Fons<sup>3</sup>, Shoji Yoshida<sup>1</sup>, and  
Hidemi Shigekawa<sup>1</sup>

<sup>1</sup> University of Tsukuba, Tsukuba, Japan

<sup>2</sup> Japan Advanced Institute of Science and Technology, Nomi, Ishikawa, Japan

<sup>3</sup> Keio University, Yokohama, Kanagawa, Japan

E-mail: mhase@bk.tsukuba.ac.jp



The integration of light and materials technology is a key to the creation of innovative sensing technologies. Sensing of electric and magnetic fields, and temperature with ultra-sensitive and high spatial-temporal resolutions have been considered as mandatory task for developing next generation nanometer scale quantum devices.<sup>[1,2]</sup> In particular, color centers in diamond crystals have attracted potential applications owing to their characteristic quantum states, although they require metallic contact to apply microwave external field.<sup>[3]</sup> Here, we build on ultrafast diamond nonlinear photonics sensor to access a surface electric field, where electro-optic sensor based on nitrogen-vacancy centers in a diamond nanotip breaks the spatial-limit of ultrafast pump-probe technique.<sup>[4-7]</sup> The 10-fs near infrared optical pulse modulates surface electric field on a prototypical 2D transition metal dichalcogenide, and we monitor the real time dynamics of local electric field with nanometer-femtosecond spatio-temporal resolutions. Our nanoscopic technique will provide a new horizon of the sensing of advanced nano materials with diamond color centers.

## References

- [1] Wu, Q.; Zhang, X. -C. *Appl. Phys. Lett.* **1996**, *68*, 1604–1606.
- [2] Taylor, J. M. *et al. Nature Phys.* **2008**, *4*, 810–816.
- [3] Pelliccione, M. *et al. Nature Nanotech.* **2016**, *11*, 700–705.
- [4] Abulikemu, A.; Kainuma, Y.; An, T.; Hase, M. *ACS Photon.* **2021**, *8*, 998–993.
- [5] Sakurai, R.; Kainuma, Y.; An, T.; Shigekawa, H.; Hase, M. *APL Photon.* **2022**, *7*, 066105.
- [6] Ichikawa, T.; Abulikemu, A.; Hase, M. *Phys. Rev. Applied.* **2023**, *19*, 024054.
- [7] Ichikawa, T.; Guo, J.; Fons, P.; Prananto, D.; An, T.; Hase, M. *Nature Commun.* **2024**, *15*, 7174.

# **Student Speaker**

# Synthesis of Terminal-Modified Semiconducting Polymers and Elucidation of the Effect of Terminal Groups

Ziwei Hu<sup>1</sup>, Takeshi Yasuda<sup>2</sup>, Takaki Kanbara<sup>1</sup>, Junpei Kuwabara<sup>1</sup>.

<sup>1</sup> Institute of Pure and Applied Sciences, University of Tsukuba (Univ. of Tsukuba), 1-1-1 Tennodai, Tsukuba 305-8573, Japan.

<sup>2</sup> Research Center for Macromolecules and Biomaterials, National Institute for Materials Science (NIMS), Ibaraki 305-0047, Japan

E-mail: s2320403@u.tsukuba.ac.jp



In recent years, organic semiconductors have gained widespread use, with their lightweight and flexibility attracting attention as next-generation materials. However, the complexity of synthesis and the high cost of semiconducting polymers hinder the expansion of their practical applications. This research utilizes a direct arylation polycondensation reaction, a convenient and environmentally friendly synthesis method,<sup>[1]</sup> to efficiently synthesize semiconducting polymers. To ensure the functionality of semiconducting polymers, a well-defined structure is crucial, including the absence of structural defects such as homocoupling or cross-linking, and the controlled terminal structures. In this research, we focused particularly on the terminal effect.

To achieve this goal, I first synthesized polymers with the same main chain and similar molecular weight but with different terminals<sup>[2]</sup> (**P1a**, **P1b**, and **P1c**, Figure 1).

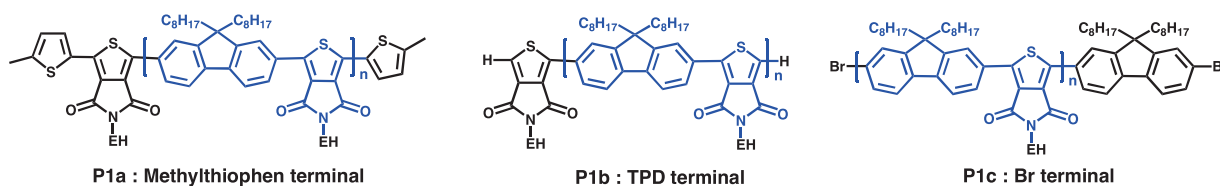


Figure 1 Polymers with different terminals

Table 1

Polymer	Thin film properties		OLED properties	
	PLQY(%)	HOMO (eV)	Max brightness (cd /m <sup>2</sup> )	Max EQE (%)
P1a	22	-6.2	9760	1.05
P1b	27	-6.2	9740	1.25
P1c	28	-6.2	2970	1.01

Next, we investigated the OLED characteristics (Table 1). **P1c** exhibited the worst device performance despite having the highest photoluminescence quantum yield (PLQY) in the film state. As the device with **P1c** shows high resistance (Figure 2), the Br terminals may act as carrier trapping sites. The device with **P1b** shows highest performance due to the high PLQY and no adverse effect of the terminals. Although the terminals accounted for only 2% of the polymer by weight, the terminals caused a significant difference (around 20%) in the external quantum efficiency (EQE) of the devices.

This research has provided valuable insights into the future improvement of organic devices.

## References

[1] J. Kuwabara, T. Kanbara, Bull. Chem. Soc. Jpn., 2019, 92, 152-161. [2] Ziwei HU, et al, 73rd Annual Meeting of the Society of Polymer Science, 2024, 2Pb060.

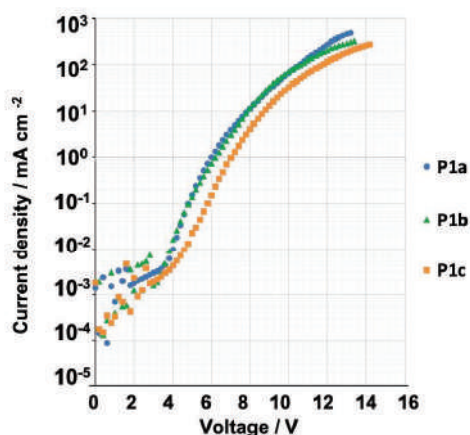


Figure 2 Current density (J) - voltage (V) characteristics ITO/PEDOT:PSS/PVK/ Polymer/TPBi/LiF/Al

# Ambient-air processed perovskite CsPbBr<sub>3</sub> thin films for solar cell applications



Xorell Ivanov Monov<sup>1</sup>, Prima Fitri Rusliani<sup>1</sup>, Shobih<sup>2</sup>, Natalita

Maulani Nursam<sup>2</sup>, Brian Yulianto<sup>1</sup>, Wilman Septina<sup>2\*</sup>

<sup>1</sup>Bandung Institute of Technology (ITB), Indonesia,

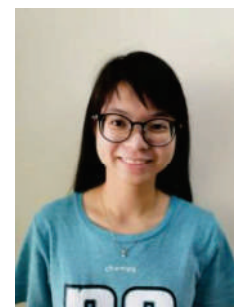
<sup>2</sup>National Research and Innovation Agency (BRIN), Indonesia

*E-mail: sorelmonov@gmail.com*

Perovskite solar cells (PSCs) have gotten a lot of attraction as a viable replacement for Silicon based solar cells due to its high efficiency reaching over 25% in 2023. Indonesia is a country located in the tropical region and has a high relative humidity. Halide-based PSCs, which has a structure of ABX<sub>3</sub> (A= MA, FA, Cs B = Pb, Sn, Bi, X = I, Br, Cl), have a problem with its stability in high humidity, which is a big problem in fabricating PSCs in Indonesia. MAPbI<sub>3</sub> PSCs are an example of a popular halide-based PSCs which has high efficiency but are usually fabricated in an inert gas environment such as nitrogen to overcome the problem with the high humidity environments, which increases cost in fabrication. CsPbBr<sub>3</sub> based PSCs are more stable towards moisture compared to MAPbI<sub>3</sub> and can be fabricated without the use of an inert gas environment which reduced the cost in fabrication. In this report, we show a fabrication of planar based CsPbBr<sub>3</sub> PSCs in a high-humidity ambient air (relative humidity 50-80%) with the use of SnO<sub>2</sub> as the electron transport layer (ETL) and a carbon-based electrode. CsPbBr<sub>3</sub> films were fabricated by multi-step spin coating of PbBr<sub>2</sub> and CsBr ink, respectively, followed by annealing in air at 250°C for 30 min. Maximum efficiency of 5.25%, Jsc of 4.99 mA/cm<sup>2</sup>, Voc of 1461.4 mV and fill factor (FF) of 72% was achieved by optimizing the fabrication processes. In addition, CsPbBr<sub>3</sub> powder has also been synthesized which can be used as a precursor to larger scalable deposition method such as thermal evaporation, drop casting and slot die coating to create larger area cells.

Keywords: perovskite solar cells, ambient air, CsPbBr<sub>3</sub>, SnO<sub>2</sub>

# Synthesis and Characteristics of Non-Edible Jatropha Oil Based Polyurethane Acrylate (PUA) Gel Polymer Electrolyte For Dye Sensitized Solar Cell Application



K.L. Chai,<sup>1</sup> Tian Khoon Lee<sup>1,4</sup>, Mohd Sukor Su'ait<sup>2</sup> and Azizan Ahmad<sup>1,3,4</sup>

<sup>1</sup>*Department of Chemical Science, Faculty of Science and Technology, Universiti Kebangsaan Malaysia, Bangi, 43600, Selangor Darul Ehsan, Malaysia*

<sup>2</sup>*Solar Energy Research Institute (SERI), Universiti Kebangsaan Malaysia, Bangi 43600, Selangor Darul Ehsan, Malaysia*

<sup>3</sup>*Department of Physics, Faculty of Science and Technology, Airlangga University (Campus C), Mulyorejo Road, Surabaya 60115, Indonesia*

<sup>4</sup>*Battery Technology Research Group (UKMBATT), Faculty of Science and Technology, Universiti Kebangsaan Malaysia, Bangi, 43600, Selangor Darul Ehsan, Malaysia*

E-mail: [tiankhoon@ukm.edu.my](mailto:tiankhoon@ukm.edu.my)

Solid and liquid electrolytes have opposing strengths: solid electrolytes offer durability and wide operating temperatures but lower ionic conductivity, while liquid electrolytes have better conductivity but risk leakage and corrosion. Gel polymer electrolytes (GPE) aim to combine the advantages of both. In this study, Jatropha oil-based polyurethane acrylate (PUA) GPEs were enhanced with varying amounts of salts and ionic liquids for dye-sensitized solar cells (DSSCs). The best-performing GPE contained 6% BMII ionic liquid, achieving an ionic conductivity of  $4.17 \times 10^{-4} \text{ S cm}^{-1}$  and a solar conversion efficiency of 5.72%. This demonstrates PUA-based electrolytes' potential for DSSC applications.

## References

- [1] Arof, A. K., Amirudin, S., Yusof, S. Z., & Noor, I. M. *Physical Chemistry Chemical Physics* **2014**, 16(5), 1856–1867.
- [2] Bandara, T. M. W. J., DeSilva, L. A., Ratnasekera, J. L., Hettiarachchi, K. H., Wijerathna, A. P., Thakurdesai, M., Preston, J., Albinsson, I., & Mellander, B. E. *Renewable and Sustainable Energy Reviews* **2019**, 103, 282–290.
- [3] Careem, M. A., Noor, I. S. M., & Arof, A. K. *Polymer Electrolytes: Characterization Techniques and Energy Applications* **2020**, 23–64.

# Doped NaSICON-Type Solid Electrolytes for Sodium-Ion Batteries from Scalable Spray-Flame Synthesis

Mohammed-Ali Sheikh<sup>1</sup> Hartmut Wiggers<sup>1,2</sup>

<sup>1</sup> Institute for Energy and Materials Processes – Reactive Fluids,  
University of Duisburg-Essen, Duisburg, Germany

<sup>2</sup> Center for Nanointegration Duisburg-Essen (CENIDE), Duisburg, Germany  
E-mail: mohammed-ali.sheikh@uni-due.de



Solid-state batteries are increasingly the focus of current research because they offer greater safety and capacity compared to battery cells with liquid electrolytes. In this context, sodium-ion batteries (SiB) are also of particular interest, as Na solid-electrolytes generally have higher ionic conductivities than Li-based ones. In addition, the raw materials for the electrodes are less critical and cost-effective. One of the best studied NaSICON materials is  $\text{Na}_3\text{Zr}_2\text{Si}_2\text{PO}_{12}$  (NZSP) with a high ionic conductivity in the order of  $10^{-4}$ – $10^{-3}$   $\text{S}\cdot\text{cm}^{-1}$  at room temperature [1, 2].

We present the spray flame synthesis (SFS) as a new approach for the synthesis of nanosized NaSICON materials. Recent studies have shown that sintering of nanoparticulate NZSP precursors enables high homogeneity and phase purity to be achieved at comparatively low temperatures due to their high specific surface area and nanoscale mixing [3].

The materials are characterized by transmission electron microscopy (TEM), X-Ray diffraction (XRD) and Raman-Spectroscopy for structural and morphological investigation. Ionic conductivities of sintered pellets are measured by impedance spectroscopy. The pristine powders consist of around 5 nm crystalline  $\text{ZrO}_2$  particles, uniformly covered with a mixed oxide shell. After a short annealing step for 1h at  $1000^\circ\text{C}$ , this mixture can be converted almost quantitatively into the desired NZSP phase. Moreover, aliovalent dopants were successfully added for the synthesis of  $\text{Na}_{3+2x}\text{A}_x\text{Zr}_{2-x}\text{Si}_2\text{PO}_{12}$  with  $\text{A} = \text{Mg}$  or  $\text{Ca}$ . Pressed pellets of Mg-doped NZSP sintered at  $1100^\circ\text{C}$  show a surprisingly high ionic conductivity of up to  $9.3\cdot 10^{-4}$   $\text{S}\cdot\text{cm}^{-1}$ .

In conclusion, spray flame synthesis is an elegant and promising possibility for the scalable production of sodium-ion solid electrolytes, which also holds great potential, especially with regard to further improvement of ionic conductivity through targeted doping.

## References

- [1] Goodenough, J.B. et al., Mater.Res.Bull. **1976**, 11, 203
- [2] Narayanan, S. et al., Solid State Ion. **2019**, 331, 22
- [3] Jalalian-Khakshour, A. et al. J.Mater.Sci. **2019**, 55, 2291

# Development of automatic synthesis system for materials research

Wei-Sheng Wang<sup>1,2</sup>, Kensei Terashima<sup>2</sup>, Yoshihiko Takano<sup>1,2</sup>

<sup>1</sup>Graduated School of Pure and Applied Sciences, University of Tsukuba,  
1-1-1 Tennodai, Tsukuba, Ibaraki 305-8573, Japan

<sup>2</sup>National Institute for Materials Science, Materials Information Technology  
Station 1-2-1 Sengen, Tsukuba, Ibaraki Japan



Email: WANG.Wei-Sheng@nims.go.jp

The rise of materials informatics and its ability to predict material properties through computational modeling has spurred a demand for robust experimental validation. Automation using robots has emerged as a promising approach to expedite this validation process. Recent advancements in robotic systems for material synthesis have been documented in diverse areas, including liquid-phase materials[1], thin-film[2], and solid-state synthesis[3]. While robots excel at repeatable movement, achieving consistent final products remains paramount for both process optimization and obtaining materials with desired properties through Bayesian optimization techniques.

This work reports the development of an automated arc-melting system (Figure 1) for the synthesis of alloys and demonstrates its successful application in the production of several superconducting samples. The system is built upon the Robot Operating System (so-called ROS2), a flexible and scalable framework for developing robust and reliable robotic applications. ROS2 provides a structured communication architecture between various system components, including the robotic arm, vacuum chamber, arc-melting furnace, and sensors. This modular design facilitates the integration of additional components and the adaptation of the system for diverse experimental setups.

The system's basic construction is nearing completion, with successful testing of key hardware components (cooling water flow, air/Ar pressure, and electric arc control). The process begins by initiating the arc on Zr stored as an oxygen trap (Figure 2), followed by its migration towards the raw material mixture. After cooling, the material is flipped and re-melted for ensuring the reaction and the homogeneity of the product.

Despite the apparent simplicity of the process, numerous parameters can be optimized, including discharge power and distance, approach speed, arc radius, and the number of melting cycles. Leveraging the system, we have successfully synthesized several samples (Figure 3), demonstrating its potential for high-throughput and reproducible production of superconducting alloys. The developed system can be quite useful for seeking new superconducting materials with enhanced properties and broader applications.



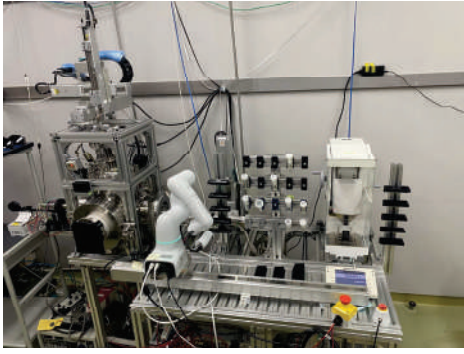


Figure 1: Automated arc-melting system.

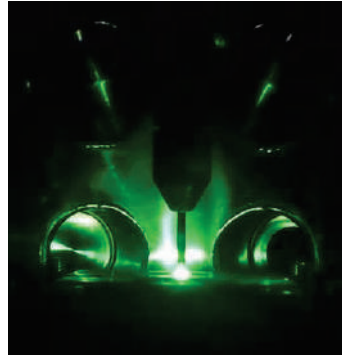


Figure 2: Arc-melting in automatic motion.

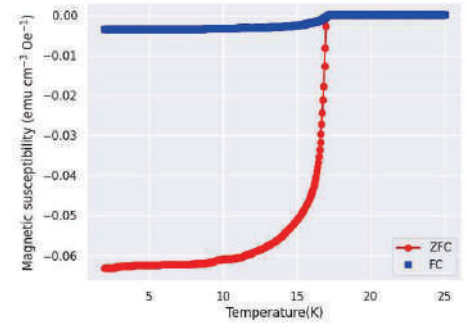


Figure 3: Magnetization data under 10 Oe, for  $Nb_3Al$  sample synthesized by the automated arc-melting system.

## References:

- [1] Benjamin Burger et al. In: *Nature* 583, 237 (2020).
- [2] Ryota Shimizu et al. In: *APL Materials* 8, 11 (2020).
- [3] Nathan J Szymanski et al. In: *Nature* 624, 86 (2023).

# Study On A Potential Of PVA/AgNO<sub>3</sub> Nano Fiber As Anti Bacterial Materials Prepared By Electrospinning For Medical Application



Hendra,<sup>1</sup> Syahla Andini Putri<sup>2</sup>

<sup>1</sup> Textile Engineering Department, Politeknik STTT Bandung, Bandung, Indonesia

<sup>2</sup> Textile Chemistry Department, Politeknik STTT Bandung, Bandung, Indonesia

E-mail: hendramahesa@yahoo.com

PVA is an attractive material among researchers and has been widely used in the fabrication of the nanofiber through electrospinning. In this paper, we dissolved PVA in distilled water and used an electrospinning technique to convert it into nanofibers. The electrospinning process, such as viscosity, the distance between the needle tip and collector, solution feed rate, and voltage, are varied to control physical properties such as fiber diameter to meet desired diameter and suitable applications such as filtration. Further, the nanofiber diameter produced by varying those parameters was then investigated using a scanning electron microscope. The results show that by increasing the electrospinning voltages from 30 KV to 38 KV, the fiber diameter was decreased while other parameters were kept constant. However, it was found that the diameter of the nanofibers appeared to increase when the solution concentration was increased from 5% to 15%. The phenomenon of decreasing the diameter of the nanofibers was also seen when the solution feed rate was increased from 0.4 ml/hour to 1.2 ml/hour. It can be seen that the diameter of the nanofibers decreased when the distance was changed from 5 cm to 10 cm, but when the distance between the needle and the collector was increased to 15 cm, the diameter of the nanofibers increased. Furthermore, we extended this research by adding AgNO<sub>3</sub> antibacterial to the PVA solution to determine the effect of AgNO<sub>3</sub> concentration in the solution on the diameter of the nanofibers and its impact on bacterial activity. The results showed that the AgNO<sub>3</sub> concentration in the solution showed a larger diameter, therefore it has a higher ability to reduce bacterial activity. This discovery will be very useful for the manufacture of materials that can be applied to the medical field, such as wound dressing materials.

## References

- [1]. Chen Wen-Jie, Xin Bin-Jie, and Wu Xiang-Ji. *J Industrial Tex.* **44**, 159-179 (2014).
- [2]. Mariia S, Tomasz M, Ele L, Ewa P. *Polymer Testing.* **113**, (2023).

# Assessment of Hydrogen Desorption and Absorption Properties of MgH<sub>2</sub>-Ni/HB composites



Natsumi Noguchi<sup>1</sup>, Kazuho Goto<sup>1</sup>, Shin-ichi Ito<sup>2</sup>, Kouji Sakaki<sup>3</sup>, Kohta Asano<sup>3</sup>, Takeshi Fujita<sup>4</sup>, Hideo Hosono<sup>5,6</sup>, Shin-ichi Orimo<sup>7,8</sup>, Takahiro Kondo<sup>2,7</sup>

<sup>1</sup> Graduate School of Pure and Applied Sciences, University of Tsukuba, Tsukuba, Ibaraki, Japan

<sup>2</sup> Department of Materials Science and Tsukuba Research Center for Energy Materials Science, Institute of Pure and Applied Sciences, University of Tsukuba, Tsukuba, Ibaraki, Japan

<sup>3</sup> National Institute of Advanced Industrial Science and Technology, Tsukuba, Ibaraki, Japan

<sup>4</sup> School of Environmental Science and Engineering, Kochi University of Technology, Kami, Kochi, Japan

<sup>5</sup> Materials Research Center for Element Strategy, Tokyo Institute of Technology, Yokohama, Kanagawa, Japan

<sup>6</sup> Research Center for Material Nanoarchitectonics, National Institute for Material Science, Tsukuba, Ibaraki, Japan

<sup>7</sup> The Advanced Institute for Materials Research (WPI-AIMR), Tohoku University, Sendai, Miyagi, Japan

<sup>8</sup> Institute for Materials Research (IMR), Tohoku University, Sendai, Miyagi, Japan

E-mail: s2430102@u.tsukuba.ac.jp

Carbon neutrality, aiming for zero greenhouse gas emissions and reducing fossil fuel dependence is a global trend. Renewable energy is advancing rapidly, but stable supply is still challenging. Against this backdrop, hydrogen energy is attracting attention because it offers a solution by storing, and transporting energy. MgH<sub>2</sub> is promising material for hydrogen storage due to Mg's abundance, and high hydrogen density (7.6wt%). Issues include the time required for hydrogen desorption and the high temperatures required for hydrogen utilization. Ni has been reported to improve the performance of MgH<sub>2</sub> as a catalyst on two-dimensional materials [1,2]. In this study, applying Ni supported hydrogen boride nanosheets (Ni/HB<sup>[3]</sup>), MgH<sub>2</sub>-Ni/HB composites were synthesized by ball milling MgH<sub>2</sub> with nano-sized. The Temperature Programed Desorption (TPD) results show that the hydrogen release temperature is 50 K lower than in the case of MgH<sub>2</sub> alone. The activation energy during hydrogen desorption was obtained from simultaneous Thermogravimetry / Differential Thermal Analysis (TG-DTA) measurements, and enthalpy ( $\Delta H$ ) and entropy ( $\Delta S$ ) during hydrogen desorption and absorption were obtained from pressure-composition-temperature (PCT) measurements. From these results, the energy diagram shown in Fig. 1 was obtained, indicating that the addition of Ni/HB did not create a new compound, but that Ni acts as a catalyst.

## References

[1] Wen, Z. et al. *ACS Appl. Mater. Inter.* **12**(45), 50333 (2020).

[2] Dan, L. et al. *ACS Appl. Energy Mater.* **5**, 4976 (2022).

[3] Noguchi, N. et al. *Molecules* **27**, 8261 (2022).

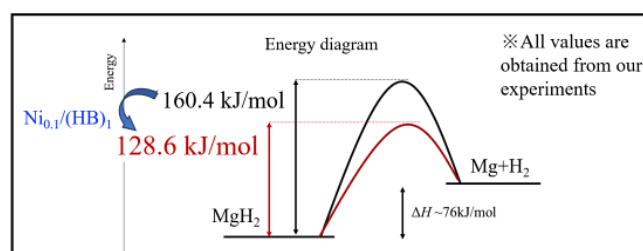
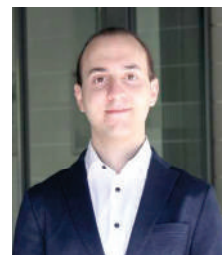


Fig. 1. Energy diagram of MgH<sub>2</sub>-(Ni<sub>0.1</sub>/HB<sub>1</sub>) composites.

# Coherent Workflows for Sustainable Electrochemical Hydrogenation Reactions with Pentlandite Catalysts



Mena-Alexander Kräenbring,<sup>1</sup> Leon Wickert,<sup>2</sup> Meinert Hansen,<sup>2</sup> Sebastian Sanden,<sup>2</sup> Kevinjeorjios Pellumbi,<sup>2</sup> Jonas Wolf,<sup>2</sup> Daniel Siegmund,<sup>2</sup> Fatih Özcan<sup>1</sup>, Ulf-Peter Apfel,<sup>2</sup> Doris Segets<sup>1</sup>

<sup>1</sup> EMPI—Particle Science and Technology, University of Duisburg-Essen, Duisburg, Germany

<sup>2</sup> Ruhr University Bochum, Bochum, Germany

E-mail: [mena.kraeenbring@uni-due.de](mailto:mena.kraeenbring@uni-due.de)

The hydrogenation of organic substances is a central process type in various industries<sup>[1]</sup>. The usage of gaseous hydrogen, which is primarily sourced from fossil fuels, entails the release of CO<sub>2</sub> during its production. In addition, the usage of gaseous hydrogen also carries a safety risk, which should be reduced as much as possible. An alternative approach is direct electrochemical hydrogenation with water or other protic liquids, where the required hydrogen is produced in situ and directly utilized. If this is driven by renewable energy, it represents a sustainable synthesis method that does not require stoichiometric reduction agents or high-temperature conditions<sup>[2]</sup>.

Transition metal chalcogenides, particularly pentlandites ( $\text{Fe}_x\text{Co}_y\text{Ni}_z\text{S}_a\text{Se}_b$ ,  $x+y+z=9$ ,  $a+b=8$ ), exhibit high conductivity and serve as efficient and affordable electrocatalysts for this purpose. The utilization of hierarchical functional layers in the final electrode greatly enhances their efficiency<sup>[3, 4]</sup>. A comprehensive approach to analyzing the vast and complex electrode production parameter space, encompassing process parameters and material variables for ink formulation and layer deposition, is critical for understanding the intricate mechanisms within the manufacturing process chain and to maximize the electrochemical conversion efficiency. For this purpose, a time-saving and cost-effective *coherent workflow* was developed which enables a systematic analysis of several parameters, maximizing the knowledge gained from each experiment while minimizing the total amount of experiments. The described procedure enables successive optimization and establishment of efficient membrane-electrode-assemblies for electroorganic reactions, offering new avenues for efficient, green, and sustainable synthesis pathways. These methods are also readily adaptable for scalable industrial applications.

- [1] Lauren S. Jackson, Fadwa Al-Taher, Chapter 23 - *Processing Issues: Acrylamide, Furan and Trans Fatty Acids, Ensuring Global Food Safety*, Academic Press (2010)
- [2] Ya Zhang, Weibin Qiu, Yongjun Ma, Yonglan Luo, Ziqi Tian, Guanwei Cui, Fengyu Xie, Liang Chen, Tingshuai Li, and Xuping Sun, *High-Performance Electrohydrogenation of N<sub>2</sub> to NH<sub>3</sub> Catalyzed by Multishelled Hollow Cr<sub>2</sub>O<sub>3</sub> Microspheres under Ambient Conditions*, ACS Catalysis (2018)
- [3] David Tetzlaff, Kevinjeorjios Pellumbi, Daniel M. Baier, Lucas Hoof, Harikumar Shastry Barkur, Mathias Smialkowski, Hatem M. A. Amin, Sven Grätz, Daniel Siegmund, Lars Borchardt and Ulf-Peter Apfel, *Sustainable and rapid preparation of nanosized Fe/Ni-pentlandite particles by mechanochemistry*, Chemical Science (2020)
- [4] Daniel Siegmund, Sebastian Metz, Volker Peinecke, Terence E. Warner, Carsten Cremers, Anna Grevé, Tom Smolinka, Doris Segets and Ulf-Peter Apfel, *Crossing the Valley of Death: From Fundamental to Applied Research in Electrolysis*, JACS Au (2021)

# Activation mechanism of carbon catalyst for oxygen reduction reaction



Kenji Hayashida<sup>1,2</sup>, Shusaku Fujita<sup>1</sup>, Shota Saito<sup>1</sup>, Rafiq Arsyad<sup>2</sup>, Kaito Homma<sup>2</sup>, Yasuo Yoshida<sup>3</sup>, Takahiro Kondo<sup>4</sup>, Satoru Takakusagi<sup>5</sup>, Junji Nakamura<sup>6</sup>, and Kotaro Takeyasu<sup>4,5</sup>

<sup>1</sup> Graduate School of Science and Technology, University of Tsukuba

<sup>2</sup> Graduate School of Environmental Science, Hokkaido University

<sup>3</sup> Department of Physics, Kanazawa University

<sup>4</sup> Institute of Pure and Applied Sciences, University of Tsukuba

<sup>5</sup> Institute for Catalysis, Hokkaido University

<sup>6</sup> International Institute for Carbon-Neutral Energy Research, Kyushu University

E-mail: [s2330104@u.tsukuba.ac.jp](mailto:s2330104@u.tsukuba.ac.jp)

Hydrogen fuel cells are essential for achieving carbon neutrality. Although platinum is widely used as a catalyst, carbon-based catalysts offer a promising and cost-effective alternative. However, their catalytic activity still requires improvement for practical use. In this study, we investigate the role of unpaired electrons such as pentagon carbons, enhance oxygen reduction reaction (ORR) activity compared to pyridinic nitrogen, which is traditionally considered the active site in carbon catalysts[1][2]. We synthesized nitrogen-doped reduced graphene oxide (NrGO) by heating graphene oxide at 950°C in NH<sub>3</sub>(NrGO-950), and post-annealed NrGO (PNrGO) by further heating NrGO-750 in Ar at 950°C and 1000°C. ORR measurements revealed that the onset potential of NrGO-950 was 0.76 V, whereas PNrGO showed improved performance with onset potentials of 0.82 V(Figure 1). This enhancement is likely due to the formation of pentagon carbons. X-ray photoelectron spectroscopy (XPS) confirmed pyridinic nitrogen amount decreases after annealing(Figure 2). This suggests high temperature treatment introduces new active sites. In my talk, I will focus on the effect of unpaired electron on ORR activity through Magnetic property measurement system.

## References

[1] Y. Tian, et al., *Angew. Chem. Int. Ed.* 2023 62, e202215295

[2] D. Guo, T. Kondo, J. Nakamura, et al., *Science*, 351, 361-365 (2016)

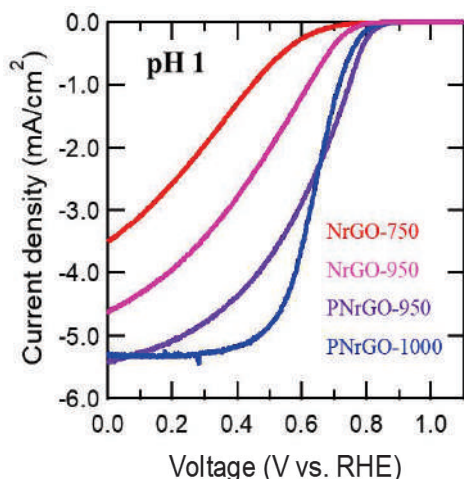


Fig 1. ORR activity of the catalysts in 0.1 M H<sub>2</sub>SO<sub>4</sub>.

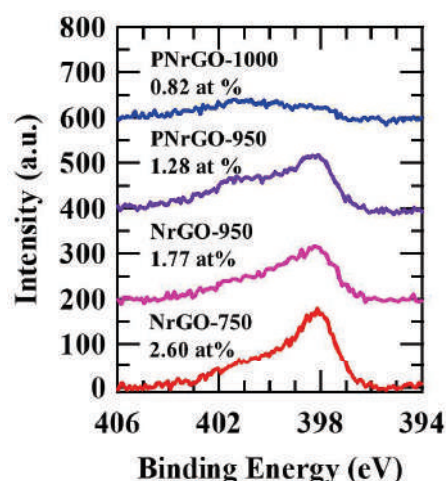


Fig 2. XPS spectra of N 1s

# Synthesis and Characterization of Nickel Cobalt Phosphate Electrode to Improve the Performance of Hybrid Supercapacitor



Miftahul-Khoiri,<sup>1</sup> Ni Luh Wulan-Septiani,<sup>2</sup> and Brian-Yulianto<sup>3</sup>

<sup>1</sup> *Magister Program of Engineering Physics, Faculty of Industrial Technology,  
Bandung Institute Technology, Ganesha 10, Bandung 40132, Indonesia*

<sup>2</sup> *Research Center for Advanced Materials, National Research, and Innovation Agency (BRIN),  
Kawasan Puspiptek, South Tangerang 15134, Indonesia*

<sup>3</sup> *Research Center for Nanosciences and Nanotechnology, Institut Teknologi Bandung, Bandung,  
40132, Indonesia*

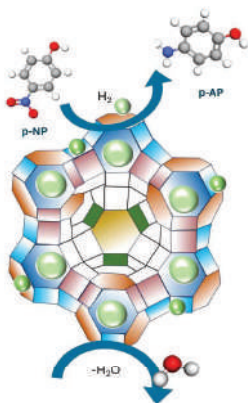
*E-mail: nilu010@brin.go.id*

In this study, nickel-cobalt phosphate has been developed as a positive electrode or pseudocapacitive materials for applied in hybrid supercapacitors. The nickel-cobalt phosphate synthesis was carried out in several different ratios of Ni:Co, i.e. 1:0, 5:1, 3:1, 2:1, 1:1, and 1:2. The phosphate formation process using nickel-cobalt glycerate as a precursor combined with triethyl phosphate (TEP) as phosphate source, followed by calcination at 600 °C under air conditions. Morphological analysis revealed that nickel-cobalt glycerate exhibited a spherical structure, nickel-cobalt TEP showed a dish-like structure, and nickel-cobalt phosphate had a cracker-like structure. Nickel cobalt phosphate also demonstrated an amorphous phase, which is highly beneficial for supercapacitor applications. Electrochemical testing in half-cells revealed that the specific capacitance of the nickel-cobalt phosphate variations was 673, 1211, 1123, 982, 948, and 510 F/g at a current density of 1 A/g in a 6 M KOH solution, respectively. The capacitance specific results were supported by BET analysis, which showed surface areas of 60.5, 47.8, 44.2, 43.3, 39.6, and 33.8 m<sup>2</sup>g<sup>-1</sup>, respectively. Meanwhile, the AC//Ni<sub>5</sub>Co<sub>1</sub>(PO<sub>4</sub>)<sub>3</sub> hybrid supercapacitor exhibited a specific capacitance of 100 Fg<sup>-1</sup>, with energy and power densities of 31.3 WhKg<sup>-1</sup> and 75 WKg<sup>-1</sup>, respectively.

# p-Nitrophenol reduction using transition metal supported zeolites

Ayush Kumar,<sup>1</sup> Kavitha Ramadass,<sup>1</sup> Gurwinder Singh,<sup>1</sup> Satish CI,<sup>1</sup> and Ajayan Vinu<sup>1,\*</sup>

<sup>1</sup> Global Innovative Centre for Advanced Nanomaterials, School of Engineering, The University of Newcastle, Callaghan, NSW 2308, Australia  
E-mail: Ayush.Kumar@uon.edu.au



The catalytic conversion of p-nitrophenol (p-NP) to p-aminophenol (p-AP) is a crucial industrial process with significant environmental and pharmaceutical implications. This reduction reaction also serves as a model system for evaluating the catalytic performance of novel materials. Existing catalysts for p-NP reduction often suffer from poor stability, low recyclability, and susceptibility to deactivation through metal leaching or nanoparticle aggregation. Zeolite overcomes these challenges by confining metal nanoparticles within their porous structure, preventing aggregation and leaching, while their high surface area and tunable pore sizes enhance catalytic activity and selectivity, leading to improved stability and recyclability for p-nitrophenol reduction<sup>1</sup>. Currently, most studies focus on ZSM-5 or hierarchical ZSM-5 derivatives for the reduction of p-NP<sup>2</sup>. There is still much to explore about other zeolite frameworks like beta-zeolites and gamma-zeolites with in-depth mechanistic studies. Our current research is focused on developing a new type of transition metal decorated with zeolites catalyst for the room temperature reduction of p-NP. Various combinations and permutation of metal loading impregnation methods are systematically explored to get the optimum catalyst. Out of all the catalysts developed, 1% Ni loaded on beta & gamma-zeolites demonstrated optimal performance, achieving 100% conversion and selectivity at optimized reaction conditions at 25°C and within 3h reaction time.

(1) Erika, D.; Nurdini, N.; Mulyani, I.; Kadja, G. T. M. Amine-functionalized ZSM-5-supported gold nanoparticles as a highly efficient catalyst for the reduction of p-Nitrophenol. *Inorganic Chemistry Communications* **2023**, 147.

(2) Aslam, S.; Subhan, F.; Yan, Z.; Yaseen, M.; Shujahat, M. H. Fabrication of gold nanoparticles within hierarchically ZSM-5-based micro-/mesostructures (MMZ) with enhanced stability for catalytic reduction of p-nitrophenol and methylene blue. *Separation and Purification Technology* **2021**, 254.



# Graphene-Enhanced Lithium-Ion and Alternative Batteries: Pioneering Malaysia's National Green Economy



Nurul Akmaliah Dzulkurnain,<sup>1</sup> Marliyana Mokhtar,<sup>1</sup> Nur Jafni Azaki<sup>1</sup>, Azizan Ahmad<sup>2</sup>, Sazlin Imaz Ismail<sup>3</sup>

<sup>1</sup> International Battery Center Sdn. Bhd., Kuala Lumpur, Malaysia

<sup>2</sup> The National University of Malaysia, Selangor, Malaysia

<sup>3</sup> NanoMalaysia Berhad, Kuala Lumpur, Malaysia

E-mail: nurulakmaliah@ibcm.com

Nowadays, rechargeable battery-based energy storage systems have received a lot of attention due to the irregular energy supply from renewable sources like solar and wind <sup>[1]</sup>. This issue has become more pressing as fossil energy reserves are depleting, and their excessive use has raised several environmental pollution concerns, which are currently the subject of intense global debate <sup>[2]</sup>. Therefore, International Battery Center Sdn. Bhd., in strategic partnership with NanoMalaysia Berhad (an agency under the Ministry of Science, Technology, and Innovation Malaysia), has developed and nurtured a local ecosystem for battery production and expertise to drive the National Green Economy agenda. Our research focuses on the production of graphene-based composite lithium-ion pouch cells, which are lighter and can store higher power and energy densities. Additionally, we are conducting research on graphene-enhanced sodium and aluminum-ion batteries <sup>[3,4]</sup>, which offer alternatives to lithium-ion technology, as sodium resources are abundantly available, and aluminum can be mined locally.

## References

- [1] Zhang, Y., Liu, S., Ji, Y., Ma, J., & Yu, H. *Advanced Materials* **2018**, 30(38), 1706310.
- [2] Zhao, L., Zhang, T., Li, W., Li, T., Zhang, L., Zhang, X. and Wang, Z., *Engineering* **2023**, 24, 172-183.
- [3] Abu Nayem, S. M., Ahmad, A., Shaheen Shah, S., Saeed Alzahrani, A., Saleh Ahammad, A. J., & Aziz, M. A. *The Chemical Record* **2022**, e202200181.
- [3] Kong, Y., Gadelhak, N. A., Chen, S., Rakov, D., Nanjundan, A. K., Yu, C., & Huang, X. *Materials Lab* **2023**, 220055-1.

# Enhancing Enzyme Electrode Performance Using Metal-Organic Frameworks for Advanced Biosensing Applications



Muhammad Rezki<sup>1</sup>, and Seiya Tsujimura<sup>2</sup>,

<sup>1</sup>*Graduated School of Pure and Applied Sciences, University of Tsukuba, 1-1-1 Tennodai, Tsukuba, Ibaraki 305-8573, Japan*

<sup>2</sup>*Division of Material Science, Faculty of Pure and Applied Science, University of Tsukuba, 1-1-1, Tennodai, Tsukuba, Ibaraki 305-5358, Japan*

E-mail: 1: [s2236006@u.tsukuba.ac.jp](mailto:s2236006@u.tsukuba.ac.jp)

2: [seiya@ims.tsukuba.ac.jp](mailto:seiya@ims.tsukuba.ac.jp)

## Content

The integration of enzyme electrodes into wearable devices, such as epidermal and implantable systems, has gained significant attention in recent years due to their potential in energy conversion and biosensing applications<sup>1,2</sup>. Despite these advancements, critical challenges persist, particularly in maintaining the stability of enzymes as biorecognition elements, enhancing electron transfer efficiency, and ensuring operational stability, especially in mediated electron transfer systems. This study addresses these challenges by utilizing Metal-Organic Frameworks (MOFs) to significantly improve enzyme electrode performance in biosensing applications. MOFs, known for their high surface area, tunable pore sizes, and biocompatible synthesis routes, provide an ideal platform for enzyme and guest molecule immobilization<sup>3</sup>. By employing a strategic approach that combines enzyme encapsulation within MOFs with tandem catalysts, we achieved notable improvements in enzyme electrode stability under harsh chemical conditions and elevated temperatures. Additionally, the sensors developed exhibited a wide linear range and low applied voltage requirements, minimizing interference from oxidizing compounds at higher voltages. Moreover, functionalizing MOFs with specific chemical groups and integrating redox mediators further enhanced electron transfer efficiency and preserved electrode stability in continuous operation. This approach offers superior performance compared to existing systems reliant on organic redox mediators, establishing a high-performance platform for advanced biosensing technologies.

## References

- (1) Saha, T.; Del Caño, R.; Mahato, K.; De la Paz, E.; Chen, C.; Ding, S.; Yin, L.; Wang, J. *Chem Rev* 2023, 123 (12), 7854–7889.
- (2) Min, J.; Tu, J.; Xu, C.; Lukas, H.; Shin, S.; Yang, Y.; Solomon, S. A.; Mukasa, D.; Gao, W.. *Chem Rev* 2023, 123 (8), 5049–5138.
- (3) Wang, Q.; Astruc, D. *Chem Rev* 2020, 120 (2), 1438–1511.

# High efficiency $\text{Sb}_2(\text{S}, \text{Se})_3$ thin-film solar cells by substrate-temperature-controlled vapor transport deposition method

Deyang Qin,<sup>1</sup> Yuxin Pan,<sup>1</sup> and Shaoqiang Chen<sup>1</sup>

<sup>1</sup> State key Laboratory of Precision Spectroscopy,  
Department of Electronic Engineering, East China Normal University,  
500 Dongchuan Road, Shanghai 200241, China

E-mail: [sqchen@ee.ecnu.edu.cn](mailto:sqchen@ee.ecnu.edu.cn)



Antimony chalcogenide ( $\text{Sb}_2(\text{S}, \text{Se})_3$ ) semiconductor is a recently emerging photovoltaic material for thin-film solar cells due to its high light absorption coefficient, and tunable absorption band gap.<sup>[1]</sup> However,  $\text{Sb}_2(\text{S}, \text{Se})_3$  solar cells produced by the vapor transport deposition (VTD) approach have not progressed significantly in the previous 3-5 years.<sup>[2]</sup> A new  $\text{Sb}_2(\text{S}, \text{Se})_3$  solar cells produced method based on a double-temperature evaporation furnace named control vapor transport deposition (STC-VTD) was carried out. The heat field distribution of the tube furnace during deposition was simulated through COMSOL Multiphysics. By first employing the modified VTD method, a solar cell with a power conversion efficiency (PCE) of 7.56% was achieved by adjusting the exact temperature control between the evaporation source and the substrate. This work proposes the notion of substrate temperature-independent control for other physical vapor preparation methods.

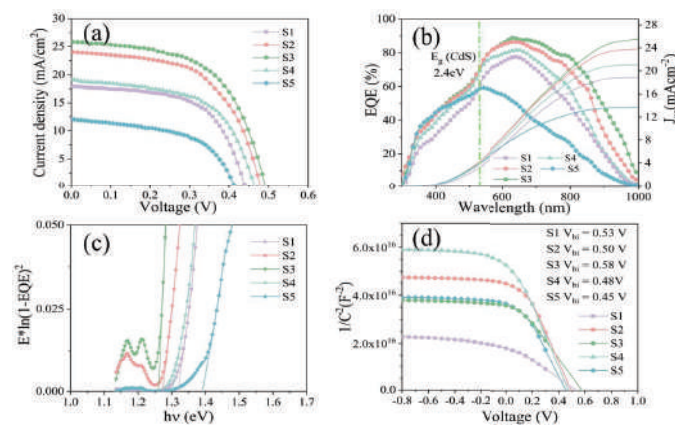


Figure 1. (a) J-V characteristics, (b) EQE spectra, (c) the bandgap energy ( $E_g$ ), (d)  $1/C^2$ -V plots of S1-S5 solar cells.

## References

- [1] Pan Y L, Hu X B, Guo Y X, *et al*, *Advanced. Functional. Mater* **2021**, 2101476.
- [2] Wang R, Wang Y Y, Pan Y L, *et al*, *Solar Energy* **2021**, 220, 942-948.

# Amorphous Silicon/Carbon Composite-Based Hierarchically Structured Supraparticles for Lithium-Ion Battery Anodes

Adil Amin,<sup>1</sup> Moritz Loewenich,<sup>2</sup> Hartmut Wiggers<sup>2,3</sup>, Fatih Özcan,<sup>1</sup> and Doris Segets<sup>1,3</sup>



<sup>1</sup>Institute for Energy and Materials Processes—Particle Science and Technology (EMPI—PST), University of Duisburg-Essen (UDE), Germany

<sup>2</sup>Institute for Energy and Materials Processes—Reactive Fluids (EMPI—RF), University of Duisburg-Essen (UDE), Germany

<sup>3</sup>Center for Nanointegration Duisburg-Essen (CENIDE), University of Duisburg-Essen (UDE), Germany

Silicon (Si), with its high theoretical lithiation capacity, has the potential to replace graphite anodes in conventional lithium-ion batteries.<sup>[1]</sup> However, its commercialization is slowed down by significant volume changes during cycling. These volume changes result in particle cracking, loss of electrical contacts, electrode delamination and unstable solid electrolyte interface (SEI) leading to fast capacity fading. Nanoparticles have solved the particle cracking issue but inherently suffer from low first cycle Coulombic efficiency<sup>[2]</sup> and difficulty in processing of Si-dominant (graphite-free) slurries into homogenous-electrodes.<sup>[3]</sup>

To address the processing challenges associated with incorporating nanoparticles into conventional manufacturing processes, we propose a post-synthesis spray drying method to produce hierarchically structured secondary particles, termed supraparticles, from gas-phase-synthesized nanoparticles.<sup>[4]</sup> Figure 1 shows that Si/C (primary particles' carbon content 4 wt.%) supraparticles exhibited improved first cycle Coulombic efficiency ~86 % and a good cycling stability, i.e. 80 % of the 3rd cycle capacity was retained after 126 cycles.

Based on nitrogen adsorption, XPS results, and analysis of supraparticle size distributions, improved first cycle Coulombic efficiency is because supraparticles have a lower surface-to-volume ratio and structuring confining most of SEI limit to their outer surface. Additionally, a thin stabilizer coating on their outer surface further helps avoid immediate electrolyte flooding leading to less abrupt reactions of electrolyte with surface. These factors collectively contribute to forming a smaller SEI volume during the initial formation cycles. Furthermore, cycling

stability is improved due to well-defined, evenly distributed pores within and around the supraparticle, accommodating Si volume expansion and preventing electrode delamination. Moreover, structuring nanoparticles into supraparticles improved slurry processing (40 wt.% solids) by achieving a moderate zero shear viscosity of 47 Pa·s and ensuring fast recovery of the wet-layer structure within 20 seconds. This also allowed precise control over electrode layer porosity (analogous Hg-porosimetry on powder level), reducing variability. Supraparticle-based electrodes showed high reproducibility with only a 2.7% standard deviation.

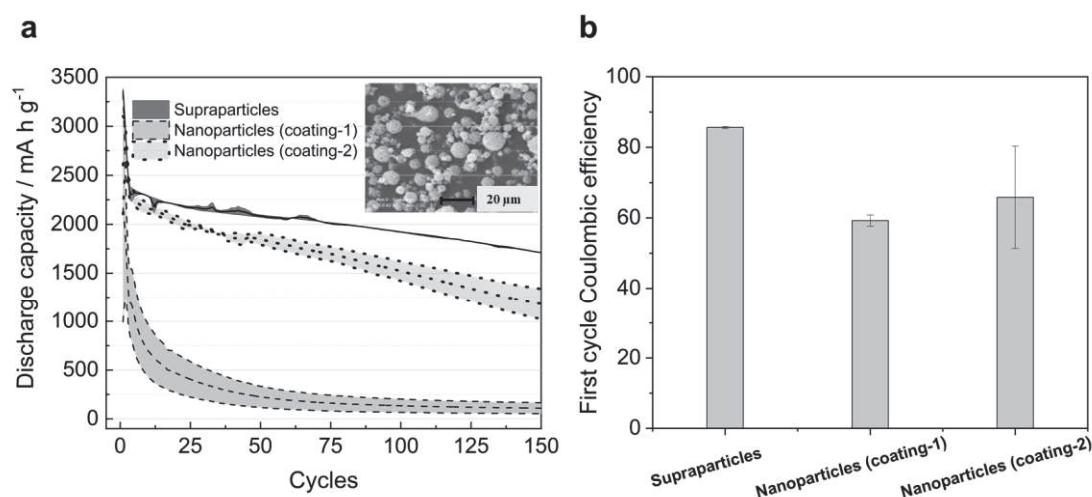


Fig.1. For nanoparticles and supraparticles: (a) Specific discharge capacity with the cycling, inset shows SEM of supraparticles; b) bar-chart showing 1<sup>st</sup> cycle Coulombic efficiency. Figure taken from Adil Amin et al.<sup>[4]</sup> and is under the CC SA 4.0 International license. Colors, legends and line styles were modified.

To conclude, our study demonstrates how combining gas-phase synthesis of impurity-free Si nanoparticles<sup>[5]</sup> with scalable spray drying can advance nanoparticle-based technologies. Our results are also highly promising in that sense that integrating these processes with conventional Roll-to-Roll systems is feasible.

## References

- [1] C. K. Chan, H. Peng, G. Liu, K. McIlwrath, X. F. Zhang, R. A. Huggins, Y. Cui, *Nature nanotechnology* **2008**, 3, 31.
- [2] X. Zhao, V.-P. Lehto, *Nanotechnology* **2021**, 32, 42002.
- [3] B. Wu, J. Quinn, J. Li, Q. Li, D. Liu, W. Martin, K. Baar, L. Zhong, C. Wang, J. Xiao, *J. Electrochem. Soc.* **2024**, 171, 50542.
- [4] A. Amin, M. Loewenich, S. O. Kilian, T. Wassmer, S. Bade, J. Lyubina, H. Wiggers, F. Özcan, D. Segets, *J. Electrochem. Soc.* **2023**, 170, 20523.
- [5] H. Wiggers, R. Starke, P. Roth, *Chem. Eng. Technol.* **2001**, 24, 261.

# Near-unity angular anisotropy of circularly polarized luminescence from microspheres of monodispersed chiral conjugated polymer

Sota Nakayama<sup>1</sup>, Hiroshi Yamagishi<sup>1</sup>, Osamu Oki<sup>1</sup>, Soh Kushida<sup>1</sup>, Junhui Chen<sup>1</sup>, Junpei Kuwabara<sup>1</sup>, Takaki Kanbara<sup>1</sup>, Wijak Yospanya<sup>2</sup>, Reiko Oda<sup>3,2</sup>, and Yohei Yamamoto<sup>1</sup>



<sup>1</sup>Department of Materials Science, Institute of Pure and Applied Sciences, and Tsukuba Research Center for Energy Materials Science (TREMS), University of Tsukuba, 1-1-1 Tennodai, Tsukuba, Ibaraki 305-8573, Japan.

<sup>2</sup>Advanced Institute of Material Research (AIMR), Tohoku University 2-1-1 Katahira, Aoba, Sendai, Miyagi, 980-8577, Japan.

<sup>3</sup>University of Bordeaux, CNRS, Bordeaux INP, CBMN, UMR 5248, F-33600 Pessac, France

E-mail: s2430087@u.tsukuba.ac.jp

## 1. Introduction

Circularly polarized luminescence (CPL) is fascinating for advanced devices such as 3D displays and optical cryptography<sup>[1]</sup>. We recently reported that a chiral  $\pi$ -conjugated polymer, (*S,S*)-PFBT (**Fig. 1a**), self-assembled into well-defined microspheres (MSs) with twisted bipolar (TB) molecular order (**Fig. 1b-d**) at the interior<sup>[2]</sup>, and it emitted intense anisotropic CPL with large dissymmetry factor ( $|g_{\text{lum}}|$ ). In this study, we prepared MS from enantiomerically pure PFBT with a series of number-average molecular weight ( $M_n$ ) and a smaller PDI. As a result, we found that MS with a certain molecular weight emitted CPL with significantly high angular anisotropy with the degree of anisotropy of almost unity.

## 2. Results and Discussion

(*S,S*)-PFBT was synthesized according to our previous report<sup>[2]</sup>. We fractionated the resulting polymer by size exclusion chromatography (SEC) and obtained five fractions of (*S,S*)-PFBT (named **f<sub>1</sub>**–**f<sub>5</sub>**, respectively). The microspherical particles of (*S,S*)-PFBT ((*S,S*)-MS) were assembled from each fraction by vapour diffusion (VD) method<sup>[2]</sup>. MSs assembled from **f<sub>2</sub>** to **f<sub>5</sub>** ((*S,S*)-MS<sub>f<sub>2</sub></sub>–**f<sub>5</sub>**) exhibited counterclockwise spiral texture (**Fig. 1f-i**) in polarized optical microscopy (POM), characteristic of the TB phase.

MS with the TB order ((*S,S*)-MS<sub>f<sub>2</sub></sub>–**f<sub>5</sub>**) showed large  $|g_{\text{lum}}|$  value that oscillated as a function  $\theta$  (**Fig. 4a**). The degree of angular anisotropy of  $g_{\text{lum}}$  ( $r = (|g_{\text{lum}}^{\text{max}}| - |g_{\text{lum}}^{\text{min}}|) / (|g_{\text{lum}}^{\text{max}}| + |g_{\text{lum}}^{\text{min}}|)$ ) were plotted in **Fig. 4b**. In definition, the  $r$  value approaches 1 with a perfectly anisotropic CPL emitters. The  $|g_{\text{lum}}^{\text{max}}|$  of (*S,S*)-MS<sub>f<sub>2</sub></sub> was 61-fold larger than its  $|g_{\text{lum}}^{\text{min}}|$  (**Fig. 4c**) and yielded  $r$  of 0.95 on average, which is the best anisotropy among minute CPL emitters reported previously<sup>[3]</sup>.

## References

- [1] J. Kumar *et al.*, *J. Phys. Chem. Lett.* **2015**, *6*, 3445. [2] O. Oki *et al.*, *J. Am. Chem. Soc.* **2021**, *143*, 8772–8779  
[3] **S. Nakayama** *et al.*, *Chem. Commun.* 2024, **2024**, 60, 7634–7637

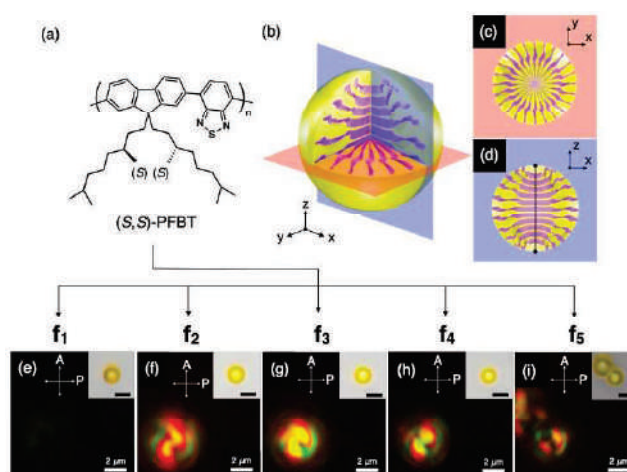


Fig. 1. (a) Molecular structure of (*S,S*)-PFBT. (b-d) Schematic representation of the TB molecular arrangement in MS and its cross-sectional views at the  $y$ - $z$  (c) and  $x$ - $z$  (d) planes. (e-i) POM micrographs (insets are the corresponding OM images, scale bars: 4  $\mu\text{m}$ ) of the fractions of (*S,S*)-PFBT.

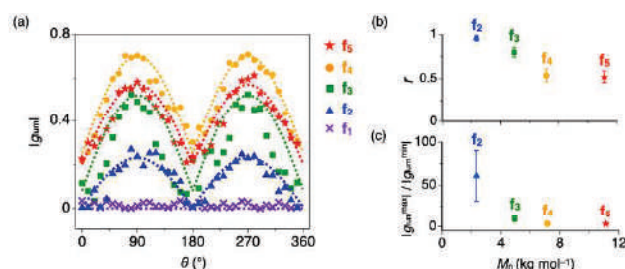


Fig. 2. (a) A plot of  $|g_{\text{lum}}|$  at 546 nm as a function of  $\theta$  (purple crosses: MS<sub>f<sub>1</sub></sub>, blue triangles: MS<sub>f<sub>2</sub></sub>, green squares: MS<sub>f<sub>3</sub></sub>, orange circles: MS<sub>f<sub>4</sub></sub>, and red stars: MS<sub>f<sub>5</sub></sub>) in angle-dependent CPL measurements of single particle of (*S,S*)-MS. Dotted curves are the fitted sine curves ( $|g_{\text{lum}}| = a + b|\sin\theta|$ ). (c,d) Plots of  $r$  (b) and  $|g_{\text{lum}}^{\text{max}}| / |g_{\text{lum}}^{\text{min}}|$  (c) as a function of  $M_n$ . Error bars represent standard deviation.

# Influence of Size and Shape of ZnO Photocatalysts in Natural Rubber Latex Foam on Antibacterial Applications



Kamonthip Singbumrung,<sup>1,4</sup> Yeampon Nakaramontri,<sup>2</sup> Chotiros  
Dokkhan,<sup>3</sup> Pasaree Laokijcharoen,<sup>3</sup> Surawut Chuangchote <sup>1,4,\*</sup>

<sup>1</sup> Department of Tool and Materials Engineering, Faculty of Engineering, King Mongkut's University of Technology Thonburi (KMUTT), 126 Prachauthit Rd., Bangmod, Thungkru, Bangkok 10140, Thailand.

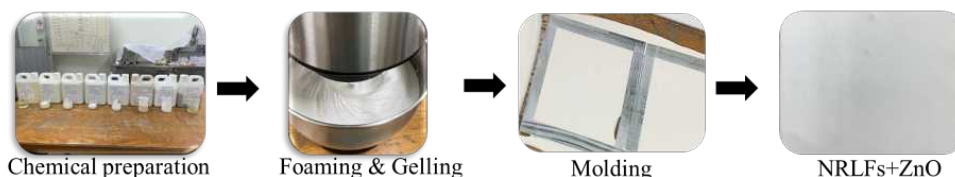
<sup>2</sup> Sustainable Polymer & Innovative Composites Material Research Group, Department of Chemistry, Faculty of Science, King Mongkut's University Thonburi, 126 Prachauthit Rd., Bangmod, Thungkru, Bangkok, Thailand.

<sup>3</sup> National Metal and Materials Technology Center (MTEC), National Science and Technology Development Agency (NSTDA), Thailand Science Park, Pathum Thani 12120, Thailand.

<sup>4</sup> Research Center of Advanced Materials for Energy and Environmental Technology (MEET), King Mongkut's University of Technology Thonburi (KMUTT), 126 Prachauthit Rd., Bangmod, Thungkru, Bangkok 10140, Thailand.

E-mail: \* surawut.chu@kmutt.ac.th

Natural rubber latex foam was made using the Dunlop technique. Zinc oxide photocatalysts were used as fillers in the latex foam. In the rubber foam preparation step, the time for rubber mixing was varied (i.e., 2, 4, 6, and 8 min). Scanning electron microscopy (SEM) was performed to study the morphology and chemical structure of the rubber foam. Different sizes and shapes of zinc oxide (i.e., particles with diameters of 50 nm, 100 nm, 300 nm, and 400 nm and wires with a 50 nm diameter and 1  $\mu$ m long) were studied. Compression properties and antibacterial ability in both dark and light conditions were investigated. It was found that the rubber foam with zinc oxide in smaller diameters has more ability to resist infection for both gram-negative and gram-positive bacteria.



# Poster Session



# Nanoarchitectonics of Biomass Carbon for Energy Storage Technology



S. Manandhar<sup>1,2</sup>, L. K. Shrestha<sup>1,2\*</sup>

<sup>1</sup>Department of Materials Science, Institute of Pure and Applied Sciences, University of Tsukuba 1-1-1, Tennodai, Tsukuba 305-8573, Ibaraki, Japan

<sup>2</sup>Research Center for Materials Nanoarchitectonics (MANA), National Institute for Materials Science (NIMS), 1-1 Namiki, Tsukuba, Ibaraki 305-0044, Japan

E-mail: [s2336013@u.tsukuba.ac.jp](mailto:s2336013@u.tsukuba.ac.jp)

## Content

With the increase in global demand of energy, it emphasizes the urgency for efficient, sustainable, and environmentally friendly energy storage technologies [1]. The exploration of biomass carbon materials has emerged as promising candidate in energy storage [2] as they offer a unique combination of high surface area, well-defined porosity, and intrinsic conductivity, making it particularly well-suited for energy storage devices like supercapacitors and batteries [3]. By employing the concept of nanoarchitectonics, the design and application of biomass carbon can be precisely tailored at the nanoscale, offering new possibilities for high-performance, sustainable energy storage technologies.

This research explores the synthesis of high surface area hierarchically porous carbon materials from *Terminalia bellirica* (Barro) seed through chemical activation using zinc chloride ( $\text{ZnCl}_2$ ) and carbonized at  $700^\circ\text{C}$  with varying weight ratios under a nitrogen atmosphere. Several characterization techniques were employed to characterize the carbon materials, and its electrochemical performance was studied using three-electrode cell in 1 M  $\text{H}_2\text{SO}_4$  aqueous electrolyte with Ag/AgCl and Pt-wire as reference and counter electrodes.

Fig. 1a and b show the cyclic voltammogram (CV) and galvanostatic charge discharge (GCD) curve with quasi-rectangular and quasi-triangular shape respectively; that indicates the electric double layer (EDLC) type charge storage mechanism. Nanoporous carbon materials prepared from Barro by  $\text{ZnCl}_2$  activation at different impregnation ratio showed better electrochemical performance for sample with 1:3 ratio that correlates with the BET surface area as well. The hierarchical micro and mesopores distribution led to better performance of the sample highlighting the importance of porosity for its potential in energy storage application.

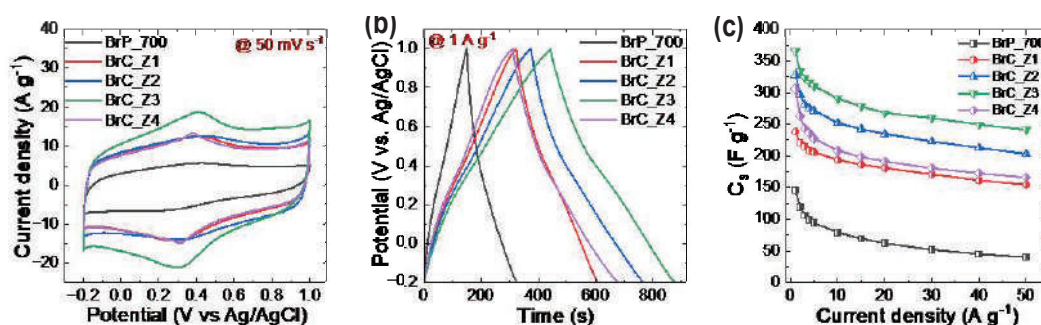


Fig. 1. a-c) CV curves at scan rate of  $50\text{ mV s}^{-1}$ , GCD curves at  $1\text{ A g}^{-1}$  current density and specific capacitance ( $C_s$ ) at different current density of prepared carbon materials

## References

- [1] N. Kumar et. al., *Nanoscale Adv.* 5 (12) (2023) 3146–3176
- [2] J. Wang et. al., *ACS Omega* 7 (26) (2022) 22689–22697
- [3] R. G. Shrestha et. al., *Nanomaterials* 10 (4) (2020) 639

# Enhancement of Reversibility and Capacity of Silicon Based Electrodes through Various Parameters



Chenxiao Ye<sup>1,2</sup>, Denis Y. W. Yu<sup>1,2</sup>

<sup>1</sup>Graduated School of Pure and Applied Sciences, University of Tsukuba, 1-1-1 Tennodai, Tsukuba, Ibaraki 305-8573, Japan

<sup>2</sup>National Institute for Materials Science, 1-1 Namiki, Tsukuba, Ibaraki 305-0044, Japan

E-mail: s2420401@u.tsukuba.ac.jp

Silicon (Si) is a promising anode material for lithium-ion batteries (LIBs) due to its high theoretical capacity. However, challenges such as significant volume expansion during charge-discharge cycles, leading to electrode degradation and increased internal resistance, and the pulverization of Si particles under strain, have limited its practical application<sup>1</sup>. In this work, we study the effect of different parameters such as Si particle size, binder type, binder amount, annealing condition, etc. on the stability of Si electrodes for LIBs. We found that the capacity and reversibility is significantly affected by the binder<sup>2</sup>. In particular, the use of polyimide (PI) binders can help improve cycle stability. An initial capacity of more than 3000 mAh g<sup>-1</sup>, close to its theoretical capacity, can be obtained from the Si electrode (Fig. 1). Available capacity is also increased after reducing the Si particle size by ballmilling (Fig. 2). The ballmilled Si electrode with PI binder retains 61% of its initial charge specific capacity after 30 cycles, with a Coulombic efficiency of 98.1%. Improved cycle stability with ballmilled Si is attributed to smaller amount of cracking of the electrode upon charge-discharge (Fig. 3). With the help of PI binders and the reduced Si particle size, the connectivity of the electrodes can be improved.

Fig.1 Charge-discharge curves of ballmilled Si electrode with PI binder.

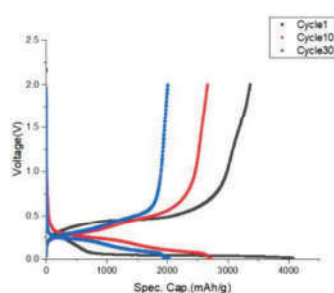


Fig.2 Cycling performance of electrode with different Si with PI binder at a current of 300 mA g<sup>-1</sup>.

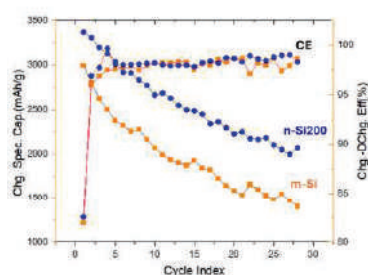
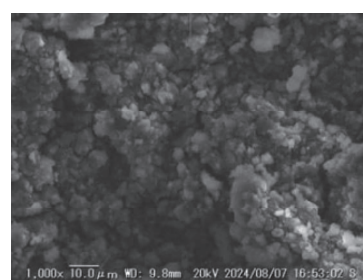


Fig.3 Scanning electron microscopy of Si electrodes after 30 cycles.



## References

1. Lee, P.-K.; Tan, T.; Wang, S.; Kang, W.; Lee, C.-S.; Yu, D. Y. W. Robust Micron-Sized Silicon Secondary Particles Anchored by Polyimide as High-Capacity, High-Stability Li-Ion Battery Anode. *ACS Applied Materials & Interfaces* 2018, 10 (40), 34132–34139. <https://doi.org/10.1021/acsami.8b09566>.
2. Zhang, M.; Wang, L.; Xu, H.; Song, Y.; He, X. Polyimides as Promising Materials for Lithium-Ion Batteries: A Review. *Nano-Micro Letters* 2023, 15 (1). <https://doi.org/10.1007/s40820-023-01104-7>.

# Energy performance advancement by tuning nanospace of hollow carbon spheres



Sabina Shahi<sup>1,2</sup>, Lok Kumar Shrestha<sup>1,2,\*</sup>

<sup>1</sup>*Department of Materials Science, Institute of Pure and Applied Sciences, University of Tsukuba 1-1-1, Tennodai, Tsukuba 305-8573, Ibaraki, Japan*

<sup>2</sup>*Research Center for Materials Nanoarchitectonics (MANA), National Institute for Materials Science (NIMS), 1-1 Namiki, Tsukuba, Ibaraki 305-0044, Japan*

E-mail: s2430108@u.tsukuba.ac.jp

## Content

Hollow carbon spheres, with their unique structural properties; hollow space at the center and carbon shells due to which they exhibit high surface area, have emerged as promising materials for energy storage applications, catalysts, chemical reactors, biomedical diagnosis and therapy and so on. We aim to enhance ion transport within these spheres, by manipulating the hollow spaces and nanopore engineering in the porous shell, optimizing their energy density performance to contribute to next generation energy storage technologies.

In this contribution, we have used fullerene as a carbon source due to its ability to self-assemble and ethylenediamine as a structure-directing agent to synthesize the hollow carbon spheres by simple dynamic liquid-liquid interfacial precipitation method. Systematic control over the nanoscale dimensions of the hollow spaces can improve ion mobility. For this, our first approach is time programmable synthesis method. By varying the incubation time from 10 minutes to 24 hours, we observed that particle size increases and hollow space decreases up to 1 hour, after which both parameters remain nearly constant. At 10 minutes, the hollowness is notably large, providing extensive internal surface area. The 1-hour sample exhibits smaller hollow space compared to the 10-minute sample, yet both structures maintain effective ion transport characteristics. Furthermore, we are performing KOH-activation to fine-tune the porosity of hollow spheres, enhancing the ion-diffusion pathways within the porous shell. After that, we are investigating the electrochemical performance of these hollow carbon spheres in an aqueous electrolyte.

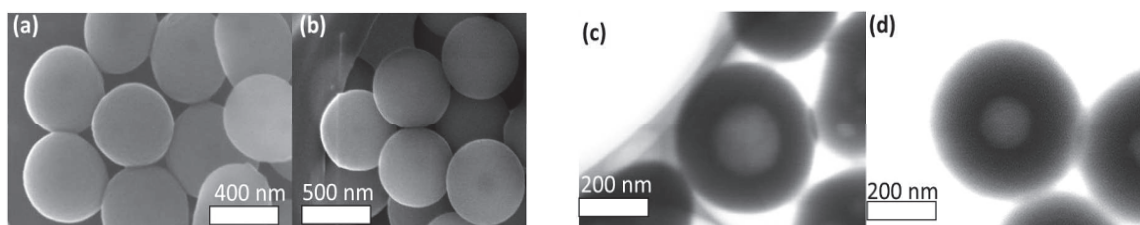


Figure: (a,b)SEM and (c,d) STEM images of synthesized hollow carbon spheres incubated at 10 min and 60 min respectively

## References

- [1] Y. Sun et al. Carbon 125 (2017) 139-145.
- [2] L.K. Shrestha et al. Nanomaterials 13 (2023) 946.

# 3D Printed Scaffold using Polycaprolactone/Fullerene (C<sub>60</sub>) Nanorod for Bone Tissue Engineering



Novi Dwi Widya Rini<sup>1,2</sup>, Arie Wibowo<sup>3,4\*</sup>, Lok Kumar Shrestha<sup>1,2\*</sup>

<sup>1</sup>Department of Materials Science, Institute of Pure and Applied Sciences, University of Tsukuba, 1-1-1 Tennodai, Tsukuba, Ibaraki 305-8573 Japan

<sup>2</sup>Research Center for Materials Nanoarchitectonics (MANA), National Institute for Materials Science (NIMS), 1-1 Namiki, Tsukuba, Ibaraki 305-0044, Japan

<sup>3</sup>Materials Science and Engineering Research Group, Faculty of Mechanical and Aerospace Engineering, Institut Teknologi Bandung, Jl. Ganesha 10, Bandung, 40132, Indonesia

<sup>4</sup>Research Center for Nanoscience and Nanotechnology, Institut Teknologi Bandung, Jl. Ganesha 10, Bandung 40132, West Java, Indonesia

E-mail: s2430105@u.tsukuba.ac.jp

Scaffolds based on polycaprolactone (PCL), fabricated using 3D printing, have been attracted in bone tissue applications because of their biocompatibility, biodegradability, and precise tailored geometry. However, adjusting the mechanical strength and hydrophilicity of the scaffold to fulfill the specific requirements for bone tissue application is yet challenging. Recently, fullerene (C<sub>60</sub>) has gained attention as a promising filler in composite materials due to its superior mechanical properties. We explored self-assembled C<sub>60</sub> nanorods (FNR) and pluronic 123 surface-modified C<sub>60</sub> nanorods (PFNR) as reinforcing fillers in the PCL scaffold. The addition of 0.013 wt% FNR improved significantly the mechanical strength compared to the pure PCL scaffold, without significant changes in the hydrophilicity. However, both the PCL scaffolds' hydrophilicity and mechanical strength could be improved by incorporating PFNR filler. As a result, the scaffold showed excellent proliferation activity of Human Wharton's Jelly Mesenchymal Stem Cells. Moreover, the FNR and PFNR-incorporated PCL scaffolds showed antibacterial activity against *Staphylococcus aureus* and *Escherichia coli* which is critical for preventing implant-associated infections. This study demonstrates that by adjusting the type and concentration of fillers, we can tune the mechanical and hydrophilicity properties of the PCL scaffold, optimizing cell proliferation and antibacterial activity for bone tissue application.

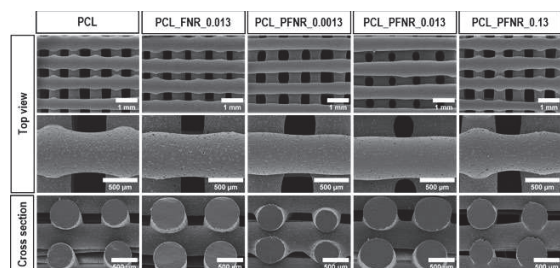


Fig. 1. The SEM images of the 3D-printed scaffolds from the top view and the cross-section view.

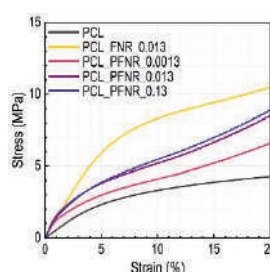


Fig. 2. Representative compressive stress-strain curves of 3D-printed scaffolds.

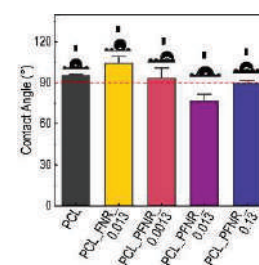


Fig. 3. Contact angles and the water droplet images on the surface of the scaffold.

## References

- [1] C. W. Wong, K. C. Tsai, L. K. Shrestha, K. Ariga, and S. H. Hsu, *Nanoscale* 14, 11152 (2022).
- [2] M. Mira, A. Wibowo, G.U.N. Tajalla, G. Cooper, P.J.D.S. Bartolo, and A. Barlian, *Mater Adv* 4, 6407 (2023).

# Observing electronic dynamics in the conduction band of 2H-MoTe<sub>2</sub> by using double-excitation ultrafast electron diffraction



Yui Iwasaki<sup>1\*</sup>, Takumi Fukuda<sup>1</sup>, Godai Noyama<sup>1</sup>, Mizuki Akei<sup>1</sup>, Hidemi Shigekawa<sup>2</sup>, Paul Fons<sup>3</sup>, Muneaki Hase<sup>2</sup>, Yusuke Arashida<sup>2</sup>, Masaki Hada<sup>2</sup>

<sup>1</sup>Graduate School of Pure and Applied Sciences, University of Tsukuba, 1-1-1 Tennodai, Tsukuba, Ibaraki 305-8573, Japan

<sup>2</sup>Institute of Pure and Applied Sciences, University of Tsukuba, 1-1-1 Tennodai, Tsukuba, Ibaraki 305-8573, Japan

<sup>3</sup>Faculty of Science and Technology, Keio University, Yokohama, Kanagawa 223-8522, Japan

\*E-mail: s2420398@u.tsukuba.ac.jp

Transition metal dichalcogenides (TMDs) are two-dimensional layered materials. MoTe<sub>2</sub>, one of the TMD materials, shows semiconductor, semimetal, and Weyl semiconductor phases in different stacking structures [1,2]. Because the characteristics of semiconductors are affected by behavior of carriers in the conduction and valence bands, it is important to understand the carrier dynamics in the conduction and valence bands. Electronic relaxations have been directly observed by two-photon photoelectron spectroscopy and time-resolved angle-resolved photoemission spectroscopy [3]. In this study, we propose a different method to understand the electronic relaxation dynamics in semiconducting materials. Double-excitation ultrafast time-resolved electron diffraction measurements under saturable absorption conditions were demonstrated to observe electronic relaxation in the conduction band of 2H-MoTe<sub>2</sub> [4]. In the experiments, we equipped a Mach-Zehnder interferometer to generate double pulse excitation with a wavelength of 400 nm for the conventional ultrafast time-resolved electron diffractometer. The pulse interval between the optical excitation pulses was adjusted by the optical stage in the interferometer. The incident fluence of one of the excitation pulses was set to 5 mJ/cm<sup>2</sup>. Our previous study found that the saturable absorption effect for a 2H-MoTe<sub>2</sub> thin film at an incident fluence of 4–12 mJ/cm<sup>2</sup> [5]. Figure 1 shows the diffraction intensity changes in the 110 diffraction spots for different pulse intervals of the two optical pulses. When the pulse intervals are 0 ps and 0.1 ps, the intensity decreases are relatively low, which suggests that the second pulses are under saturable absorption conditions. By using exponential fitting curve, the time constant of momentum relaxation of electrons is estimated to be 100 fs, which is comparable with the duration of optical pump pulse, ~100 fs. In conclusion, we found that momentum relaxation of electrons occurred within 100 fs in the conduction band of 2H-MoTe<sub>2</sub> by using double-excitation ultrafast time-resolved electron diffraction measurements. For further study, we plan to measure the time constant of momentum relaxation more precisely by using an ultrafast time-resolved electron diffraction setup with shorter excitation optical pulses (<35 fs) [6].

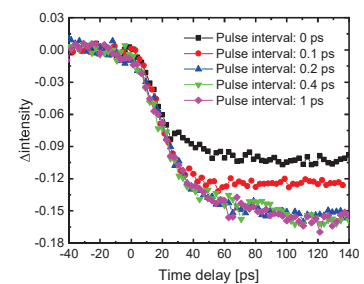


Fig. 1. Intensity changes in the 110 diffraction spots for different pulse intervals. [4]

## References

- [1] D. H. Keum, *et al.*, *Nat. Phys.* **11**, 482 (2015).
- [2] K. Deng, *et al.*, *Nat. Phys.* **12**, 1105 (2016).
- [3] U. De Giovannini, *et al.*, *Nano Lett.* **16**, 7993 (2016).
- [4] Y. Iwasaki, T. Fukuda, M. Hada, *et al.*, *Appl. Phys. Lett.* **123**, 181901 (2023).
- [5] T. Fukuda, M. Hada, *et al.*, *J. Phys. Chem. C* **127**, 13149 (2023).
- [6] K. Takubo, M. Hada, *et al.*, *Rev. Sci. Instrum.* **93**, 053005 (2022).

# T Perovskite photonic crystal of CsPbBr<sub>3</sub> on patterned substrates and its laser properties

Luoting Yang<sup>1</sup>, Zhan Su<sup>1</sup>, Fuyi Cao<sup>1</sup>, Yawen He<sup>1</sup>, Cong Wang<sup>1</sup>, Shoujie Ye<sup>1</sup>,

Guoen Wen<sup>1</sup> and Shaoqiang Chen<sup>1</sup>

<sup>1</sup>State Key Laboratory of Precision Spectroscopy, Department of Electronic

Engineering, East China Normal University, Shanghai 200241, China.

Corresponding author: 1245933637@qq.com



All-inorganic perovskite nanocrystals have gained significant attention for their exceptional optoelectronic properties, including high quantum yield, tunable emission wavelengths, and strong stability, making them promising for applications in photodetectors, solar cells, LEDs, and lasers. However, challenges such as low light utilization, poor crystallization quality, and limited long-term stability hinder commercialization. To address these issues, photonic crystals (PCs) have been developed as effective light-control structures. PCs not only enhance device performance but also provide additional benefits, including flexibility, vibrant colors, and partial transparency, paving the way for more efficient and advanced optoelectronic devices.

In this work, all-inorganic perovskite CsPbBr<sub>3</sub> crystals are grown on the patterned PSS substrate. The crystal is expected to form the structure of photonic crystal. And PL and TRPL tests have been done when the photonic crystal is observed to produce laser. The properties of the laser produced by perovskite photonic crystal is different greatly from other perovskite crystals grown on the same substrates in the same condition, which is worth further research.

# Synthesis and properties and azobenzene containing macrocycles and molecular cages

Mads Nybo Sørensen,<sup>1</sup> Masaru Kondo,<sup>2</sup> Takashi Nakamura<sup>3</sup>

<sup>1</sup>Degree Programs in Pure and Applied Sciences, University of Tsukuba, 1-1-1 Tennodai, Tsukuba, Ibaraki 305-8571, Japan

<sup>2</sup>School of Pharmaceutical Sciences, University of Shizuoka, 52-1 Yada, Surugaku, Shizuoka 422-8526, Japan

<sup>3</sup>Institute of Pure and Applied Sciences, University of Tsukuba, 1-1-1 Tennodai, Tsukuba, Ibaraki 305-8571, Japan

E-mail: [Sorensen@dmb.chem.tsukuba.ac.jp](mailto:Sorensen@dmb.chem.tsukuba.ac.jp)



Macrocyclic receptors are capable of strongly binding guests, but for some applications such as sensors and catalysts, it is desirable for the binding to be reversible. The binding can often be reversed through heating, adding competing ligands, or changing solvents. These methods are not always repeatable or practical, so we set out to design a receptor that could bind guests with binding affinities that can be regulated with irradiation of light.

We aim to create supramolecular structures consisting of photoresponsive units and recognition sites. Azobenzene<sup>1</sup> was chosen as the photoresponsive unit as it can undergo reversible *cis-trans* isomerization by irradiation, changing the geometry of the entire molecule. Azobenzene has been widely applied as a chemically stable, easy to synthesize supramolecular building blocks. Salen complexes can be formed through condensation of a diamine and a salicylaldehyde, and act as recognition sites that can bind guests through coordination in the axial site.<sup>2</sup> Macrocycles containing multiple salen recognition sites can be formed by using building blocks containing two salicylaldehyde moieties and diamines. Building blocks with three or more units can yield three-dimensional cages. The size of the cages depends on the angle and flexibility of the substituents.<sup>3</sup>

Based on these considerations we designed the azobenzene bis-salicylaldehyde **1**. **1** was reacted with diamine **4** to yield salen-based macrocycle H<sub>6</sub>**2**, and with triamine **5** to yield molecular cage H<sub>6</sub>**3** (Figure 1). The structures of the ligands and their metal complexation were investigated as well as their photochemical properties.

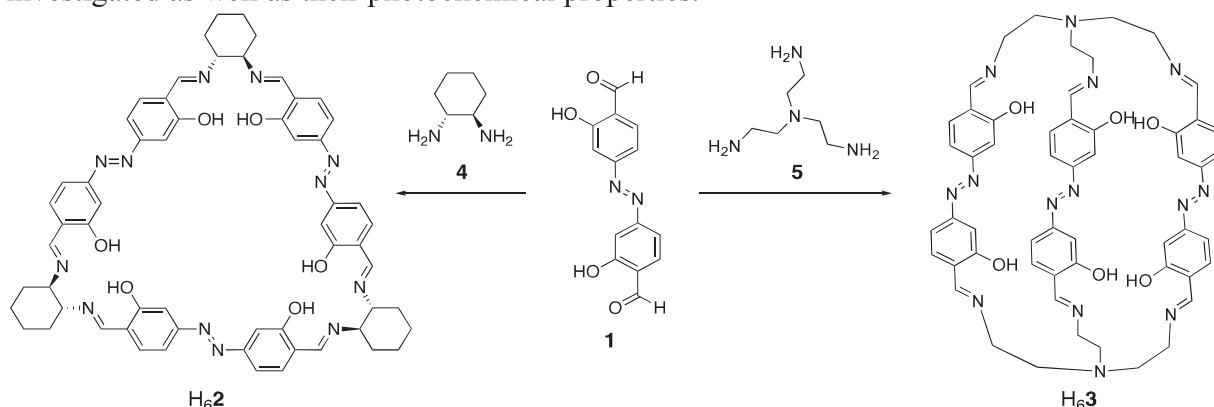


**Figure 1.** Synthesis of macrocycle H<sub>6</sub>**2** and molecular cage H<sub>6</sub>**3** from azobenzene bis-salicylaldehyde **1**.

## References

- [1] J. Vapaavuori, C. G. Bazuin, A. Priimagi, *J. Mater. Chem. C* **2018**, *6*, 2168.
- [2] T. Nakamura, Y. Kawashima, E. Nishibori, T. Nabeshima, *Inorg. Chem.* **2019**, *58*, 7863.
- [3] T. Yuan, Z. Q. Wang, X.-Q. Gong, Q. Wang, *Tetrahedron Lett.* **2020**, *61*, 152626.

# Carrier Properties and The Possible Cause for Low Donor Activation of As-doped BaSi<sub>2</sub> Thin Films

Nurfauzi Abdillah<sup>1</sup>, Yuka Fukaya<sup>1</sup>, Kaoru Toko<sup>1</sup>, Takashi Suemasu<sup>1</sup>

<sup>1</sup>Institute of Pure and Applied Sciences, University of Tsukuba, 1-1-1 Tennodai, Tsukuba, Ibaraki 305-8573, Japan

E-mail: s2326034@u.tsukuba.ac.jp



## Introduction

Barium Disilicide (BaSi<sub>2</sub>) is deemed as one of the alternative materials for thin film solar cells due to its fitting electrical and optical properties [1]. Currently, the main hindrance towards high performing BaSi<sub>2</sub> homojunction solar cells is the fabrication of high-quality n-type BaSi<sub>2</sub> layer [1]. Previously, the fabrication and enhancement of n-type As-doped BaSi<sub>2</sub> thin film has been demonstrated grown by molecular beam epitaxy (MBE) using GaAs as the source of arsenic doping [2,3]. However, the carrier concentration is not well controlled. In our recent experiments, the ratio between electron and arsenic concentration is low in the range of 5 – 10%. In this study, we vary the Ba-to-Si deposition rate ratio ( $R_{Ba}/R_{Si}$ ) to optimize the electron concentration and discuss the potential culprit of the low donor activation of As-doped BaSi<sub>2</sub>.

## Experimental Method

In this work, As-doped BaSi<sub>2</sub> films were grown on top of p-Si(111) substrates using MBE method. The steps of thin-film growth are carried out as in the previous report [2]. The substrate temperature ( $T_S$ ) during growth was set to 550°C and GaAs crucible temperature ( $T_{GaAs}$ ) was set to 650°C and 700°C. The  $R_{Ba}/R_{Si}$  was varied between 1.6 – 3.1. The carrier concentration and mobility were measured at room temperature using Van der Pauw method. The photoresponsivity was measured using a xenon lamp and a 25-cm focal length single monochromator (Bunko Keiki SM-1700A and RU-60N). SIMS measurements are carried out to identify the arsenic concentration incorporated into the grown films.

## Results and Discussion

Fig. 1 shows the measured carrier concentration and hall mobility in respect to the varying  $R_{Ba}/R_{Si}$ . In this case,  $T_{GaAs}$  is set to 700°C. As can be seen, n-type films are obtained at  $R_{Ba}/R_{Si}$  of 2.2 and 2.8. In general, increasing (decreasing) trend can be observed for carrier concentrations (mobility) towards higher  $R_{Ba}/R_{Si}$ . For the n-type films themselves, the carrier concentrations from  $5.95 \times 10^{17} \text{ cm}^{-3}$  to  $9.96 \times 10^{17} \text{ cm}^{-3}$  by increasing the  $R_{Ba}/R_{Si}$  from 2.2 to 2.8. This improvement can be attributed to more vacant silicon sites available to be occupied during the growth process. Subsequently, donor activation also increases, from 6% to 10%.

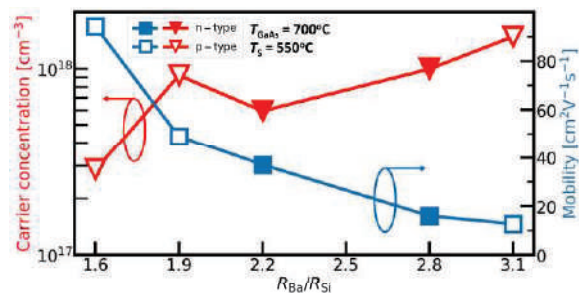


Fig. 1. Carrier Properties vs  $R_{Ba}/R_{Si}$ . Red marker denotes carrier concentration while blue marker denotes mobility

## References

- [1] T. Suemasu and D. B. Migas, *Phys. Status Solidi A* **219**, 2100593 (2022).
- [2] S. Aonuki, Y. Yamashita, K. Toko, and T. Suemasu, *Jpn. J. Appl. Phys.* **59**(SF), SFFA01 (2020).
- [3] S. Aonuki, Z. Xu, Y. Yamashita, K. Gotoh, K. Toko, N. Usami, ... and T. Suemasu, *Thin Solid Films* **724**, 138629 (2021).



# Manganese-doped perovskite microcavities are used in laser resonators

Pei Zhenhao<sup>1</sup>

<sup>1</sup> *Institute of East China Normal University, Shanghai, CHINA*

*E-mail: 51265904119@stu.ecnu.edu.cn*



Colloidal CsPbX<sub>3</sub> (X = Br, Cl, and I) perovskite nanocrystals exhibit adjustable bandgaps across the visible spectrum and high photoluminescence quantum yields in the green and red regions. However, their development for optoelectronic applications is constrained by the lack of efficient blue-emitting perovskite nanocrystals.<sup>[1]</sup>

To date, various ions have been explored as dopants for CsPbX<sub>3</sub> nanocrystals.<sup>[2]</sup> Among these, Mn<sup>2+</sup> doped CsPbBr<sub>3</sub> nanocrystals were synthesized using the ligand-assisted reprecipitation method at room temperature, exhibiting tunable photoluminescence from green to deep blue. A blue-emitting nanocrystal with a central wavelength of 465 nm and a full width at half maximum (FWHM) of 0.8 nm was achieved. This blue shift indicates successful Mn<sup>2+</sup> incorporation into the perovskite lattice. The shift can be attributed to the smaller ionic radius of Mn<sup>2+</sup> compared to Pb<sup>2+</sup>, which leads to lattice contraction.<sup>[3]</sup> However, no direct Mn<sup>2+</sup> emission was detected in these compounds, leaving questions regarding the energy transfer mechanisms within the system that require further investigation.

## References

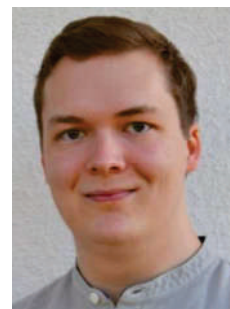
- [1] D. Parobek, B. J. Roman, Y. Dong, H. Jin, E. Lee, M. Sheldon, and D. H. Son, “Exciton-to-dopant energy transfer in Mn-doped cesium lead halide perovskite nanocrystals,” *Nano Lett.* 16, 7376–7380 (2016).
- [2] Yang, W. S.; Park, B. W.; Jung, E. H.; Jeon, N. J.; Kim, Y. C.; Lee, D. U.; Shin, S. S.; Seo, J.; Kim, E. K.; Noh, J. H.; et al. Iodide Management in Formamidinium-Lead-Halide-Based Perovskite Layers for Efficient Solar Cells. *Science* 2017, 356, 1376–1379.
- [3] Yi, C.; Luo, J.; Meloni, S.; Boziki, A.; Ashari-Astani, N.; Gratzel, C.; Zakeeruddin, S. M.; Rothlisberger, U.; Gratzel, M. Entropic stabilization of mixed A<sup>+</sup> cation ABX<sub>3</sub> metal halide perovskites for high performance perovskite solar cells. *Energy Environ. Sci.* 2016, 9, 656–662.

# Spray-Flame Synthesis of Mn and V Substituted Perovskite-Type LaCoO<sub>3</sub>

Leon Müller<sup>1</sup>, A. Hareendran<sup>2</sup>, C. Leroy<sup>2</sup>, M. Muhler<sup>2</sup>, C. Schulz<sup>1</sup>,  
H. Wiggers<sup>1</sup>

<sup>1</sup> *Institute for Energy and Materials Processes – Reactive Fluids, University of Duisburg-Essen, Duisburg, Germany*

<sup>2</sup> *Technical Chemistry, Ruhr-University Bochum, Bochum, Germany*  
E-mail: leon.mueller@uni-due.de



Reducing the environmental impact of chemical processes and water electrolysis is one of the most important challenges for a sustainable future. Heterogeneous catalysts play a major role in energy-intensive processes, so they provide a great opportunity for improvements in energy efficiency by exploring novel and highly active materials. Especially transition metal-based perovskites with the general composition ABO<sub>3</sub> are highly versatile catalysts due to their compositional flexibility. LaCoO<sub>3</sub> in particular has one of the highest catalytic activities for oxygen evolution reaction (OER) [1] and substitutional doping of A- and B-site cations in LaCoO<sub>3</sub>-type structures is widely used to tailor their electronic properties for OER.[2]

Spray-flame synthesis (SFS) is an elegant alternative compared to wet-chemical methods for obtaining nanoscale, ligand free mixed metal oxide particles in one step via gas-phase synthesis. SFS of such materials including substitutional doping will be discussed. Characterization was conducted by X-ray diffraction (XRD), Raman spectroscopy and transmission electron microscopy (TEM) for structural and morphological investigation as well as by X-ray photoelectron spectroscopy (XPS) for confirmation of elemental composition. Typically, the particles show high crystallinity and count median diameters below 10 nm. Rietveld-refinement of the X-ray diffractograms proved phase purity for all materials except for Vanadium contents above LaCo<sub>0.9</sub>V<sub>0.1</sub>O<sub>3</sub>. Catalytic tests of the perovskite materials for alcohol oxidation and oxygen evolution reaction (OER) showed highest conversion of cyclohexane for LaCo<sub>0.5</sub>V<sub>0.5</sub>O<sub>3</sub>, greatest OER activity utilizing LaCoO<sub>3</sub>. LaCo<sub>0.5</sub>Mn<sub>0.5</sub>O<sub>3</sub> was the material with highest conversion and selectivity for thermal ethylene glycol oxidation while LaCo<sub>0.95</sub>V<sub>0.05</sub>O<sub>3</sub> was the most promising one for electrochemical ethylene glycol oxidation.

## References

- [1] T.Yun et al. Nat. Commun. 2021, 12, 824
- [2] C. Sun et al., Adv. Energy Mater. 2021, 11, 2000459

# Carbon Composites from Novel Metal Organic Framework on Fullerene Assemblies (MOFOF) for Energy Conversion Application



Rabindra Nath Acharyya<sup>1,2</sup>, Katsuhiko Ariga<sup>1,3</sup>, Lok Kumar Shrestha<sup>1,2,\*</sup>

<sup>1</sup>Research Center for Materials Nanoarchitectonics (MANA), National Institute for Materials Science (NIMS), 1-1 Namiki, Tsukuba 305-0044, Ibaraki, Japan

<sup>2</sup>Graduated School of Pure and Applied Sciences, University of Tsukuba, 1-1-1 Tennodai, Tsukuba, Ibaraki 305-8573, Japan

<sup>3</sup>Department of Advanced Materials Science, Graduate School of Frontier Sciences, The University of Tokyo, 5-1-5 Kashiwanoha, Kashiwa, Chiba 277-8561, Japan

E-mail: [s2336012@u.tsukuba.ac.jp](mailto:s2336012@u.tsukuba.ac.jp)

## Content

Fullerenes, is a spherical zero-dimensional molecule composed of hexagonal and pentagonal rings, with a network of sp<sup>2</sup>-hybridized carbon atoms [1]. It can be assembled into various nanostructures with unique shapes and distinct properties. Besides, metal-organic frameworks (MOFs) are a group of porous materials with a large surface area and tunable porosity, and their combination into composites with various materials has shown promises in various applications, including gas/energy storage and catalysis [2, 3]. MOFs and their composites are often used as precursor to create functional carbon materials that has a huge potential for their applications in energy storage, catalysis, and environmental remediation [4]. Here in, a novel method is reported for synthesis of MOFOF by layer-by-layer approach. Fullerene nanostructures, especially fullerene nanotube (FNT) was synthesized by using a dynamic liquid–liquid interfacial precipitation (DLLIP) method involving self-assembly at the interface between a good solvent (Mesitylene) higher C<sub>60</sub> solubility, and anti-solvent (IPA) lower C<sub>60</sub> solubility. Then, FNT was oxidized by using concentrated H<sub>2</sub>SO<sub>4</sub> and HNO<sub>3</sub> (1:1). MOF was grown on oxidized FNT by layer-by-layer approach using the metal ions (Co(NH<sub>3</sub>)<sub>2</sub>.6H<sub>2</sub>O) and ligands (2-methylimidazol). After growing the MOF-on-FNT, MOFOF was characterized by using SEM, Raman FTIR, XRD, XPS and pyrolysis at different temperature and N-doped to get the hierarchical carbon composites. Therefore, combination of fullerene nanoarchitectonics and MOFs can be a promising material to develop of a new class advanced hierarchical carbon composites material with unique properties and functionalities for energy storage and conversion applications.

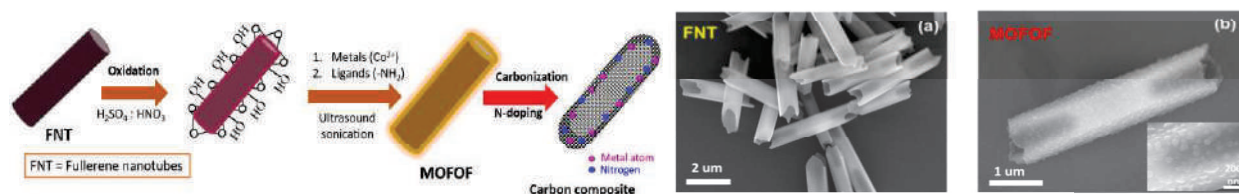


Fig. Experimental overview and SEM images of (a) FNT ; (b) MOFOF

## References

- [1] K. Ariga, L. K. Shrestha, *Mater. Adv.* **2**(2), 582-597 (2021)
- [2] B.N. Bhadra, L.K. Shrestha, Y. Yamauchi, K. Ariga, *ACS Appl. Mater. Inter.* **16**, 41363–41370 (2024)
- [3] Y. Xue, S. Zheng, H. Xue, H. Pang, *J. Mater. Chem. A.* **7**, 7301-7327 (2019)
- [4] K. Ariga, T. Mori, L. K. Shrestha, J. P. Hill, *Sci. Technol. Adv. Mater.* **20**, 51-95 (2019)

# Influences of Cobalt on the Coercivity of $(\text{Sm}_8\text{Zr}_2)(\text{Fe}_{1-x}\text{Co}_x)\text{Ti}_y\text{V}_z\text{Cu}_{0.5}$ -Based Magnets

S. Toni <sup>1,2,\*</sup>, N. Kulesh <sup>2</sup>, H. Sepehri-Amin <sup>1,2</sup>

<sup>1</sup>Graduated School of Pure and Applied Sciences, University of Tsukuba, 1-1-1 Tennodai, Tsukuba, Ibaraki 305-8573, Japan

<sup>2</sup>National Institute for Materials Science, 1-2-1 Sengen, Tsukuba, Ibaraki 305-0047, Japan

E-mail: [s2430109@u.tsukuba.ac.jp](mailto:s2430109@u.tsukuba.ac.jp)



High-performance permanent magnets are widely used in green energy conversion applications such as electric vehicles and wind turbines. Current research interest is focused on the development of high-performance permanent magnets without reliance on scarce elements. Rare-earth lean  $\text{SmFe}_{12}$ -based compounds with  $\text{ThMn}_{12}$ -type crystal structure have attracted a great attention as a potential compound for the next generation high-performance permanent magnets due to their excellent intrinsic magnetic properties; large saturation magnetization  $\mu_0 M_s = 1.64$  T, magnetic anisotropy field  $\mu_0 H_A = 12$  T, and Curie temperature  $T_c = 555$  K [1]. One problem is that this phase is thermodynamically unstable and partial substitution of Sm or Fe with non-magnetic phase stabilizing elements is necessary to realize 1:12 phase which is at the expense of saturation magnetization [2]. To realize a sufficiently large magnetization, it is necessary to design an alloy with a minimal amount of stabilizing elements. An alternative approach is to partially substitute Fe with Co, as was demonstrated for  $\text{Sm}_{0.8}\text{Zr}_{0.2}(\text{Fe}_{0.8}\text{Co}_{0.2})_{11.5}\text{Ti}_{0.5}$  compound, which exhibits  $\mu_0 M_s = 1.53$  T,  $\mu_0 H_A = 8.4$  T, and  $T_c = 830$  K [3]. Remaining challenge toward industrial application of these material is to transfer their excellent intrinsic magnetic properties to the extrinsic ones; large coercivity and remanence. In this study, we investigated the effect of Co addition on the coercivity of  $(\text{Sm}_8\text{Zr}_2)(\text{Fe}_{1-x}\text{Co}_x)\text{Ti}_y\text{V}_z\text{Cu}_{0.5}$ -based melt-spun ribbons.

Figure 1 shows coercivity as a function of Co content in the optimally annealed ribbons with compositions of  $\text{Sm}_8\text{Zr}_2\text{Fe}_{(76.5-x)}\text{Co}_x\text{Ti}_5\text{V}_8\text{Cu}_{0.5}$  and  $\text{Sm}_8\text{Zr}_2\text{Fe}_{(76.5-x)}\text{Co}_x\text{Ti}_8\text{V}_5\text{Cu}_{0.5}$ . It was found that the coercivity reduction upon addition of Co is more rapid in V-rich sample than that of Ti-rich sample. Figure 2 shows x-ray diffraction (XRD) patterns of these samples. By applying partial least squares (PLS) regression to XRD data, it was found that the presence of  $\alpha$ -Fe in V-rich samples could be the reason for the rapid coercivity reduction. In addition, the formation of a  $\text{TbCu}_7$ -type phase structure must also be considered when determining how coercivity is reduced. Based on detailed microstructure characterizations, we will discuss the origin for the rapid coercivity reduction upon addition of Co in the samples with different Ti/V ratios.

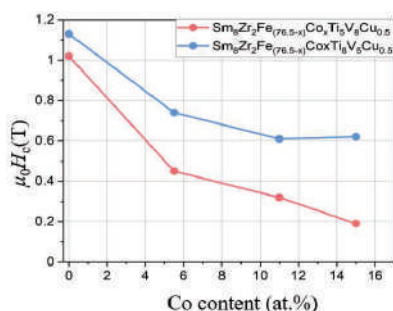


Figure 1. SQUID results show that coercivity decreases as cobalt content rises.

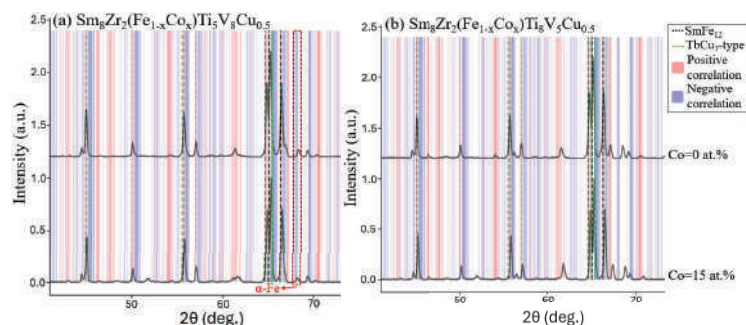


Figure 2. XRD results show the development of phases that arise in (a)  $\text{Sm}_8\text{Zr}_2(\text{Fe}_{1-x}\text{Co}_x)\text{Ti}_5\text{V}_8\text{Cu}_{0.5}$  and (b)  $\text{Sm}_8\text{Zr}_2(\text{Fe}_{1-x}\text{Co}_x)\text{Ti}_8\text{V}_5\text{Cu}_{0.5}$  before and after 15 at.% cobalt addition.

## References

- [1] Hirayama, Y., Takahashi, Y. K., Hirose, S. & Hono, K. *Scripta Materialia* **138**, 62–65 (2017).
- [2] Tozman, P., Sepehri-Amin, H., Ohkubo, T., Hono, K. *Journal of Alloys and Compounds* **855**, 157491 (2021).
- [3] Tozman P., Sepehri-Amin H., Hono, K. *Scripta Materialia* **194**, 113686 (2021).

# Highly dopable ESIPT molecule-based microsphere WGM laser.



Shunya A<sup>1</sup>, Hiroshi Y<sup>1</sup>, Tsuneaki S<sup>2</sup>, Yohei Y<sup>1</sup>.

<sup>1</sup>Graduated School of Pure and Applied Sciences, University of Tsukuba, 1-1-1 Tennodai, Tsukuba, Ibaraki 305-8573, Japan

<sup>2</sup>Faculty of Molecular Chemistry and Engineering, Kyoto Institute of Technology, 1 Hashikami-cho, Matsugasaki, Sakyo-ku, 606-8585 Kyoto, Japan

E-mail: s2320400@u.tsukuba.ac.jp

Laser devices based on organic materials have been actively studied due to their advantages, such as the ability to easily tune the oscillation wavelength through molecular design. Especially whispering gallery mode (WGM) microsphere resonators created by molecular self-assembly have attracted attention due to their small mode volumes and high Q-values. While various materials have been investigated to realize high-performance laser devices, this study suggests Excited-State Intramolecular Proton Transfer (ESIPT) molecules that can be doped at high concentrations. ESIPT molecules have been reported to be excellent laser dyes because of their large Stokes shift due to the four-level emission process. In this study, a low-threshold laser oscillation was achieved by using a polymer that does not aggregate easily even at high concentrations, ensuring a high gain at high concentrations.

Microsphere laser cavities were created by self-assembly using the mini-emulsion method. C4-CC-HBT (Fig1), based on 2-(2-hydroxyphenyl) benzothiazole (HBT) was doped into PMMA to fabricate microspheres, and the laser oscillation characteristics were confirmed by Fs-laser pumping (Fig2). The relationship between doping concentration and threshold was confirmed by measuring the threshold for spheres with different doping concentrations. As a result, this ESIPT molecule was able to create spheres without aggregation or crystallization in a high concentration range ( $\sim 40\text{wt}\%$ ), confirming laser oscillation. Furthermore, the threshold of laser oscillation was found to decrease significantly as the concentration of ESIPT molecules increased (Fig3).

While previous studies have mainly focused on molecular design to increase quantum yield for low-threshold laser materials, this study suggests a different approach. By designing molecules that can be doped at high concentrations, large gains can be ensured, and low-threshold laser oscillation can be expected.

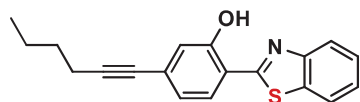


Fig1. C4-CC-HBT

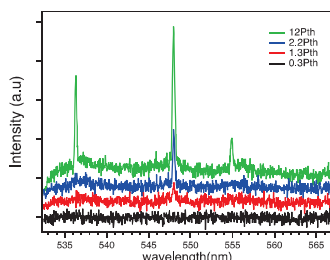


Fig2. Lasing property

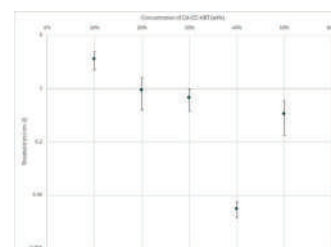


Fig3. Plot of threshold and concentration

## References

[1] Wanying Zhang, et al. *Langmuir* **2019** 35 (43), 14031-14041

# Relationship between Heat Storage Properties and Crystallite Size of Lambda-Type Titanium Pentoxide



Riku Seiki,<sup>1</sup> Tomoko Kubota,<sup>1</sup> Akito Fujisawa,<sup>1</sup> Akhmad Fadel Fadilla,<sup>1</sup> Shin-ichi Ohkoshi,<sup>2</sup> Hiroko Tokoro<sup>1</sup>

<sup>1</sup> Department of Materials Science, Faculty of Pure and Applied Sciences, The University of Tsukuba, 1-1-1 Ten-nodai, Tsukuba, Ibaraki 305-8577, Japan

<sup>2</sup> Department of Chemistry, School of Science, The University of Tokyo, 7-3-1 Hongo, Bunkyo-ku, Tokyo, Japan

E-mail: s2430085@u.tsukuba.ac.jp

[Introduction] The lambda-type trititanium pentoxide ( $\lambda$ -Ti<sub>3</sub>O<sub>5</sub>) was reported as a pressure-responsive heat-storage material to preserve thermal energy in the long-term<sup>[1, 2]</sup>. In this study, we developed a synthesis method for  $\lambda$ -Ti<sub>3</sub>O<sub>5</sub> simply by preparing a precursor using titanium chloride (TiCl<sub>4</sub>) as a starting material and evaluated the heat-storage properties<sup>[3]</sup>.

[Experiment] A mixed solution of H<sub>2</sub>O, TiCl<sub>4</sub>, and NH<sub>3</sub> was prepared in a round bottle flask. The solution was stirred at 50 °C for 20 hours in an oil bath. The precipitation was extracted from the solution by centrifugation, washed with ethanol, and heated at 60 °C for 24 hours. Then the obtained precursor was sintered under a hydrogen flow of 0.5 dm<sup>3</sup> min<sup>-1</sup> at 1100 °C for 5 hours to synthesized a black powder sample.

[Result] XRF measurement indicated that the composition formula was Ti<sub>3.00(5)</sub>O<sub>5.00(5)</sub> (Calculated: Ti 64.22, O 35.78 wt%; Found: Ti 64.53, O 35.47 wt%). SEM image showed that the particle size is 299 ± 54 nm. PXRD pattern with Rietveld analysis indicated that the obtained sample was a single phase of  $\lambda$ -Ti<sub>3</sub>O<sub>5</sub> (monoclinic, *C*2/*m*; *a* = 9.8332(2) Å, *b* = 3.78568(7) Å, *c* = 9.9688(2) Å,  $\beta$  = 91.259(2) °) and the crystallite size was estimated 57 ± 3 nm. The pressure threshold ( $P_{th}$ ) for converting 50 % of  $\lambda$ -Ti<sub>3</sub>O<sub>5</sub> to  $\beta$ -Ti<sub>3</sub>O<sub>5</sub> was approximately 300 MPa. The transition enthalpy ( $\Delta H_{trans}$ ) for converting pressure-induced  $\beta$ -Ti<sub>3</sub>O<sub>5</sub> to  $\lambda$ -Ti<sub>3</sub>O<sub>5</sub> was 144 kJ L<sup>-1</sup> at 462 K. The examination of the relationship between the crystallite size and these two heat-storage properties (the  $P_{th}$  and the  $\Delta H_{trans}$ ) demonstrated that a reduction in crystallite size and an increase in ratio of surface atoms intensify the influence of surface energy on the Gibbs free energy and consequently it decreased the  $\Delta H_{trans}$ . Additionally, thermodynamics analyses showed that the reduction in  $\Delta H_{trans}$  makes the energy barrier between  $\lambda$ -Ti<sub>3</sub>O<sub>5</sub> and  $\beta$ -Ti<sub>3</sub>O<sub>5</sub> less like to dissipate, consequently it increased the  $P_{th}$ . Understanding the relationship is essential for developing more effective heat storage materials.

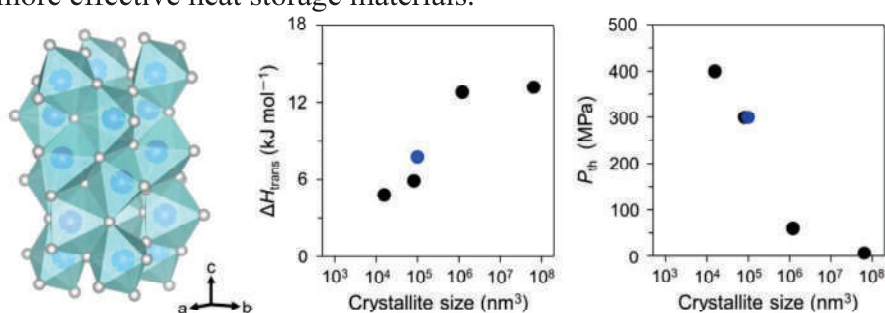


Fig. 1: Crystal structure of  $\lambda$ -Ti<sub>3</sub>O<sub>5</sub> (left),  $\Delta H_{trans}$  versus crystallite size plot (center), and  $P_{th}$  versus crystallite size plot (right). Black circles indicate previously reported data whereas blue circles indicate the present study.

## References

[1] S. Ohkoshi, et. al., *Nature Chem.* **2010**, 2, 539-545. [2] H. Tokoro, et. al., *Nature Commun.* **2015**, 6, 7037. [3] T. Kubota, R. Seiki, A. Fujisawa, A.F. Fadilla, F. Jia, S. Ohkoshi, H. Tokoro. et. al., *Materials Advances*, **2024**, 5, 3832-3837.

# Effect of Alkyl Chain Length on Photoinduced Crystal-Liquid Phase Transition in Para-Alkoxy Azobenzenes

Zhichao Wei<sup>1,2</sup>, Minghao Gao<sup>1,2</sup>, Keegan McGehee<sup>2</sup>, Dennis Kwaria<sup>2</sup>, Makoto Saikawa<sup>1,2</sup>, Yasuo Norikane<sup>2,1</sup>

<sup>1</sup>Graduate School Science and Technology, University of Tsukuba, 1-1-1 Tennodai, Tsukuba, Ibaraki 305-8573, Japan

<sup>2</sup>Electronics and Photonics Research Institute, National Institute of Advanced Industrial Science and Technology (AIST), 1-1-1 Higashi, Tsukuba, Ibaraki 305-8565, Japan

E-mail: [s2320402@u.tsukuba.ac.jp](mailto:s2320402@u.tsukuba.ac.jp)



## Introduction

Generally, the phase transition of a substance is induced by changes in temperature. However, certain organic materials, such as azobenzene derivatives,<sup>[1]</sup> exhibit a reversible photoinduced crystal-liquid phase transition (PCLT) at a constant temperature driven by *trans*→*cis* and *cis*→*trans* photoisomerizations. The molecular and crystal structures of azobenzenes are crucial in determining its photo-responsive properties. Our laboratory has previously reported that azo compounds with an asymmetric azo core and two *p*-alkoxy chains can undergo PCLT<sup>[2,3]</sup> In contrast to the previous azo compounds, azo molecules with simple single *p*-alkoxy chains have not been systematically investigated. The aim of the research is to explore the relationship between PCLT properties and alkyl chain length in the series of compounds Azo-OC<sub>n</sub> (**Fig.1a**). The structure-property relationships will be further discussed by crystal structure analysis. (**Fig.1d**)

## Results and Discussion

Eighteen compounds were synthesized. PCLT properties of most compounds were investigated under a polarizing microscope (POM) with exposure of ultraviolet and blue light irradiation at room temperature (**Fig.1b**). To study the rate of PCLT response across compounds, we observed the kinetics of the loss of birefringence at crossed polarizer orientation under POM with exposure of UV light (**Fig.1c**).<sup>[3]</sup> To further characterize the structure-property relationship of the compounds, we conducted thermal *cis*→*trans* isomerization kinetics, differential scanning calorimetry and single crystal X-ray diffraction experiments.

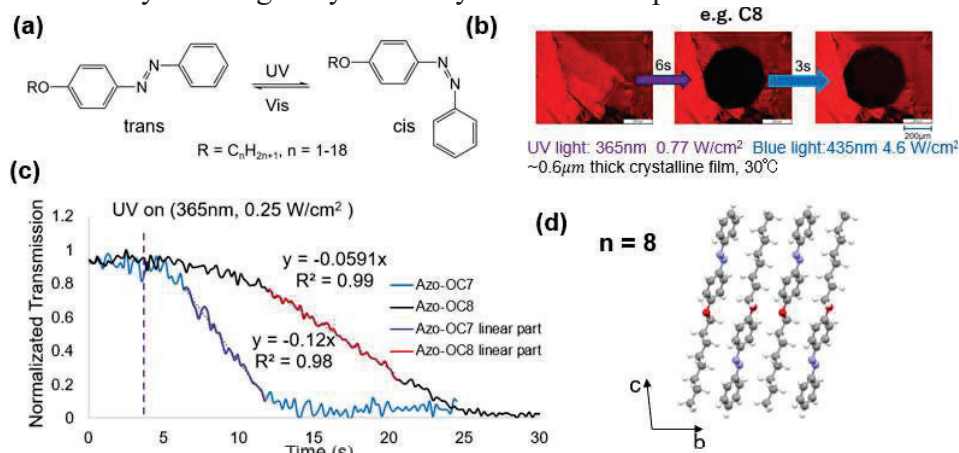


Fig.1. (a) The molecular structure of target compounds; (b) photomelting of Azo-OC8 under POM; (c) linear fitting typical data obtained by PCLT kinetics; (d) crystal structure of Azo-OC8.

## References

- [1] Y. Norikane, *et al.* *Chem. Commun.* **47**, 1770 (2011).
- [2] Y. Norikane, *et al.* *Org. Lett.* **16**, 5012 (2014).
- [3] Y. Norikane, *et al.* *J. Photopolym. Sci. Tech.* **29**, 149 (2016).

**Title: Computational Insights into Schottky barrier height of vertical Graphene and Borophene with  $XSi_2N_4$  ( $X= Mo, W$ ) monolayers.**

**Ammara Firdous<sup>1</sup>, Jalil Abdul<sup>2</sup>**

<sup>1</sup>Graduated School of Pure and Applied Sciences, University of Tsukuba, 1-1-1 Tenmodai, Tsukuba, Ibaraki 305-8573, Japan<sup>2</sup> Allama Iqbal Open University, Islamabad, Pakistan.

**E-mail: s2420400@u.tsukuba.ac.jp**



**Introduction:** Graphene a well-known, improved material monolayer has paved the way for the quest for new 2D materials in the exploration of remarkable experimental and theoretical study of extraordinary physical characteristics and functionalities. The Synthesis of  $MoSi_2N_4$  monolayer [1], an air-stable 2D semiconductor unlocks the extraordinary folds of structural, mechanical, transport, and optical properties, while its enigmatic of electrical contacts with 2H, 2H' Phase metals are yet to lighten up.

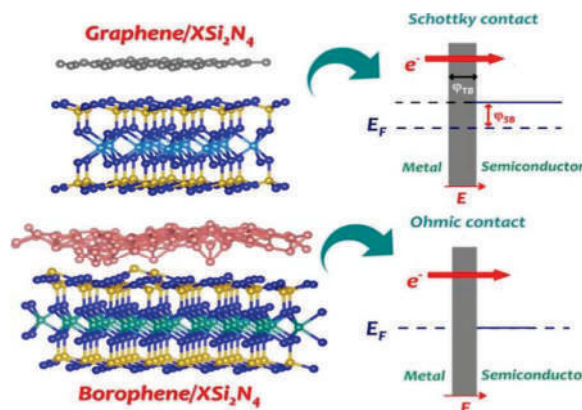
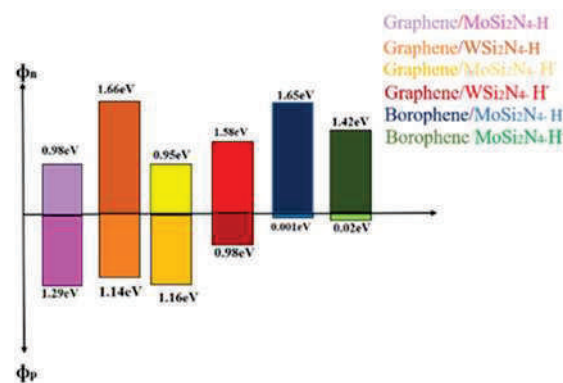


Figure 1: Schematics of Schottky and Ohmic Contacts among Graphene and Borophene based heterostructures.

**Methodology:** In this work, we devoted our efforts to calculating Structural Stability, Bonding Nature, Band Width, Schottky Barrier heights, and tunneling probabilities of  $XSi_2N_4$  based electrical contacts with metals using the First principle density functional theory calculations.

**Results:**  $XSi_2N_4$  ( $X=Mo, W$ ) with Graphene and Borophene exhibits extremely low Schottky barrier heights with high Tunneling Probability among interfaces in comparison with other 2D-heterostructures. The Novel Borophene Vertical contacts showed higher charge carrier mobility with more structural stability in comparison with graphene. The tunneling probability is determined to be 21.3% and 36.4% for these interfaces[2], showing a high efficiency of carrier injection. Our findings highlight the potential uses of Borophene-based heterostructures in barrier engineering and Ohmic contact design.



**References:**

[1] Q. Wang *et al.*, “Efficient Ohmic contacts and built-in atomic sublayer protection in  $MoSi_2N_4$  and  $WSi_2N_4$  monolayers,” *NPJ 2D Mater Appl*, vol. 5, no. 1, 2021, doi: 10.1038/s41699-021-00251-y.

[2] A. Jalil, T. Zhao, A. Firdous, A. Kanwal, S. R. Ali Raza, and A. Rafiq, “Computational Insights into Schottky Barrier Heights: Graphene and Borophene Interfaces with H- and  $\acute{H}$ - $XSi_2N_4$  ( $X = Mo, W$ ) Monolayers,” *Langmuir*, vol. 40, no. 16, pp. 8463–8473, Apr. 2024, doi: 10.1021/acs.langmuir.3c04045.



# Flower-like Cu<sub>2</sub>ZnSnS<sub>4</sub> (CZTS) Transition Metal Sulphides (TMS) as a Micro-structured Electrode in Lithium Rechargeable Battery



Maryam Hassan,<sup>1</sup> Muhammad Amirul Aizat Mohd Abdah,<sup>2</sup> Puvaneswaran Chelvanathan,<sup>2</sup> Yusran Sulaiman,<sup>3,4</sup> Fatin Saiha Omar,<sup>5,6</sup> Hassan Ahmoum,<sup>7</sup> Paolo Scardi,<sup>8</sup> and Mohd Sukor Su'ait\*<sup>1</sup>

<sup>1</sup> Solar Energy Research Institute (SERI), Universiti Kebangsaan Malaysia (UKM), Bangi, Malaysia

<sup>2</sup> Department of Chemistry, Faculty of Science, Universiti Teknologi Malaysia (UTM), Johor Bahru, Malaysia

<sup>3</sup> Department of Chemistry, Faculty of Science, Universiti Putra Malaysia (UPM), Serdang, Malaysia

<sup>4</sup> Functional Devices Laboratory, Institute of Advanced Technology, Universiti Putra Malaysia (UPM), Serdang, Malaysia

<sup>5</sup> Department of Applied Physics, Faculty of Science and Technology, Universiti Kebangsaan Malaysia (UKM), Bangi, Malaysia

<sup>6</sup> Battery Technology Research Group (UKMBATT), Polymer Research Centre (PORCE), Faculty of Science and Technology, Universiti Kebangsaan Malaysia (UKM), Bangi, Malaysia

<sup>7</sup> Faculty of Medicine and Pharmacy, Ibnu Zohr University, Agadir, Morocco

<sup>8</sup> Department of Civil, Environmental and Mechanical Engineering, University of Trento, Mesiano, Italy

\* E-mail: mohdsukor@ukm.edu.my

Lithium rechargeable batteries exhibit the advantages of high energy density with a broad range of potential applications, from portable electronics to highly energy-demanding electric vehicles. Recently, transition metal chalcogenides have been regarded as a promising candidate for a microstructure electrode in electrochemical energy storage devices because it has a higher theoretical capacity ( $\sim 847 \text{ mAh g}^{-1}$ ) compared to a commercial lithium-ion battery (LIB) ( $\sim 372 \text{ mAh g}^{-1}$ ).<sup>[1]</sup> Thus, this work aims to explore the capacity performance and cycling stabilities of the transition metal chalcogenide, Cu<sub>2</sub>ZnSnS<sub>4</sub> (CZTS) microstructure electrode using galvanometric method. The CZTS was synthesised *via* the sol-gel method followed by sulphurisation at 550 °C under nitrogen atmosphere. The structural analysis showed that the CZTS nanoflower took on morphology of kesterite phase and possessed an average chemical stoichiometric composition of Cu<sub>2.2</sub>Zn<sub>1.9</sub>Sn<sub>1.5</sub>S<sub>4</sub>.<sup>[2]</sup> The as-prepared CZTS-Li half-cell configuration exhibited high reversible capacity but lacked cycling performance at room temperature under a potential window from 3.00 to 0.01 V (vs. Li<sup>+</sup>/Li). The achieved initial discharge capacity is obtained at  $\sim 578.89 \text{ mAh g}^{-1}$ , which suggests that the kesterite CZTS can be a promising electrode material for lithium-CZTS rechargeable batteries.

## References

- [1] Wan, H., Peng, G., Yao, X., Yang, J., Cui, P., Xu, X. *Energy Storage Materials* **2016**, *4*, 59–65.
- [2] Tamin, C., Chaumont, D., Heintz, O., Chassagnon, R., Leray, A., Geoffroy, N., Guerineau, M., Adnane, M. *Boletín de la Sociedad Española de Cerámica y Vidrio* **2021**, *60*, 380–390.

# Monodispersed Organic Microcavities from Inkjet Printer as Biological Optical Probes

Kariana Kusuma Dewi<sup>1</sup>, Hiroshi Yamagishi<sup>2</sup>, Yohei Yamamoto<sup>3</sup>

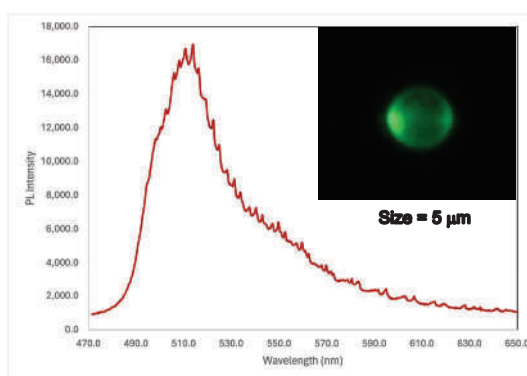
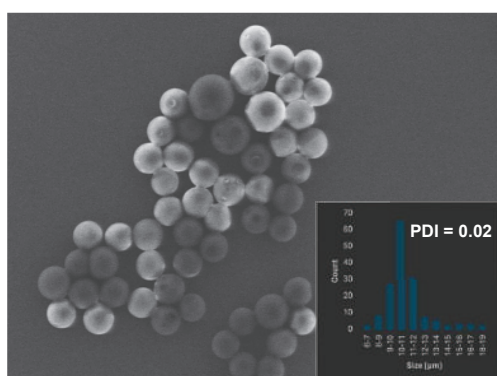
<sup>1</sup>Department of Materials Science, Institute of Pure and Applied Sciences

<sup>2</sup>Tsukuba Research Center for Energy Materials Science (TREMS), University of Tsukuba, Tsukuba, Ibaraki 305-8573, Japan School of Pure and Applied Sciences, University of Tsukuba, 1-1-1 Tennodai, Tsukuba, Ibaraki 305-8573, Japan



E-mail: s2336011@u.tsukuba.ac.jp

Biological detection based on optical devices have been developed largely in the last decade because of their high sensitivity. Proteomics is an example among them for characterizing a series of biological substances simultaneously, namely, it is a methodology for the comprehensive identification of proteins in the whole proteome of a cell. The library of the proteins provides key clues for understanding normal and abnormal behaviors of the cell and for elucidating important cellular pathways and pathogenesis.<sup>[1]</sup> In this study, we used an inkjet printer specialized for viscous liquid to produce organic WGM microresonator with a monodisperse size distribution. Typically, 1,2-dichlorobenzene solution of polystyrene (PS) with 9,10-bis(phenylethyl)anthracene (BPEA) as a luminescent dye was shot as tiny droplets onto aqueous solution containing sodium dodecyl sulfate (SDS, 2 mg mL<sup>-1</sup>). PS microspheres were successfully fabricated, and the concentration of PS was varied to make spheres with different diameters. The SEM images revealed that the size of the microspheres was controllable in a range of 5-15 μm by changing the concentration of PS in the mother solvent and the monodispersity of microsphere is calculated by polydispersity index (PDI). The optical performances were evaluated using a microscopic photoluminescence spectroscopy. We can evaluate WGM based on the periodic sharp peaks that appear together with a broad emission band originating from the spontaneous emission of BPEA. Based on the results, the resonance peaks of WGM are not significantly sharp, which might be due to the relatively low quality of the microspheres, however we get a clearly WGM peaks after decreasing the size into 5 μm. The perfect microsphere with a smooth surface might generate highly sharp peaks, meaning that the quality of the microspheres should be improved furthermore.



## References

[1] I. Y. Zhao et.al, Biosensors for Single-Cell Analysis 7, 36 (2022)

# A study on Thermoelectric Properties of PANI/ZnSb nanocomposite flexible films

Anmol Sharma<sup>1,a,b</sup>, N.S. Chauhan<sup>2,b</sup>, Takao Mori<sup>3,a,b</sup>

<sup>a</sup> Graduated School of Pure and Applied Sciences, University of Tsukuba, 1-1-1 Tennodai, Tsukuba, Ibaraki 305-8573, Japan

<sup>b</sup> Research Center for Materials Nanoarchitectonics (MANA), National Institute for Materials Science (NIMS), 1-1 Namiki, Tsukuba, Ibaraki 305-0044 Japan

Email:

<sup>1</sup> [s2330105@u.tsukuba.ac.jp](mailto:s2330105@u.tsukuba.ac.jp); [SHARMA.anmol@nims.go.jp](mailto:SHARMA.anmol@nims.go.jp)

<sup>2</sup> [CHAUHAN.NagendraSingh@nims.go.jp](mailto:CHAUHAN.NagendraSingh@nims.go.jp)

<sup>3</sup> [MORI.Takao@nims.go.jp](mailto:MORI.Takao@nims.go.jp)



## Abstract

Flexible Thermoelectric (TE) materials [1] can convert waste heat energy into electrical power, providing a potential energy source for numerous Internet of Things (IoT) devices without relying on batteries or cells. Traditional TE materials such as Bi<sub>2</sub>Te<sub>3</sub>, SnTe, PbTe, and ZnSb offer excellent TE properties but lack flexibility. In contrast, hybrid organic-inorganic materials have gained attention for their flexibility combined with promising TE performance, making them suitable for various IoT applications. Conducting organic polymers like PEDOT:PSS [2], PANI [3], PTh, and PPy are notable for their mechanical flexibility, easy processing, non-toxicity, and cost-effectiveness. Among these, polyaniline (PANI) stands out due to its favorable TE properties, including low intrinsic thermal conductivity and high electrical conductivity. However, many existing TE materials involve toxic or scarce elements, such as tellurium (Te) and selenium (Se). Our research focuses on incorporating non-toxic, cost-effective inorganic TE materials into a PANI matrix, specifically using ZnSb [4]—a non-toxic, inexpensive, and efficient TE material. We aim to explore the TE properties of flexible PANI/ZnSb hybrid films. Unlike traditional TE materials, the PANI/ZnSb hybrid offers both flexibility and promising TE performance (though not comparable with traditional ZnSb). ZnSb was synthesized via high-energy ball milling and incorporated into the PANI matrix at varying weight percentages (20% to 70%). The hybrid films were prepared through a solution-based method, involving dispersion in m-cresol, mixing with PANI/CSA, and subsequent casting and drying. The PANI/70% ZnSb composite achieved a high power factor of approximately  $\sim 10 \mu\text{W}/\text{m}\cdot\text{K}^2$  at 330 K, primarily due to an enhanced Seebeck coefficient,  $S \sim 52 \mu\text{V}/\text{K}$  at 330 K (Fig. 1). The high loading of ZnSb improved TE performance by increasing Seebeck coefficient despite a reduction in electrical conductivity. These findings suggest that incorporating non-toxic, cost-effective materials into flexible TE composites can yield significant performance improvements. Future work is anticipated to enhance performance further through the use of nanostructured ZnSb fillers.

## References

1. Y. Du et al. Applied Materials Today 12 366–388 (2018)
2. Wang, L., Zhang, Z., Liu, Y. et al. Nat Commun. 9, 3817 (2018)
3. Wang, Y., Zhang, S. M., and Deng, Y., J. Mater. Chem. A, 4, 3554–3559 (2016)

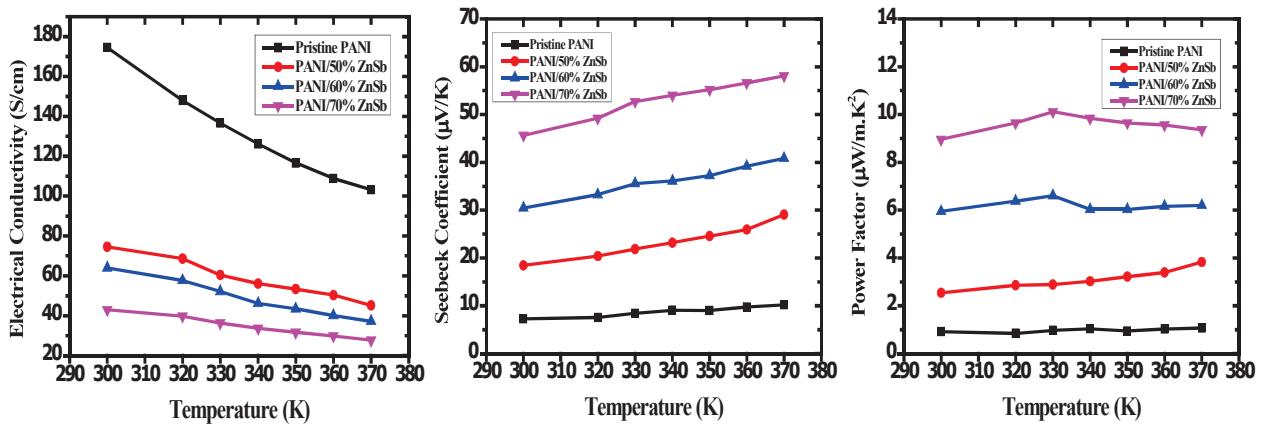


Fig. 1. Thermoelectric properties of PANI/ZnSb

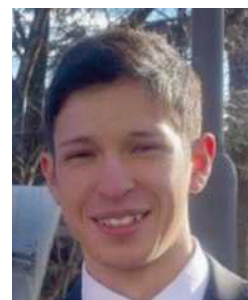
# Controlling the Rotational Behavior of Chiral Polymer Spheres with Optical Tweezers

Makoto Okumura<sup>1</sup>, Soh Kushida<sup>1</sup>, Ken-ichi Yuyama<sup>2</sup>, Yohei Yamamoto<sup>1</sup>

<sup>1</sup>Graduated School of Pure and Applied Sciences, University of Tsukuba, 1-1-1 Tennodai, Tsukuba, Ibaraki 305-8573, Japan

<sup>2</sup>Graduated Graduate School of Science Department of Chemistry, Osaka metropolitan University, Sugimoto, Sumiyoshi Ward, Osaka, 558-8585, Japan

E-mail: s2420399@u.tsukuba.ac.jp



## Content

When circularly polarized light (CPL) is applied to birefringent particles within an optical trapping system, the particles undergo rotational motion. This phenomenon occurs because the spin angular momentum of the CPL is transferred to the particles upon alteration of the light's polarization state after scattering<sup>[1]</sup>. Numerous studies have explored the optically induced rotation of achiral birefringent particles. However, in the case of chiral birefringent particles, such as cholesteric liquid crystal droplets, it has been observed that only one handedness of the CPL, which satisfies the Bragg reflection condition, induces rotation<sup>[2]</sup>.

In this study, we aimed to control the rotation of twisted bipolar spheres with a helicoidal structure composed of chiral  $\pi$ -conjugated polymers, as depicted in Figure 1, by applying various polarization states and intensities. The spheres have birefringence and lower chirality regime due to their helical structure, which may lead to the fabrication of novel micro-machines that show different rotation behavior for left and right CPL.

The spheres were fabricated using Poly(9,9-bis((S)-3,7-dimethyloctyl)-2,7-fluorene-alt-benzothiadiazole) via the vapor diffusion method. Initially, we investigated the orientation of the spheres relative to the electric field direction of linearly polarized light (LPL) at 1064 nm using a polarization optical microscope. It was found that the bipolar axis of the sphere was oriented perpendicular to the light incidence direction.

We have demonstrated the capability to manipulate the orientation of twisted dipolar microspheres composed of chiral conjugated polymers by irradiating them with LPL. As a subsequent step, we are currently investigating the relationship between the chirality of the polymer and the handedness of the light when the spheres undergo rotation in more detail.

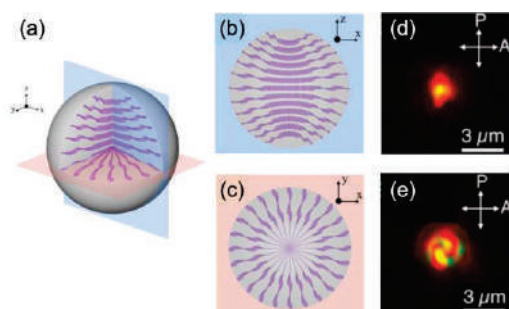


**Fig 1.** Schematic representation of polymer configuration within a chiral microsphere (a) and its cross-section views (b, c). Corresponding POM micrographs (d, e).

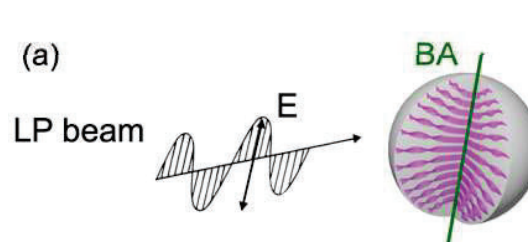


**Fig 2.** Alignment of bipolar axis (BA) with E field when irradiated by linearly polarized beam

## References

[1] Shangran Xie et al., *Sci. Adv.* **7**, eabf6053 (2021)

[2] Donato, M., Mazzulla, A., Pagliusi, P. et al. *Sci Rep.* **6**, 31977 (2016)

# Contact material optimization for the $\text{Mg}_3(\text{Sb,Bi})_2$ based thermoelectric compounds.

Aamir Muhammad Fasih<sup>1,2</sup>, R. Chetty<sup>2</sup>, B. Jayachandran<sup>2</sup>, T. Mori<sup>1,2\*</sup>

<sup>1</sup>Graduated School of Pure and Applied Sciences, University of Tsukuba, 1-1-1 Tennodai, Tsukuba, Ibaraki 305-8573, Japan

<sup>2</sup>International Center for Materials Nanoarchitectonics (MANA), National Institute for Materials Science (NIMS), 1-1 Namiki, Tsukuba 305-0044, Japan.

E-mail: [s2236004@s.tsukuba.ac.jp](mailto:s2236004@s.tsukuba.ac.jp)



Thermoelectric (TE) materials convert unutilized heat into electricity, which is one of the most promising technologies for harvesting energy [1,2]. Recently,  $\text{Mg}_3(\text{Sb,Bi})_2$  based TE compounds have received much attention due to their high thermoelectric conversion efficiencies [3,4]. However, there is still room to improve conversion efficiencies further by optimizing contact materials that provide both good electrical and thermal contact at their interfaces. In this study, the influence of sintering temperature on both the TE properties and electrical contact resistivity of the  $\text{Mg}_3(\text{Sb,Bi})_2$  based compounds is investigated. The TE element of SS/ $\text{Mg}_3(\text{Sb,Bi})_2$ /SS were fabricated by spark plasma sintering (SPS) at different temperatures of 973K, 1023K and 1073K for 5 minutes. Powder XRD of sintered  $\text{Mg}_3(\text{Sb,Bi})_2$  compounds confirm the phase purity. The effect of sintering shows no significant variation in the TE properties of  $\text{Mg}_3(\text{Sb,Bi})_2$  compounds. Specific contact resistivity of all the samples with interfaces was obtained by measuring the resistance drop across the interfaces using the resistance profiler. The contact resistivity of SS/ $\text{Mg}_3(\text{Sb,Bi})_2$ /SS decreased with increasing sintering temperature, which is most likely a result of improved densification and bonding strength at the interfaces. Further, the conversion efficiency was evaluated by measuring the power generation characteristics. Maximum conversion efficiency of 9.3% is obtained for the SS/ $\text{Mg}_3(\text{Sb,Bi})_2$ /SS at the temperature difference of 370 K. Thermal stability is ensured after 30 days at 673K.

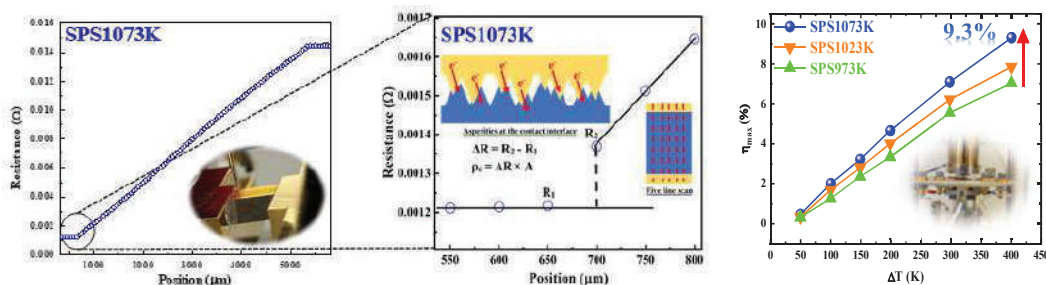


Fig.1: Contact resistance and conversion efficiency of SS/ $\text{Mg}_3(\text{Sb,Bi})_2$ /SS.

## Acknowledgments

This work is supported by the JST Mirai Program (JPMJMI19A1). AMF acknowledges support from MEXT Fellowship as well.

## References

- [1] L. E. Bell et al, Cooling, Heating, Generating Power, and Recovering Waste Heat with Thermoelectric Systems, *Science* 321, 1457 (2008).
- [2] T. Mori and S. Priya, Materials for energy harvesting: At the forefront of a new wave, *MRS Bull.*, 43, 176–180 (2018).
- [3] Z. Liu et al, and T. Mori, Demonstration of ultrahigh thermoelectric efficiency of ~ 7.3% in  $\text{Mg}_3\text{Sb}_2/\text{MgAgSb}$  module for low-temperature energy harvesting, *Joule*, 5, 1196–1208 (2021).
- [4] Z. Liu et al and T. Mori, Maximizing the performance of n-type  $\text{Mg}_3\text{Bi}_2$  based materials for room-temperature power generation and thermoelectric cooling, *Nat. Commun.*, 13, 1120 (2022).

# Systematic study of structural effects for proton and oxygen transport on nitrogen-doped carbon catalysts

Ravi Singh,<sup>1,2\*</sup> Katsuhiko Ariga,<sup>3,4</sup> Lok Kumar Shrestha,<sup>3,6</sup> Kotaro Takeyasu,<sup>5,6</sup>

<sup>1</sup> Graduate School of Science and Technology, University of Tsukuba, Japan

<sup>2</sup> Graduate School of Environmental Science, Hokkaido University, Japan

<sup>3</sup> Research Center for Materials Nano architectonics (MANA), National Institute for Materials Science, Japan

<sup>4</sup> Graduate School of Frontier Sciences, The University of Tokyo, Japan

<sup>5</sup> Institute for Catalysis, Hokkaido University, Japan

<sup>6</sup> Institute of Pure and Applied Sciences, University of Tsukuba, Japan

\*e-mail: s2336014@u.tsukuba.ac.jp



Proton exchange membrane fuel cells (PEMFCs) are pivotal for advancing clean energy technologies, with their efficiency being significantly influenced by the oxygen reduction reaction (ORR) at the cathode. While Pt-based catalysts have been the standard, their high cost necessitates exploring alternative catalysts. Although nitrogen-doped carbon as non-Pt-group metal catalysts show potential, their performance is hampered by low mass transport [1]. In nitrogen-doped carbon catalysts, the effect of pore size and distribution on oxygen mass transport has been well investigated. On the other hand, the current in the region below the limiting current density is dominated by proton diffusion. It is not at all clear what kind of macrostructure or surface structure is the key factor in proton transport. In order to fabricate catalysts with high performance, it is essential to design a structure that allows both oxygen and proton diffusion. However, it is difficult to systematically change the micro- and macrostructure of nitrogen-doped carbon catalysts prepared in a top-down method.

In the present study, by bottom-up synthesis using fullerenes as starting materials, we aimed to systematically change the structure of nitrogen-doped carbon catalysts and reveal the structural effects on mass transport. In the synthesis, carbon frames composed of fullerenes were prepared using the liquid-liquid interface precipitation (LLIP) method. Nitrogen doping was then performed by oxidation with mixed acids and heat treatment at 950°C in ammonia.

Figure 1 shows SEM images of the synthesized carbon tubes. It can be seen that the pore diameter and length of the tube are systematically varied. Figure 2 shows the measured activity of the synthesized nitrogen-doped carbon tubes. Although proton transport was slightly reduced for the catalyst using ethanol in the synthesis, overall, the pore size and length of the tubes did not significantly affect the overall activity. This means that structures larger than submicron do not significantly affect proton transport. The performance of nitrogen-doped carbon with controlled micropore distribution and surface graphiticity will also be compared, and structures that are effective for both proton and oxygen transport will be discussed.

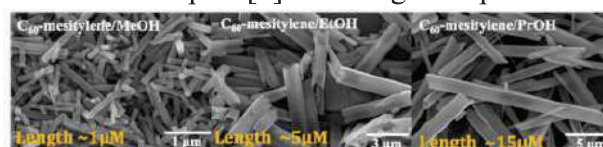


Fig1. Systematic increase of length in order from MeOH till PrOH

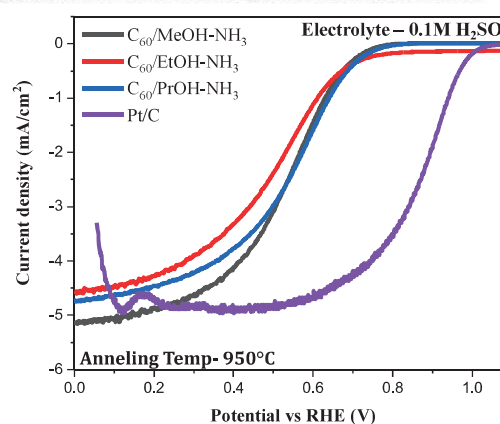


Fig 2. ORR measurement of the alcohol chain length catalyst



# Development of Flower like-nanocomposite Based $\text{Mg}(\text{Ti}_{0.99}\text{Sn}_{0.01})\text{O}_3$ Decorated on Reduced Graphene Oxide (rGO) as Supercapacitor Electrodes



Syadza Aisyah Hermadianti,<sup>1,2,5</sup> Murni Handayani,<sup>2,3,\*</sup> Muhammad Aulia Anggoro,<sup>1,2,5</sup> Desinta Dwi Ristiana,<sup>2</sup> Isa Anshori,<sup>4,5,\*</sup> Agung Esmawan,<sup>6</sup> Yosephin Dewiani Rahmayanti,<sup>2</sup> Andi Suhandi,<sup>7</sup> Gerald Ensang Timuda,<sup>2</sup> Gagus Ketut Sunnardianto,<sup>8,9,10</sup> Bambang Wisnu Widagdo,<sup>11</sup> and Frida Ulfah Ermawati,<sup>12,\*</sup>

<sup>1</sup> Department of Nanotechnology, Graduate School, Bandung Institute of Technology, Bandung, 40132, Indonesia

<sup>2</sup> Research Center for Nanotechnology Systems, National Research and Innovation Agency (BRIN), Tangerang Selatan, 15314, Indonesia

<sup>3</sup> Department of Chemical Engineering, Pamulang University (UNPAM), Pamulang, Tangerang Selatan, Banten, 15417, Indonesia

<sup>4</sup> School of Electrical Engineering and Informatics, Bandung Institute of Technology, Bandung, 40132, Indonesia

<sup>5</sup> Research Center for Nanoscience and Nanotechnology (RCNN), Bandung Institute of Technology, Bandung, 40132, Indonesia

<sup>6</sup> Department of Physics, Faculty of Mathematics and Natural Sciences, Universitas Gadjah Mada, Yogyakarta, 55281, Indonesia

<sup>7</sup> Research Center for Advanced Materials, National Research and Innovation Agency (BRIN), Tangerang Selatan, 15314, Indonesia

<sup>8</sup> School of Materials Science and Engineering, Nanyang Technological University, 50 Nanyang Avenue, Singapore 639798, Singapore

<sup>9</sup> Research Center for Quantum Physics, National Research and Innovation Agency (BRIN), Tangerang Selatan, 15314, Indonesia

<sup>10</sup> Research Collaboration Center for Quantum Technology 2.0, Bandung 40132, Indonesia

<sup>11</sup> Department of Informatic Engineering, Pamulang University, Tangerang Selatan, 15310, Indonesia

<sup>12</sup> Physics Department, Faculty of Mathematics and Natural Sciences, Universitas Negeri Surabaya, Surabaya, 60213, Indonesia

E-mail: [murn003@brin.go.id](mailto:murn003@brin.go.id), [dosen02710@unpam.ac.id](mailto:dosen02710@unpam.ac.id), [isaa@staff.stei.itb.ac.id](mailto:isaa@staff.stei.itb.ac.id) and [frida.ermawati@unesa.ac.id](mailto:frida.ermawati@unesa.ac.id)

The objective of this study was to synthesize ceramic materials of  $\text{Mg}(\text{Ti}_{0.99}\text{Sn}_{0.01})\text{O}_3$  and decorate them on reduced graphene oxide, thereby forming a nanocomposite of rGO/ $\text{Mg}(\text{Ti}_{0.99}\text{Sn}_{0.01})\text{O}_3$  (rGO/MTS001). Ascorbic acid was used as a reducing agent, while MTS001 was synthesized by solution mixing method. The successful synthesis results were confirmed by XRD (X-Ray Diffraction), UV-Vis (UV-Visible) analysis, FT-IR (Fourier Transform Infrared Spectroscopy), Raman Spectra, and SEM-EDS (Scanning Electron Microscopy-Energy Dispersive X-Ray Spectroscopy). The SEM Analysis revealed that the

MTS001 has a flower-like morphology, and the nanocomposites of rGO/MTS001 were decorated on the rGO's surface. The electrochemical performance of rGO/MTS001 and MTS001 was investigated by determining the specific capacitance obtained in 1 M H<sub>2</sub>SO<sub>4</sub> solution by cyclic voltammetry, followed by galvanostatic charge–discharge analysis using a three-electrode setup. The rGO/MTS001 achieved a specific capacitance of 361.97 Fg<sup>-1</sup>, compared to MTS001 (194.90 Fg<sup>-1</sup>). The capacitance retention of rGO/MTS001 nanocomposite also depicted excellent cyclic stability of 95.72% after 5000 cycles at a current density of 0.1 Ag<sup>-1</sup>. The result showed that the nanocomposite of ceramics with graphene materials has a potential for high performance supercapacitor electrodes.

# Development of an efficient and air-stable Pd(II) precatalyst

Li Weiqi<sup>1</sup>, Takaki Kanbara<sup>1</sup>, Junpei Kuwabara<sup>1</sup>.

<sup>1</sup> Institute of Pure and Applied Sciences, University of Tsukuba, 1-1-1 Tennodai, Tsukuba 305-8573, Japan.

E-mail: s2420404@u.tsukuba.ac.jp

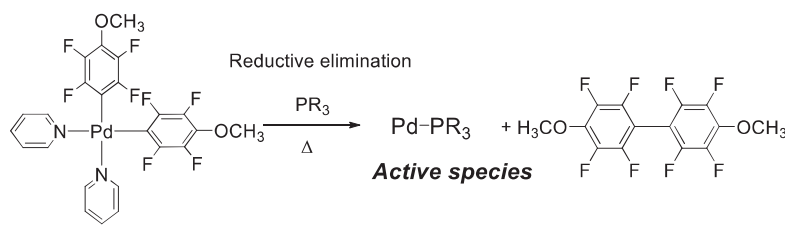


## 1. Introduction

Cross-coupling reactions are widely used in synthesizing pharmaceuticals and electronic materials, and palladium (Pd) complexes are common catalysts in these reactions. Pd precatalysts are classified by valence into Pd(II) and Pd(0). The active species are typically Pd(0) with a supporting ligand, such as phosphorus ligands. Due to the instability of the Pd(0) active species, stable precatalysts are used to generate the active species in the reaction system. Pd(II) precatalysts are stable during storage. However, converting Pd(II) to the active Pd(0) species requires a reduction process that causes side reactions.<sup>[1][2]</sup> In contrast, Pd(0) precatalysts do not need the reduction process.<sup>[3]</sup> However, the main disadvantage of Pd(0) precatalysts is instability in air. This research develops a new method for reducing the Pd(II) precatalyst to generate an active species [Pd(0)PR<sub>3</sub>] without side reactions.

## 2. Method

To develop this new precatalyst, a method is built up to reduce Pd(II) precatalyst, which will directly generate active species [Pd(0)PR<sub>3</sub>] without side reactions. For example, biaryl complexes of fluorobenzene are stable, making them easy to be isolated and stored. By adding ligands that promote reductive elimination, a Pd(0) species is generated along with producing a biaryl compound (Scheme 1). This controlled reduction process from the Pd(II) precatalyst prevents the undesired side reaction.<sup>[4]</sup>



## 3. Results and Discussion

I have currently synthesized the following precatalysts and reacted each of them with ligand P<sup>t</sup>Bu<sub>3</sub> at 100 ° C to verify their performance as precatalysts. Table 1 shows conversion rates from precatalyst to the active species after 24 h. The results show Pd(2,3,5,6-tetrafluoroanisole)<sub>2</sub>(pyridine)<sub>2</sub> is the best precatalyst among the tested complexes due to its high conversion rate.

Table 1. Conversion Rate of Active Species

[Precatalyst] + P <sup>t</sup> Bu <sub>3</sub>	Conversion Rate of Active Species
[Pd(C <sub>6</sub> F <sub>5</sub> ) <sub>2</sub> (tmeda)]	3%
[Pd(C <sub>6</sub> F <sub>5</sub> ) <sub>2</sub> (acetonitrile) <sub>2</sub> ]	18%
[Pd(C <sub>6</sub> F <sub>5</sub> ) <sub>2</sub> (pyridine) <sub>2</sub> ]	57%
[Pd(2,3,5,6-tetrafluoroanisole) <sub>2</sub> (pyridine) <sub>2</sub> ]	85%

## 4. Conclusion

The Pd(II) precatalysts coordinating with pyridine ligands perform better than those with tmeda or acetonitrile ligands in the steps of reductive elimination and generating active species. Therefore, pyridine-coordinated Pd(II) precatalysts are expected to show higher initial catalytic activity. In future research, I will investigate a wider variety of precatalysts and promoting ligands to evaluate their performance in catalytic activity and stability in air.

## References

- [1] F. Ozawa, A. Kubo, T. Hayashi, *Chem. Lett.* **1992**, 21, 2177–2180.
- [2] J. Kuwabara, M. Sakai, Q. Zhang, T. Kanbara, *Org. Chem. Front.* **2015**, 2, 520–525.
- [3] R. Sato, T. Kanbara, J. Kuwabara, *Organometallics* **2020**, 39, 235–238.
- [4] E. Gioria, J. del Pozo, J. M. Martínez-Illarduya, P. Espinet, *Angew. Chem., Int. Ed.* **2016**, 55, 13276–13280.

# Organic Switchable Organic Droplet Lasers for Laser Display

Masato Kato<sup>1</sup>, Junnosuke Miyagawa<sup>1</sup>, Shun-ichiro Noguchi<sup>1</sup>, Naoki Takada<sup>2</sup>, Soumei Baba<sup>2</sup>, Satoshi Someya<sup>3</sup>, Ankit Kumar Singh<sup>4</sup>, Jer-Shing Huang<sup>4</sup>, Yohei Yamamoto<sup>1</sup>, and Hiroshi Yamagishi<sup>1\*</sup>

<sup>1</sup> Department of Materials Science, Institute of Pure and Applied Sciences, and Tsukuba Research Center for Energy Materials Science (TREMS), University of Tsukuba, 1-1-1 Tennodai, Tsukuba, Ibaraki 305-8573, Japan.

<sup>2</sup> Research Institute for Energy Conservation, National Institute of Advanced Industrial Science and Technology (AIST), Tsukuba, Ibaraki 305-8564, Japan.

<sup>3</sup> Department of Mechanical Engineering, Tokyo Denki University, Senjyu Asahicho, Adachiku, Tokyo 120-8551, Japan.

<sup>4</sup> Nanooptics Research Group, Leibniz Institute of Photonic Technology, Albert-Einstein Strasse 9, Jena D-07745, Germany.

E-mail: s2320333@u.tsukuba.ac.jp



## 1. Introduction

Flat panel laser displays are enthusiastically pursued owing to the high brightness, high power conversion efficiency, and wide color gamut. Despite of the demands, the mechanical assembly of the laser panel displays is far more difficult due to the complexity and cost of fabricating the dense array of blue, green, and red laser oscillators in conventional semiconductor technologies. Here we invented the novel configuration of laser panel displays which employs the organic droplet lasers as each pixel. Organic droplet lasers, we recently reported<sup>[1]</sup>, consist of ionic liquids and organic dyes as optical resonators and gain materials, which exhibit exceptional chemical and physical stability, just drop-casting the solution onto the superhydrophobic substrate by inkjet printer. The droplet is highly deformable by external force, therefore we assumed that electric field can also deform droplet to spheroid, inducing the attenuation of Q-factor. We aim to develop the concept of the electrical Q-switching of droplet laser and integrate to laser panel displays.

## 2. Result and discussion

We fabricated the device which has the droplet laser arrays inside and sandwiched with hydrophobic substrate and ITO electrode. When applied the electric field, the peak shift and intensity decline of the lasing mode were observed in photoluminescence (PL) spectra. Angle-dependent observation revealed that the Q-factor was attenuated with the increased electric field, leading to the increment of laser threshold, especially at the detection angle of 20°. The threshold change enabled the continuous electrical Q-switching along with the electric field signals. Finally, we fabricated 2×3 droplet laser array device and successfully controlled each oscillator by electric field.

## References

[1] Yamagishi, H., Fujita, K., Miyagawa, J., Mikami, Y., Yoshioka, H., Oki, Y., *et al.* Pneumatically Tunable Droplet Microlaser. *Laser Photon. Rev.* **17**, 2200874 (2023).

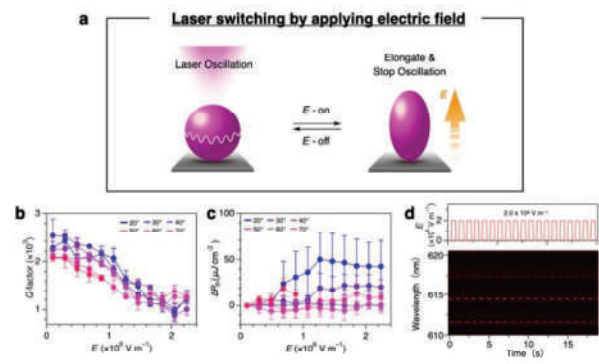


Fig.1. (a)Schematic representations of droplet deformation by electric field. (b,c) Plot of the Q-factor (b) and  $\Delta P_{th}$  (c) of a droplet with the increased electric field. (d) Continuous switching of the PL spectra along with periodic electric field.

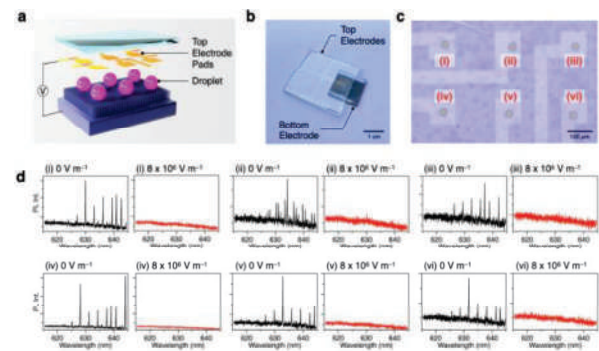


Fig.2. (a)Schematic representations of 2×3 droplet array device. (b,c) macroscopic (b) and microscopic (c) image of the device. (d) Individual switching of droplet laser array by electric field.

# Investigation of Regioselectivity and Reactivity in the Cross-Dehydrogenative Coupling Reaction of Disubstituted Benzenes with Polyfluoroarenes

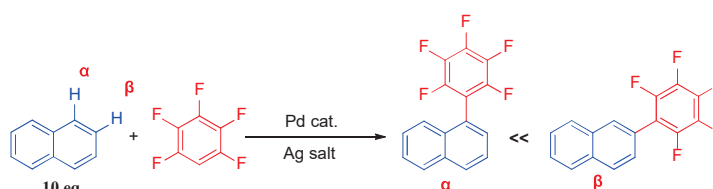
Tianya Xiong<sup>1</sup>, Tomoki Iida<sup>1</sup>, Takaki Kanbara<sup>1</sup>, Junpei Kuwabara<sup>1</sup>

<sup>1</sup> Institute of Pure and Applied Sciences, University of Tsukuba, 1-1-1 Tennodai, Tsukuba 305-8573, Japan.

E-mail: [s2320404@u.tsukuba.ac.jp](mailto:s2320404@u.tsukuba.ac.jp)



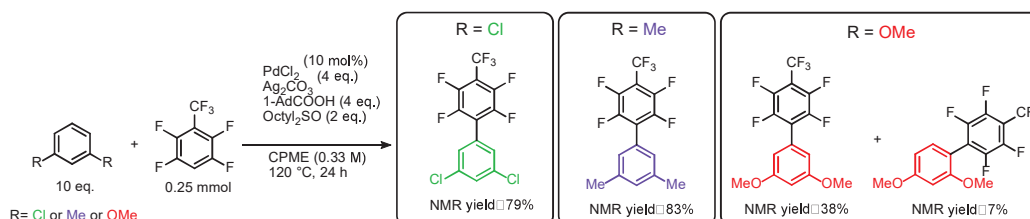
Recently we reported cross-dehydrogenative coupling (CDC) reaction of naphthalene with polyfluoroarene proceeded at the  $\beta$ -position where the steric hindrance is small, in contrast to the general  $\alpha$ -position selectivity (Scheme 1).<sup>1)</sup> This study investigates whether reactions with disubstituted benzenes also exhibit similar regioselectivity (Scheme 2). We also examined the influence of electronic factors of substituents on reactivity.



Scheme 1. CDC reaction of naphthalene with polyfluoroarene<sup>1)</sup>

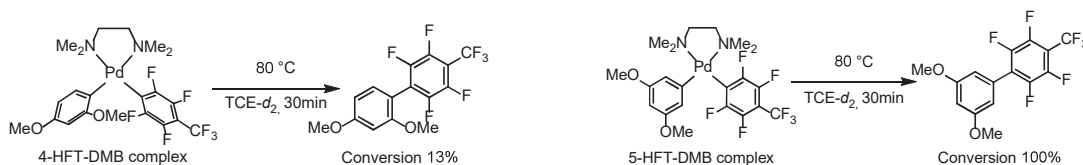
As shown in Scheme 2, heptafluorotoluene (HFT) was preferentially introduced into the position with the smallest steric hindrance in the disubstituted benzenes. However, dimethoxybenzene also reacted at the 4-position, showing low regioselectivity. Among the disubstituted benzenes studied, dimethoxybenzene (R = OMe) exhibited the lowest reactivity.

As shown in Scheme 2, heptafluorotoluene (HFT) was preferentially introduced into the position with the smallest steric hindrance in the disubstituted benzenes. However, dimethoxybenzene also reacted at the 4-position, showing low regioselectivity. Among the disubstituted benzenes studied, dimethoxybenzene (R = OMe) exhibited the lowest reactivity.



Scheme 2. Regioselectivity and yields of the CDC reaction of the disubstituted benzenes with HFT

Since the cause of this regiospecificity is associated with the difference in the reaction rate of the reductive elimination steps<sup>2)</sup>, we focused on the reductive elimination steps of the *m*-dimethoxybenzene complexes. We compared the reductive elimination of the 4-position and 5-position complexes (Scheme 3). As a result, the reaction conversion rate of the 4-position complex was 13% after 30 minutes at 80 °C, while the 5-position complex was completely consumed under the same conditions. This indicates that reductive elimination at the 5-position occurs rapidly due to the small steric hindrance. Additionally, reductive elimination also takes place at the 4-position, despite its significant steric hindrance, leading to the low regioselectivity observed in dimethoxybenzene.



Scheme 3. The reductive elimination reactions of the *m*-dimethoxybenzene complexes

## References

- [1] R. Sato; T. Iida; T. Kanbara; J. Kuwabara, *Chem. Commun.*, **2022**, 58, 11511-11514.
- [2] T. Iida, R. Sato, Y. Yoshigoe, T. Kanbara, J. Kuwabara, *Dalton Trans.*, **2024**, 53, 13340-13347.

# Exploration and evaluation of new elements of non-metallic substances r-BS by high-pressure synthesis

Li Jinyu<sup>1</sup>, Masashi Miyakawa<sup>2</sup>, Takashi Taniguchi<sup>2</sup>, Takahiro Kondo<sup>1</sup>

<sup>1</sup> Graduated School of Pure and Applied Sciences, University of Tsukuba, 1-1-1 Tennodai, Tsukuba, Ibaraki 305-8573, Japan

<sup>2</sup> National Institute for Materials Science, 1-1 Namiki, Tsukuba, Ibaraki 305-0044, Japan

E-mail: s2420403@u.tsukuba.ac.jp



## 1. Introduction

Rhombohedral boron monosulfide (r-BS) has shown excellent performance as an electrocatalyst for oxygen evolution reaction in water electrolysis [1,2]. Because r-BS is a layered two-dimensional material, its specific surface area is predicted to be large if the r-BS is exfoliated to be BS nanosheets. As well as high surface area, BS nanosheets are expected to be improved hydrogen storage material according to the theoretical prediction [3]. Therefore, my research first focuses on the actual synthesis of r-BS, while improving its specific surface area by exfoliating r-BS to be BS nanosheets for better applications in hydrogen storage and electrochemistry.

## 2. Method

r-BS was synthesized according to the reported procedures [4]. Briefly, a mixture of powdered sulfur and amorphous boron in a 1:1 atomic ratio was heated to 1873 K at 5.5 GPa and then quenched to room temperature. The resulting bulk r-BS (30 mg) was mixed with 10 mL of acetonitrile and homogenized with different time (from 30 min to 2h) to attempt a progressive exfoliation. The bulk r-BS and dried powder obtained from the supernatant after homogenization for 2h were subjected to scanning electron microscopy (SEM).

## 3. Results and Discussion

Bulk r-BS was successfully synthesized, which was corroborated by powder X-ray diffraction analysis of the resulting powder. SEM image of the bulk r-BS shows angular particles, whose grain size is mostly larger than 10  $\mu\text{m}$  (Figure 1a). In contrast, SEM image of the dried powder obtained from the supernatant after homogenization for 2h shows that the size of the particles was found to be smaller (Figure. 1b). This result indicated that the bulk-r-BS was exfoliated into BS nanosheets in acetonitrile by progressive homogenization. In the poster presentation, the detail of the exfoliation and characterizations will be shown.

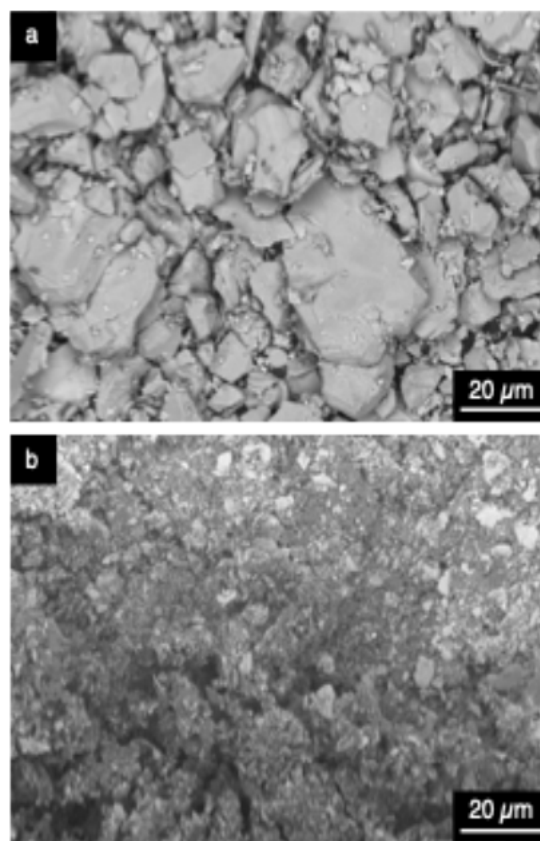


Figure 1. SEM images of (a) synthesized bulk-r-BS and (b) that of dried powder obtained from the supernatant after 2h homogenization.<sup>†</sup>

## References

- [1] L. Li, S. Hagiwara, T. Kondo, et al., *Chemical Engineering Journal* 471 (2023) 144489.
- [2] L. Li, N. Watanabe, T. Kondo, et al., *Sci. Technol. Adv. Mater.* 24 (2023) 2277681.
- [3] P. Mishra, et al., *J. Appl. Phys.* 127 (2020) 184305.
- [4] H. Kusaka, T. Kondo, et al. *J. Mater. Chem. A* 9 (2021) 24631.

# The synthesis of visible-light-driven photocatalyst material using rGO/ZnO/Fe<sub>2</sub>O<sub>3</sub> derived from zinc dross for synthetic dye degradation



William Justin Budiman<sup>1</sup>, Andri Hardiansyah<sup>2,3</sup>, Valentinus Alphano Dabur<sup>1</sup>, Nurfina Yudasari<sup>2</sup>, Isnaeni<sup>2</sup>, Lina Jaya Diguna<sup>4</sup>, Dominic Kowal<sup>5</sup>, Muhammad Danang Birowosuto<sup>5</sup>, and Arie Wibowo<sup>1,6</sup>

<sup>1</sup> Materials Science and Engineering Research Group, Faculty of Mechanical and Aerospace Engineering, Institut Teknologi Bandung, Bandung 40132, Indonesia

<sup>2</sup> Research Center for Nanotechnology Systems, National Research and Innovation Agency, South Tangerang 15314, Indonesia

<sup>3</sup> Collaboration Research Center for Advanced Energy Materials, National Research and Innovation Agency Institut Teknologi Bandung, Jl. Ganesha 10, Bandung 40132, Indonesia

<sup>4</sup> Department of Renewable Energy Engineering, Universitas Prasetiya Mulya, Kavling Edutown I.1, Jl. BSD Raya Utama, BSD City, Tangerang 15339, Indonesia

<sup>5</sup> Łukasiewicz Research Network - PORT Polish Center for Technology Development, Stabłowicka 147, Wrocław, 54-066, Poland

<sup>6</sup> Research Center for Nanoscience and Nanotechnology, Institut Teknologi Bandung, Bandung 40132, Indonesia.

E-mail: valentinus50@gmail.com

Further investigation is ongoing into the use of zinc oxide (ZnO) as a photocatalyst to mitigate water contamination<sup>[1]</sup>. Nevertheless, ZnO has limitations by a large energy bandgap, which confines its effectiveness to the ultraviolet (UV) light range, and a short recombination period<sup>[2]</sup>. In order to address these challenges, ZnO is enhanced with iron (III) oxide (Fe<sub>2</sub>O<sub>3</sub>) to decrease the energy gap, allowing it to operate within the visible light spectrum<sup>[3]</sup>. Additionally, we use reduced graphene oxide (rGO) to prolong the duration of the recombination process<sup>[2]</sup>. Zinc oxide (ZnO) and iron duplex oxide (Fe<sub>2</sub>O<sub>3</sub>) are derived from zinc dross, whereas reduced graphene oxide (rGO) is produced via the environmentally friendly Tour process<sup>[4]</sup>. This synthesis process provides a simple and sustainable solution for future wastewater treatment applications.

## References

- [1] Ong, C. B.; Ng, L.Y.; Mohammad, A.W. *Renewable and Sustainable Energy Reviews* **2018**, *81*, 536-551.
- [2] Budiarso, I. J.; Dabur, V. A.; Rachmantyo, R.; Judawisastra, H.; Hu, C.; Wibowo, A. *Materials Advances* **2024**, *5*, 2668-2688.
- [3] Diguna, L. J.; Fitriani, A. D.; Liasari, B. R.; Timuda, G. E.; Widayatno, W. B.; Wismogroho, A.S.; Shuwen, Z.; Birowosuto, M. D.; Amal, M. I. *Crystals* **2021**, *11*.
- [4] Kumar, N.; Salehiyan, R.; Chauke, V.; Botlhoko, O. J.; Setshedi, K.; Scriba, M.; Masukume, M.; Ray, S. S. *FlatChem* **2021**, *27*.

# Enhancing Thermoelectric and Mechanical Properties of $\text{YbMg}_2(\text{Bi,Sb})_2$ Zintl Phase through Anion site substitution



Kushal Mehrotra<sup>1,2</sup>, Andrei Novitskii<sup>2</sup>, Takao Mori<sup>1,2,\*</sup>

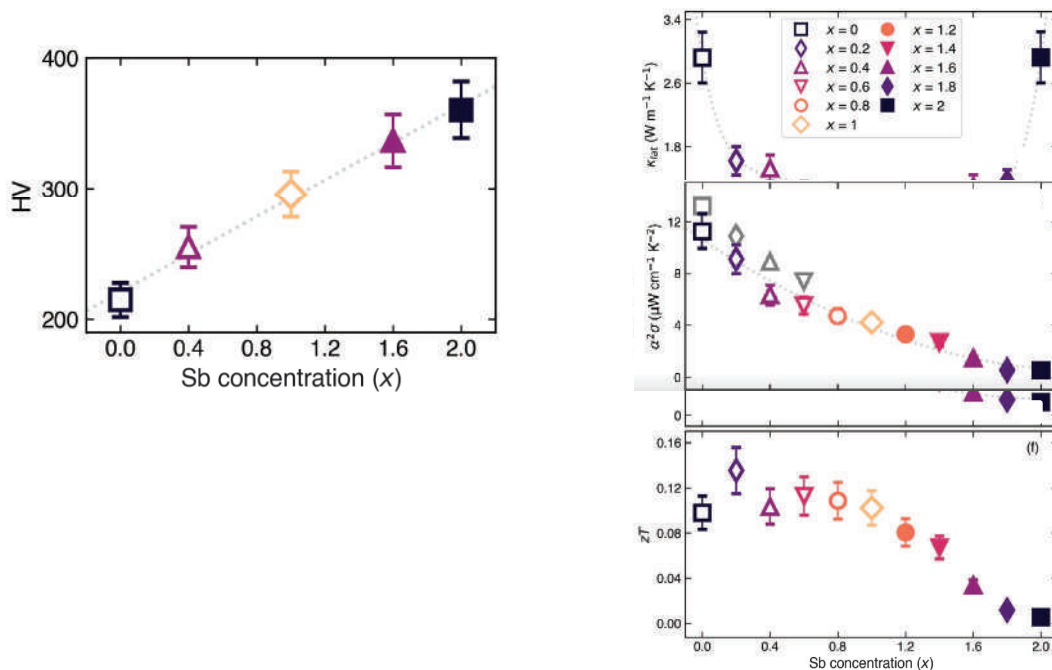
<sup>1</sup>Graduated School of Pure and Applied Sciences, University of Tsukuba, 1-1-1 Tennodai, Tsukuba, Ibaraki 305-8573, Japan

<sup>2</sup>International Center for Materials Nanoarchitectonics (WPI-MANA), National Institute for Materials Science (NIMS), 1-1 Namiki, Tsukuba, Ibaraki, 305-0044, Japan.

E-mail: MORI.Takao@nims.go.jp

## ABSTRACT

In this comprehensive study, we investigate the chemical bonding strength, thermoelectric performance, and mechanical properties of  $\text{YbMg}_2(\text{Bi,Sb})_2$  Zintl phases, with a focus on understanding the impact of anion site substitution within the  $\text{YbMg}_2\text{Bi}_{2-x}\text{Sb}_x$  system. Exploiting the unique 'Phonon-Glass, Electron-Crystal' (PGEC) characteristic inherent in Zintl phases, we specifically substitute the Bi site with isoelectric Sb, revealing intriguing insights into the thermoelectric transport behavior. The partial substitution results in a reduction of carrier concentration and induces lattice deformation due to the distinct atomic radius and mass of Bi and Sb. This, in turn, leads to a simultaneous decrease in power factor and thermal conductivity. Notably, the substantial reduction (41%) in thermal conductivity outperforms the decrease in power factor (19%) for the composition  $\text{YbMg}_2\text{Bi}_{1.8}\text{Sb}_{0.2}$ . Consequently, the Sb substitution yields a superior thermoelectric performance compared to pristine  $\text{YbMg}_2\text{Bi}_2$ , achieving a remarkable  $zT$  of approximately 0.8 at 723K. Despite the stronger chemical bonding introduced by Sb alloying, the compound exhibits lower lattice thermal conductivity, attributed to rigorous point defect scattering. Crucially, the chemical bonding toughening contributes to improved mechanical properties<sup>[1]</sup>, as reflected by the increasing Vickers hardness values from pure Bi (214.6) to pure Sb (360.4) composition, essential for the durable operation of thermoelectric generators. This research not only broadens the understanding of Zintl phases<sup>[2]</sup> but also introduces a novel approach to chemical bonding engineering for enhanced thermoelectric applications, providing valuable insights for future advancements in the field





**References:**

[1] Z. Liang and Z. Ren. New insights into the effect of chemical bonding strength on thermoelectric performance and stability in  $\text{YbMg}_2\text{Bi}_2$  toward practical thermoelectric applications. *Materials Today Physics*. 28, 100858, (2022)

[2] W. Peng, S. Chanakian, and A. Zevalkink. Crystal chemistry and thermoelectric transport of layered  $\text{AM}_2\text{X}_2$  compounds. *Inorganic Chemistry Frontiers*. 5 (8), 1744-1759, (2018)

# Combinatorial sputtering synthesis of TbCu<sub>7</sub>-type Sm-Fe based compounds: A study on phase, composition, and extrinsic magnetic properties.



Dilipan Angayarkanni Ramamurthy<sup>1,2</sup>, Sepehri-Amin Hossein<sup>1,2</sup>,  
Rajkumar Modak<sup>1</sup>, Varun Kumar Kushwaha<sup>1</sup>, Yuya Sakuraba<sup>1,2</sup>,  
Ken-ichi Uchida<sup>1,2</sup>, Kazuhiro Hono<sup>1,2</sup>, Yukiko Takahashi<sup>1,2</sup>

<sup>1</sup>National Institute for Materials Science, Tsukuba, Japan.

<sup>2</sup>Graduate School of Science and Technology, University of Tsukuba, Japan.

E-mail: [s2230115@u.tsukuba.ac.jp](mailto:s2230115@u.tsukuba.ac.jp)

Sm-Fe-based permanent magnetic compounds have emerged as a potential next generation permanent magnets due to the combination of low supply risk, cost-effectiveness, and sustainability [1,2]. In this work, TbCu<sub>7</sub>-type SmFe<sub>x</sub> ( $x=6.4$  to  $12.7$ ) and SmFe<sub>x</sub>N ( $x=6.8$  to  $12.8$ ) composition spread thin films were fabricated using a combinatorial sputtering system to study the effect of composition on the phase formation and extrinsic magnetic properties. A high-throughput phase and composition analysis was carried out using x-ray diffraction and x-ray fluorescence measurements respectively, at different Fe:Sm ratio positions on the thin film. The Fe:Sm ratio significantly affects the formation of main TbCu<sub>7</sub>-type phase and the secondary ferromagnetic  $\alpha$ -Fe phase. The optimal Fe:Sm ratio, which exhibits the highest fraction of the TbCu<sub>7</sub>-type phase free from  $\alpha$ -Fe, was identified as SmFe<sub>9.8</sub> and SmFe<sub>9.5</sub>N. The coercive field ( $\mu_0H_c$ ) was estimated using a position-dependent polar-magneto-optical Kerr effect hysteresis loops and was found to range from 1.1 T (for SmFe<sub>6.8</sub>N) to 0.06 T (SmFe<sub>12.8</sub>N). The remanent magnetization ( $\mu_0M_r$ ) values estimated using a superconducting quantum interference device-vibrating sample magnetometer measurements (on cut samples) ranges from 0.8 T to 1.2 T for the  $\alpha$ -Fe-free compositions. The optimal composition, SmFe<sub>9.5</sub>N, exhibits a  $\mu_0H_c$  of  $\sim 0.8$  T and a  $\mu_0M_r$  of  $\sim 1.2$  T. Furthermore, microstructural characterization was carried out on the SmFe<sub>9.5</sub>N using scanning transmission electron microscopy to correlate with its phase and magnetic properties. Overall, this study demonstrates the effect of composition variation on the phase and extrinsic magnetic properties of this compound, facilitating the selection of desired compositions with targeted magnetic properties.

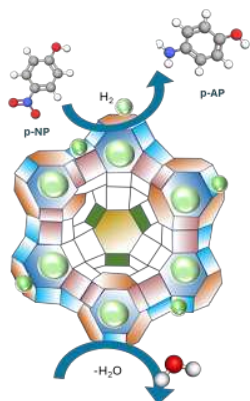
## References

- 1) K. Binnemans, J. Sustain.Metall., 4, 126-146, 2018
- 2) Y.K. Takahashi, H. Sepehri-Amin, T. Ohkubo, Sci. Technol. Adv. Mater. 22 (2021) 449-460.

# p-Nitrophenol reduction using transition metal supported zeolites

Ayush Kumar,<sup>1</sup> Kavitha Ramadass,<sup>1</sup> Gurwinder Singh,<sup>1</sup> Satish CI,<sup>1</sup> and Ajayan Vinu<sup>1,\*</sup>

<sup>1</sup> Global Innovative Centre for Advanced Nanomaterials, School of Engineering, The University of Newcastle, Callaghan, NSW 2308, Australia  
E-mail: Ayush.Kumar@uon.edu.au



The catalytic conversion of p-nitrophenol (p-NP) to p-aminophenol (p-AP) is a crucial industrial process with significant environmental and pharmaceutical implications. This reduction reaction also serves as a model system for evaluating the catalytic performance of novel materials. Existing catalysts for p-NP reduction often suffer from poor stability, low recyclability, and susceptibility to deactivation through metal leaching or nanoparticle aggregation. Zeolite overcomes these challenges by confining metal nanoparticles within their porous structure, preventing aggregation and leaching, while their high surface area and tunable pore sizes enhance catalytic activity and selectivity, leading to improved stability and recyclability for p-nitrophenol reduction<sup>1</sup>. Currently, most studies focus on ZSM-5 or hierarchical ZSM-5 derivatives for the reduction of p-NP<sup>2</sup>. There is still much to explore about other zeolite frameworks like beta-zeolites and  $\gamma$ -zeolites with in-depth mechanistic studies. Our current research is focused on developing a new type of transition metal decorated with zeolites catalyst for the room temperature reduction of p-NP. Various combinations and permutation of metal loading impregnation methods are systematically explored to get the optimum catalyst. Out of all the catalysts developed, 1% Ni loaded on beta &  $\gamma$ -zeolites demonstrated optimal performance, achieving 100% conversion and selectivity at optimized reaction conditions at 25°C and within 3h reaction time.

(1) Erika, D.; Nurdini, N.; Mulyani, I.; Kadja, G. T. M. Amine-functionalized ZSM-5-supported gold nanoparticles as a highly efficient catalyst for the reduction of p-Nitrophenol. *Inorganic Chemistry Communications* **2023**, *147*.

(2) Aslam, S.; Subhan, F.; Yan, Z.; Yaseen, M.; Shujahat, M. H. Fabrication of gold nanoparticles within hierarchically ZSM-5-based micro-/mesostructures (MMZ) with enhanced stability for catalytic reduction of p-nitrophenol and methylene blue. *Separation and Purification Technology* **2021**, *254*.



お客様に寄り添い、暮らしを豊かにする

ダイハツは、それぞれの地域、お客様一人ひとりの生活に、  
真摯に向き合い、自分らしく軽やかなライフスタイルを実現できる  
製品・サービスをお届けしてまいります。



# Open Science for All!

# STAM Science and Technology of Advanced Materials

## Platinum OA Campaign to publish articles free of charge

Limited time offer  
end on  
March 31, 2025



STAM tandfonline

IF:7.4

With rising article processing charges (APCs) becoming a global issue, the National Institute for Materials Science (NIMS) has decided to collaborate with Empa in supporting an APC-free campaign by "Science and Technology of Advanced Materials (STAM) (IF=7.4)," an international journal specializing in materials science. Authors will be exempted from STAM's usual APC (US\$1200 / £ 925 / €1060 / ¥131,000) and will be able to publish open access papers (platinum OA) for free until March 31, 2025, the 25th anniversary of STAM's first issue. NIMS will contribute to the expansion of open science through STAM's APC-free publishing campaign.



**STAM Advisory Member**  
Institute Professor / Honorary Professor, Tokyo Institute of Technology  
Distinguished Fellow, NIMS

**Hideo Hosono**

I have published a number of review articles and original research papers in STAM. I was pleased to learn that our 2010 review article on amorphous IGZO-TFTs has been cited 1,600 times. When we published our efforts to explore new superconducting materials in another review, I was even allowed to enlist unsuccessful materials thanks to STAM's unique policy. I find STAM to be a valuable resource for materials scientists.



国立研究開発法人 物質・材料研究機構  
National Institute for Materials Science

